INFORMATION TO USERS

This material was produced from a microfilm copy of the original document. While the most advanced technological means to photograph and reproduce this document have been used, the quality is heavily dependent upon the quality of the original submitted.

The following explanation of techniques is provided to help you understand markings or patterns which may appear on this reproduction.

- 1. The sign or "target" for pages apparently lacking from the document photographed is "Missing Page(s)". If it was possible to obtain the missing page(s) or section, they are spliced into the film along with adjacent pages. This may have necessitated cutting thru an image and duplicating adjacent pages to insure you complete continuity.
- 2. When an image on the film is obliterated with a large round black mark, it is an indication that the photographer suspected that the copy may have moved during exposure and thus cause a blurred image. You will find a good image of the page in the adjacent frame.
- 3. When a map, drawing or chart, etc., was part of the material being photographed the photographer followed a definite method in "sectioning" the material. It is customary to begin photoing at the upper left hand corner of a large sheet and to continue photoing from left to right in equal sections with a small overlap. If necessary, sectioning is continued again beginning below the first row and continuing on until complete.
- 4. The majority of users indicate that the textual content is of greatest value, however, a somewhat higher quality reproduction could be made from "photographs" if essential to the understanding of the dissertation. Silver prints of "photographs" may be ordered at additional charge by writing the Order Department, giving the catalog number, title, author and specific pages you wish reproduced.
- 5. PLEASE NOTE: Some pages may have indistinct print. Filmed as received.

Xerox University Microfilms

300 North Zeeb Road Ann Arbor, Michigan 48106

76-30,182

ALLEN, Raymond William Kenneth, 1948-COLLECTION OF HYDROPHILIC AND HYDROPHOBIC PARTICLES BY SUSPENDED WATER DROPS.

McGill University (Canada), Ph.D., 1975 Engineering, chemical

Xerox University Microfilms, Ann Arbor, Michigan 48106

© 1976

RAYMOND WILLIAM KENNETH ALLEN

ALL RIGHTS RESERVED

COLLECTION OF HYDROPHILIC AND HYDROPHOBIC PARTICLES BY SUSPENDED WATER DROPS

by

R.W.K. Allen

A thesis submitted to the Faculty of Graduate Studies and Research in partial fulfilment of the requirements for the degree of Doctor of Philosophy

Department of Chemical Engineering
McGill University
Montreal

June 12, 1975

R.W.K. Allen

COLLECTION OF HYDROPHILIC AND HYDROPHOBIC PARTICLES BY SUSPENDED WATER DROPS

Abstract

A new technique has been developed to measure the collection efficiencies of water drops suspended in a free laminar jet. It involves using a forward light scattering particle counter to monitor continuously the number of particles collected by a drop. The advantage of this method is that it allows the gathering of data for any aerosol.

Results are presented for three different hydrophilic aerosols. They agree very well with those of other workers and with the theoretically expected values. Results are also presented for four different hydrophobic aerosols, both liquid and solid. In every case, the hydrophobic particles are collected less efficiently than the hydrophilic particles under similar conditions.

Furthermore, a theory has been developed to account for the total change in the surface energy of the system as the particle passes through the drop surface. The energy necessary for complete penetration is derived and used to calculate

'penetration efficiencies'. It was found that there is a correlation between these calculated values and the experimental results. An analysis of the collision process predicts that there may be two types of collision regime. The first type refers to low energies of approach where the particle does not enter the drop but may still be captured on its surface. The second regime covers high energies of approach where the particle either penetrates through the drop surface or rebounds into the air stream. The existence of this second regime has been confirmed by the agreement found in this work between the theory and the experimentation.

LA CAPTATION DE PARTICULES HYDROPHILES ET HYDROPHOBES PAR GOUTTES D'EAU SUSPENDUES

Sommaire

L'auteur développe une nouvelle technique afin de mesurer l'efficacité de captation de gouttes d'eau suspendues dans un jet d'air libre et laminaire. Cette technique s'agit d'employer un spectophotomètre à aérosol pour conter continuellement le nombre de particules amassé par la gouttelette.

L'avantage de cette méthode vient du fait qu'elle permet de rassembler des données expérimentales sur n'importe quel aérosol.

L'auteur présente des résultats pour trois aérosols hydrophiles différents. Ceux-ci s'accordent bien avec les résultats d'autres travailleurs et avec les valeurs qui sont à prévoir théoriquement. Des résultats sont également présentés pour quatre aérosols hydrophobes différents, liquides autant que solides. Dans chaque cas, les particules hydrophobes sont captées de façon moins efficace que les particules hydrophiles.

En outre, l'auteur propose une théorie qui vise à expliquer ce qui se passe à l'égard de l'énergie superficielle du système lorsque la particule traverse la surface de la gouttelette. Il fait une estimation de l'énergie requise pour une pénétration complète et se sert de cette quantité afin de trouver 'l'efficacité de pénétration'. L'auteur a découvert

qu'il y a une corrélation entre ces valeurs calculées et les résultats expérimentaux. Une analyse du processus de collision prédit qu'il y a probablement deux genres de régimes gouvernant la collision. Le premier type reporte aux situations où l'énergie d'approche est basse et où la particule n'entre pas dans la gouttelette bien qu'elle puisse être captée sur la surface. Le deuxieme régime comprend les situations où l'énergie d'approche est élévée et où la particule passe à travers la surface de la goutte d'eau ou rebondit dans le courant d'air. L'existence de ce deuxième régime se confirme du fait que l'auteur a trouvé un accord entre la théorie et l'expérimentation.

Acknowledgements

The author wishes to express his sincere gratitude to his supervisor, Dr. E.J. Farkas, for his help in the administration of this project. Thanks are also due to the students and staff of the Chemical Engineering Department of McGill University, and especially to David Reay for his help in some aspects of the programming.

The author wishes to acknowledge Miss Pat Fong for the typing of this manuscript.

The financial support for this dissertation received from the National Research Council of Canada is also gratefully acknowledged.

Thanks are inadequate for Rosemarie without whom this work would have been impossible.

Table of Contents

	Page	e
ACKNOWLED	GEMENTS v	
TABLE OF	CONTENTS vi	
LIST OF F	IGURES ix	
INTRODUCT:	ION 1	
	XPERIMENTAL METHOD AND RESULTS FOR HYDROPHILIC ARTICLES	
Chapter 1	Collision Efficiencies of Spherical Droplets in Potential Flow	
1.1	Definition of terms and theoretical calculation of collection efficiency	
1.2	Review of previous experimental work 17	
Chapter 2	Experimental Equipment and Procedure 23	
2.1	Principle of operation 24	
2.2	Experimental equipment	
2.2.1	the aerosol generator 26	
2.2.2	the droplet support and sampling probe assembly	
2.2.3	the particle counter 38	
2.3	Experimental Procedure	
Chapter 3	Experimental Results for Hydrophilic Particles. 47	
3.1	Data reduction	
3.2	Experimental results 53	
3.3	Discussion of experimental method 58	

		Page	3
	PART II	COLLECTION OF HYDROPHOBIC PARTICLES BY WATER DROPLETS	
	Chapter 4	Definition of the Problem	
	4.1	Literature review 69	
	4.2	Experimental procedure 77	
	4.3	Comparison of results for hydrophobic and hydrophilic particles	
	Chapter 5	Collision Dynamics for Hydrophobic Particles 87	
	5.1	Energy considerations in the collision process . 88	
	5.1.1	collisions where complete penetration does not occur	
	5.1.2	collisions for which the particle penetrates the droplet	
	5.1.3	the approach energy 94	
	5.2	Penetration of the droplet surface 97	
	5.3	Interactive forces	
	5.3.1	van der Waals forces	
	5.3.2	electrostatic forces	
	5.3.3	viscous forces122	
C	Chapter 6	Results and Discussion128	
	6.1	Calculation of penetration efficiencies129	
	6.2	Comparison of penetration efficiencies with experimental results	
	6.3	Discussion of rebound criteria for the paraffin wax example147.	
	6.4	Criteria for the neglect of the surface interactive forces	

		Page
CONCLUSION	***************************************	,164
CLAIMS TO C	ORIGINALITY	,167
NOMENCLATUR	RE	168
REFERENCES	••••••	173
APPENDICES	••••••	177
Appendix A	Theoretical Calculations	177
A.1	Logic flow chart of computer program	178
A.2	Listing of program used to calculate collection and penetration efficiencies	
A.3	Sample output for calculations of collection and penetration efficiencies	186
Appendix B	Experimental Calculations	189
B.1	Table of experimental operating conditions	190
B.2	Listing of computer program to reduce experimental data	192
B.3	Experimental results	199

List of Figures

Figure Number		Page
1.1	Particle Trajectories around a Spherical Body	9
1.2	Theoretical Variation of Collection Efficiency with Impaction Parameter	16
1.3	Experimental Data of Walton and Woolcock	19
1.4	Comparison of Previous Experimental Work	21
2.1	Schematic Diagram of Apparatus	27
2.2	Schemiatic Diagram of the Aerosol Generator	29
2.3	Cross-sectional View of the Droplet Holder and Sampling Probe Assembly	33
2.4	Calibration Curve for Hot Wire Anemometer	39
2.5	Velocity and Turbulence Profiles in the Laminar Jet	40
2.6	Schematic Diagram of the Particle Counter	42
3.1	Geometry of Drop on Filter Surface	48
3.2	Comparison of Experimental Results with TheoryFerrous Sulphate Aerosol	. 54
3.3	Comparison of Experimental Results with TheoryMethylene Blue Aerosol	55
3.4	Comparison of Experimental Results with TheoryWater Aerosol	56
4.1	Variation of Collection Efficiency with Impaction Parameter at Various Values of Maccording to Pemberton	71
4.2	Comparison of the Best Fit Lines for the Experimental Data	83
4.3	Comparison of the Best Fit Lines for the Paraffin Wax Data with MacDonald's Theory	85

Figure Number		Page
5.1	Variation of Approach Energy with Separation at $K = 7.0$ and $K = 1.5$	96
5.2	Sessile Drop on a Solid Surface	98
5.3	Penetration of the Particle into the Droplet Surface	98
5.4	Correlation of Penetration Energy with Penetration	104
5.5	Approach of a Particle to a Deformable Surface	116
5.6	Electrostatic Gain as a Function of Separation	121
5.7	Energy Loss to Viscous Forces as a Function of Separation	127
6.1	Variation of Penetration Efficiency with Impaction Parameter for Different Contact Angles at We = 10.5	130
6.2	Variation of Penetration Efficiency with Impaction Parameter for Different Weber Numbers at $\theta = 102^{\circ}$	132
6.3	Effect of Radius Ratio and G on the Penetration Efficiency	133
6.4	Variation of Penetration Efficiency with Impaction Parameter for Different Values of M	135
6.5	Experimental Measurements of Collection Efficiency as a Function of Impaction Parameter Paraffin Wax	140
6.6	Experimental Measurements of Collection Efficiency as a Function of Impaction Parameter Paraffin Wax	141
6.7	Experimental Measurements of Collection Efficiency as a Function of Impaction Parameter Paraffin Oil	142
6.8	Experimental Measurements of Collection Efficiency as a Function of Impaction Parameter	1/13

Figure	e Number	Page
6.9	Experimental Measurements of Collection Efficiency as a Function of Impaction Parameter Talc	- 145
6.10	Experimental Measurements of Collection Efficiency as a Function of Impaction Parameter Talc	146
6.11	Comparison of Energy Functions with Gap Width for the Collision Mechanisms	149
	Variation of U _R with Angle of Incidence Computed using Potential Flow around the Collector	153

		·	Page
	<u>P1</u>	ates	
Plate	1	Experimental Apparatus	28
Plate	2	Droplet Holder and Sampling Probe Assembly	34
Plate	3	Suspended Water Drop	36

Introduction

The study of the deposition of particles from a fluid stream onto a collecting body is at least 50 years old. The interest shown in this topic was at first sporadic but has grown steadily in both degree and scope over recent years. It now extends to a wide range of disciplines including meteorology, environmental technology, and aeronautical, mining, and chemical engineering. In the last 25 years, the study of particles dispersed in a gas stream has acquired the status of a new discipline, referred to as aerosol science, of which deposition phenomena are a major preoccupation.

Concomitant with this increasing interest has been a growth in the number of mechanisms proposed for the capture of particles by collectors. The work presented in this thesis is primarily concerned with one of the oldest of these mechanisms, inertial impaction. It therefore considers aerosols which are relatively large in diameter, greater than about 5 microns (µ),* which have sufficient inertia that they deviate significantly from the fluid streamlines when they are close to a collector. The modern work on this subject still concerns itself with the same two parameters that were originally proposed by Albrecht in 1931 (2). He was the first to introduce the concept of an efficiency and he defined it as the ratio of the projected area of the obstacle to the area of the stream from which

 $^{^*}$ 1 $_{\text{U}} = 10^{-6}$ metres

particles impinge on the collector. The reciprocal of this quantity is used today and generally called the collection efficiency. Albrecht also introduced a form of the 'impaction parameter' which is used to describe the magnitude of a particle's inertia relative to the viscous drag forces.

Numerical solution of the equations describing the trajectories of individual particles close to a submerged, spherical or cylindrical obstacle was first accomplished by Langmuir (41). This led to an alternative definition of collection efficiency which was equivalent to, but conceptually different from, that of Albrecht. Langmuir's approach reduced the problem from a consideration of a cloud of aerosol to a study of the behaviour of a single particle in that cloud. Thus the collection efficiency was redefined in terms of the starting point in the trajectory of a particle which just touches the collector. By 1960, Fonda and Herne (31) were able, owing to the advent of high speed computers, to perform these calculations with far greater accuracy. However, solutions have only been possible under circumstances where the equations describing the flow field around the body can be simplified. This has meant that there have only been solutions for potential and viscous flow. These have proved very useful despite the constraint of using an approximate analytical expression for the flow around the collector. Recently, however, Beard and Grover (5) have overcome this constraint by making use of some

of the modern formulations for the flow around a sphere at intermediate Reynolds numbers (Re). Their results show that, at high Re, potential flow assumptions provide a fair estimate of the collection efficiency.

All of these works rested upon four basic assumptions which are often referred to as the Langmuir model. They are that:

- a) inertial mechanisms dominate the collection process which is then considered to occur only on the forward half of the sphere.
- b) the drag on the aerosol particle may be computed from Stokes' law.
- c) the particle is sufficiently small that it does not affect the flow field around the collector.
- d) every particle which is brought to the surface of the collector is captured.

Each of these assumptions has been examined in the literature. For example, several workers have found that, for particles smaller than lµ, inertial deposition may cause collection on the rear of a collector. Others have studied the problem of two colliding particles of comparable size and found that the flow fields interact. The last assumption, however, is the least studied of all, certainly for collisions between aerosols and liquid drops. Thus, whilst considering situations in which

the first three points are valid, this thesis addresses itself mainly to an examination of the fourth assumption.

It seems obvious that the tendency of liquid or solid hydrophobic particles to adhere to a water surface will be much less than that of hydrophilic particles. The ways and degree to which this is so are the concern of this work. order to observe successfully the effects of hydrophobicity, it is necessary to have experimental data over a wide range of However, there is a paucity of information aerosol materials. with respect to the capture of particles by liquid drops and this is directly related to the experimental difficulties involved in the measurement of such collection. A review of the results reported in the literature shows that there is a great discrepancy between the findings of various workers. Moreover, there is no general method for measuring the quantity collected by the water droplet. Each experimenter has developed his own method of analysis applicable to his individual aerosol. Even the most general of these methods, some form of counting procedure, carries the constraint that the particle be an in-In order to study the effect of the nature of soluble solid. the particle on the collection efficiency, a new experimental technique is therefore required which should be as general as possible in its application. In the present work, a new method of measurement is developed which seems to meet this need.

This work thus falls naturally into two main parts. The

first deals exclusively with hydrophilic particles for which the capture efficiency can be considered to be 100%. The method developed is described and the results from it for completely wettable particles are discussed. The second part reports the use of this technique in the study of hydrophobic aerosols, both solid and liquid, and discusses the collision process as it occured under experimental conditions. An attempt is made to isolate the important factors involved in the variation of collection with wettability.

PART I

EXPERIMENTAL METHOD AND RESULTS FOR HYDROPHILIC PARTICLES

Chapter 1

COLLISION EFFICIENCIES OF SPHERICAL DROPLETS IN POTENTIAL FLOW

In order to place the problem of the collection efficiency of hydrophilic particles in context, it is first necessary to define the terms which are used throughout the discussion and to review the available literature.

1.1 Definition of Terms and Theoretical Calculation of Collection Efficiency

The collection efficiency E is a term which has been used almost universally since its introduction by Albrecht in 1931 (2). As an air stream moves relative to a spherical body, the fluid streamlines in the immediate vicinity of the sphere diverge. A particle in the stream is subject both to the drag forces from the fluid and to its own inertia. Thus not all the particles in the volume swept by the droplet actually impinge upon it. Only a central core of the fluid is in fact cleaned of particles. The collision efficiency of the droplet is defined as the ratio of the cross-sectional area of this core to the projected area of the drop. It may be expressed either as a percentage or as a fraction. In this work, it is consistently referred to as a percentage.

There is an alternative method of conceptualising the collision efficiency which stems from a knowledge of the

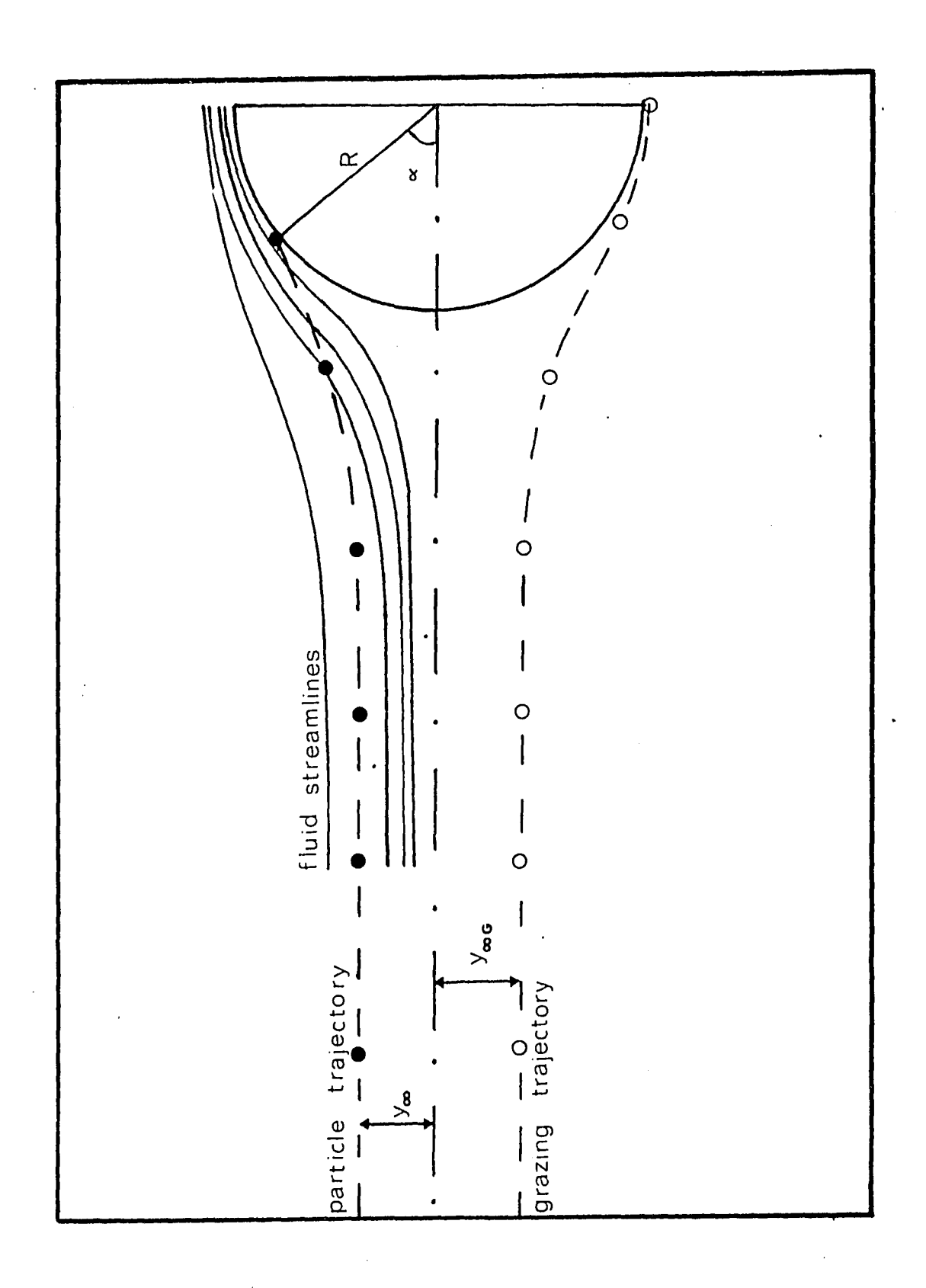
trajectories of individual particles approaching the drop. At large distances, the particle moves, with the streamlines, parallel to the axis of the drop. As it nears the obstacle, it is moved laterally by the viscous drag, whilst its own inertia tends to maintain its instantaneous direction of motion. Thus particles whose trajectories lie initially close to the axis of the drop tend to collide with it, whilst those which are originally far from the axis tend to be swept past. In between these two extremes, there is what is known as the grazing trajectory, which occurs when the particle just touches the droplet at the equator (See Figure 1.1). If the initial distance of this particle from the axis is y_c, then all particles closer to the axis than $y_{\infty G}$ are collected, whilst all those further from the axis than this value are not. radius of the drop is R, the collection efficiency can be found from the grazing trajectory by:

$$E = \frac{Y_{\infty G}^2}{R^2}$$
 (1.1)

As the particle approaches the collector, its inertia tends to overcome the viscous drag of the fluid so that it moves towards the body. However, an infinitely small particle with no inertia follows the streamlines and does not collide. A convenient measure of the ratio of inertial effects to viscous effects on the particle is the quantity referred to in

Figure 1.1

PARTICLE TRAJECTORIES AROUND A SPHERICAL BODY



this work as the impaction parameter K. It is defined by:

$$\kappa = \frac{1}{9} \cdot \frac{d^2 U_{\infty}^{\rho} p}{D u} \tag{1.2}$$

where d is the particle diameter, U_{∞} is the free stream velocity of the aerosol, μ is the viscosity of the gas, and ρ_p is the density of the particle. This dimensionless group has variously been termed the Stokes criterion or number, the inertial parameter, or the impact number. It comes from the Stokes law of viscous drag which, when substituted into the dimensionless equation of motion of the particle, gives a coefficient of $\frac{1}{K}$ to the velocity term.

The collection efficiency of aerosols larger than 5μ is predominantly a function of K. For this reason, graphs of collection efficiency versus impaction parameter are used exclusively in this work to represent both the theoretical and experimental results. Various methods of presenting this relationship are to be found in the literature, such as E versus $\ln K$, E versus K, \sqrt{E} versus $\ln K$, \sqrt{E} versus K, and $\ln E$ versus $\ln K$. Since none of these methods offers any particular advantage, the data in the present work are presented in the most commonly used format, which is a plot of E versus $\ln K$.

The collection efficiency exhibits a dependence on three other dimensionless quantities besides the impaction parameter: the radius ratio a/R, the gravitational settling velocity G,

and the Reynolds number. The radius ratio is a measure of the effect of interception on the collection efficiency. Interception is the mechanism which accounts for the finite size of the aerosol such that only the edge of the particle rather than the centre has to impinge upon the collector to ensure collision. At low radius ratios the effect is small, whilst at very large values of a/R the flow field of the aerosol particle affects the flow around the collector and the fluid mechanics change.

The dimensionless gravitational settling velocity is the ratio of the terminal velocity, calculated according to Stokes law, to the free stream velocity:

$$G = \frac{1}{18} \cdot \frac{d^2g}{\mu U_{\infty}} (\rho_p - \rho_f)$$
 (1.3)

where $\rho_{\rm f}$ is the density of the fluid. As the particle and collector approach each other, the vertical component of the particle's velocity is reduced owing to the gravitational settling effect. The collection efficiency is thereby diminished. The effect of G is fairly small in most practical situations.

The last dimensionless group on which the collection efficiency depends is the Reynolds number.* It is the second

 $Re = \rho_f U_{\infty} D/\mu$

most important parameter in that it characterises the flow around the collector and thus the trajectories of the particles before collision. Before calculations of the theoretical collection efficiency can be made, the value of Re must be assumed. Up until the work of Beard and Grover (5), computations of E had only been made for potential and Stokes flow, the two conditions where an analytical expression is available for the fluid flow around the forward half of the collector. These situations provide two almost parallel curves on an E versus K plot. are widely used as approximations to real situations which can be expected to lie between the two curves. Beard and Grover's work (4, 5) has made use of the numerical results of Le Clair et al (41a) for the stream functions about spheres at intermediate Re. They have calculated E versus K curves for Reynolds numbers of 1, 10, 20, 100, 200, and 400. Their results were found to fall between the viscous and the potential flow situations.

For the second part of this work, it was necessary to have a theoretical model to describe the trajectories of a particle approaching a water drop. It was decided to use potential flow assumptions to approximate the flow field around the forward half of the sphere since the work presented here is only for situations where inertial forces are important. This necessarily means high values of K and of Re. Comparison of the potential flow model with Beard and Grover's calculations

for K > 1.0 at Re = 400 show that there is only a difference of 6%. The potential flow model is therefore adequate for the work involved in the second part of this thesis. However, the experimental results for hydrophilic particles taken at lower values of K will be compared with both Beard and Grover's calculations and the potential flow model.

The computer program listed in Appendix A2 was used to calculate the trajectories of particles close to a spherical collector. This program is a version of the one described by Reay (59). It follows the method of Fonda and Herne (31) which uses the Langmuir model. In dimensionless terms with respect to the free stream velocity and the drop radius, the particle's equation of motion in the x direction (x vertically downwards) is:

$$\frac{dU'_{px}}{dt'} = \frac{1}{K} (U'_{px} - U'_{fx} - G)$$
 (1.4)

and in the y direction:

$$\frac{du'_{py}}{dt'} = \frac{1}{K} (u'_{py} - u'_{fy})$$
 (1.5)

with boundary conditions at t=0, $U'_{px}=-1$, and $U'_{py}=0$, where U' is the dimensionless velocity and subscript p refers to the particle and subscript f to the fluid. The velocity of the fluid around the sphere may be found from the potential

flow solution. In dimensionless cartesian coordinates with the origin at the centre of the sphere the fluid velocity is given by:

$$U'_{fx} = -1 - \frac{y'^2 - 2x'^2}{2(x'^2 + y'^2)^{5/2}}$$
 (1.6)

$$U'_{fy} = -\frac{3x'y'(x'^2 + y'^2 - 1)}{4(x'^2 + y'^2)^{5/2}}$$
 (1.7)

The particle trajectory was computed by numerically integrating Equations (1.4) and (1.5) using the fourth order Runge-Kutta-Merson technique (40) starting from a point 15 drop diameters upstream of the collector. An initial value of y'_{∞} was set at 0.65 and the value of y'_{∞} , which gave a grazing trajectory, was found by a dichotomous search. collision efficiency was then equal to the square of this dimensionless value. The logic flow chart of this program is shown in Appendix Al. A trajectory was considered high if the particle missed the collector, that is, did not come within a distance of 1 + a/R of the centre of the drop before it reached the equator. A trajectory was considered low if the centre of the particle did come within that distance. Trajectories were calculated until the values of $\mathbf{y}_{\mathbf{x}}$ for the most recent high and the most recent low trajectory differed by less than 0.1%. A sample output is shown in Appendix A3.

The results obtained for values of K between 0.1 and

10 and for various values of a/R and G are shown in Figure
1.2. The collection efficiency curve for viscous flow around
the collector is also shown. The results are identical to the
computations of Fonda and Herne and of Flint and Howarth (20).
With a means of predicting the collection efficiency of a
sphere at high Reynolds numbers, the next step is to compare
these calculations with experimentally measured values to see
whether or not the Langmuir model is appropriate.

Figure 1.2

THEORETICAL VARIATION OF COLLECTION EFFICIENCY WITH IMPACTION PARAMETER

	a/R = 0,	G = 0
	a/R = 0.005,	G = 0
	a/R = 0,	G = 0.025
	a/R = 0,	G = 0.05
	2/P - 0	C = 0 (viccous flow)

1.2 Review of Previous Experimental Work

This section briefly reviews the work that has been reported in order to compare the results obtained both between workers and with the theoretically predicted values. There have been relatively few experimental investigations of the collection of small particles by larger spherical collectors despite the theoretical interest which has been shown in the topic. One of the earliest experimental works is by Ranz and Wong (58) who studied the collection of a sulphuric acid mist $(0.3-1.3\mu)$ flowing horizontally onto a 0.9 mm. platinum sphere. They obtained results which lie parallel to the theoretical curve but considerably above it.

Chronologically, the next study is by McCully et al (47) who were concerned with rainfall formation. They allowed water drops to fall through a column containing a polydisperse dust of glass beads from 1 to 15μ in diameter. They present graphs of collection efficiency versus particle diameter but do not give details of either the size or the terminal velocity of the drops. It is therefore impossible to correlate these collection efficiencies with the impaction parameter. Picknett (57) also reported an experiment to measure the collection efficiencies of free falling water drops in air. The drops used were 0.04 mm. in diameter and the aerosol was a water mist $(2-20\mu)$. He gave values of E as a function of a/R and found that the collection efficiency increased as the drops became

of comparable size.

The classic experimental work on this subject was published by Walton and Woolcock in 1960 (70). They suspended a water droplet on a glass capillary in an upward flowing aerosol of methylene blue $(2.5\mu$ and 5.0μ). They measured collection efficiencies at air velocities of 670, 390, and 200 cm./sec. Their results, which are generally considered to be the best available, are shown in Figure 1.3. As may be seen, they correlate with the theoretical line which lies 5 - 10% above the best fit curve through their experimental data.

Goldshmid and Calvert (25) studied the impaction of polystyrene (0.8 - 2.85 μ) and sulphur (0.6 - 2.94 μ) aerosols on a series of different collecting drops. Their data were gathered at low K and correlate with neither the theory nor the experimental results of Walton and Woolcock.

Rosinski et al (62) conducted a set of experiments to measure the collection efficiency of zinc sulphide particles (1.14µ) by condensing and evaporating water droplets. They took readings at a single, very low, impaction number and obtained results which varied considerably according to the droplet growth rate.

Starr and Mason (68) studied the collection of pollens by falling water drops. They used three types of spores $(4.5\mu,\ 5.2\mu,\ and\ 12.8\mu)$ and measured values of E as a function of the drop diameter. They found a maximum in collection

Figure 1.3

EXPERIMENTAL DATA OF WALTON AND WOOLCOCK (70)

Impaction Parameter

efficiency for collector diameters of 0.4 mm. Their data may be reexpressed in terms of the impaction parameter and from this it is evident that the results cover only K values between 0.2 and 0.4 and between 1.5 and 6.0. However, their results correlate well with those of Walton and Woolcock and seem to be the second best available.

In a study of the trajectories of individual glass beads in the vicinity of a 1 mm. glass sphere, Berg et al (6) found 4 values for collision efficiency, all of which agree well with the potential flow theory. However, their results only cover a small range of impaction parameter.

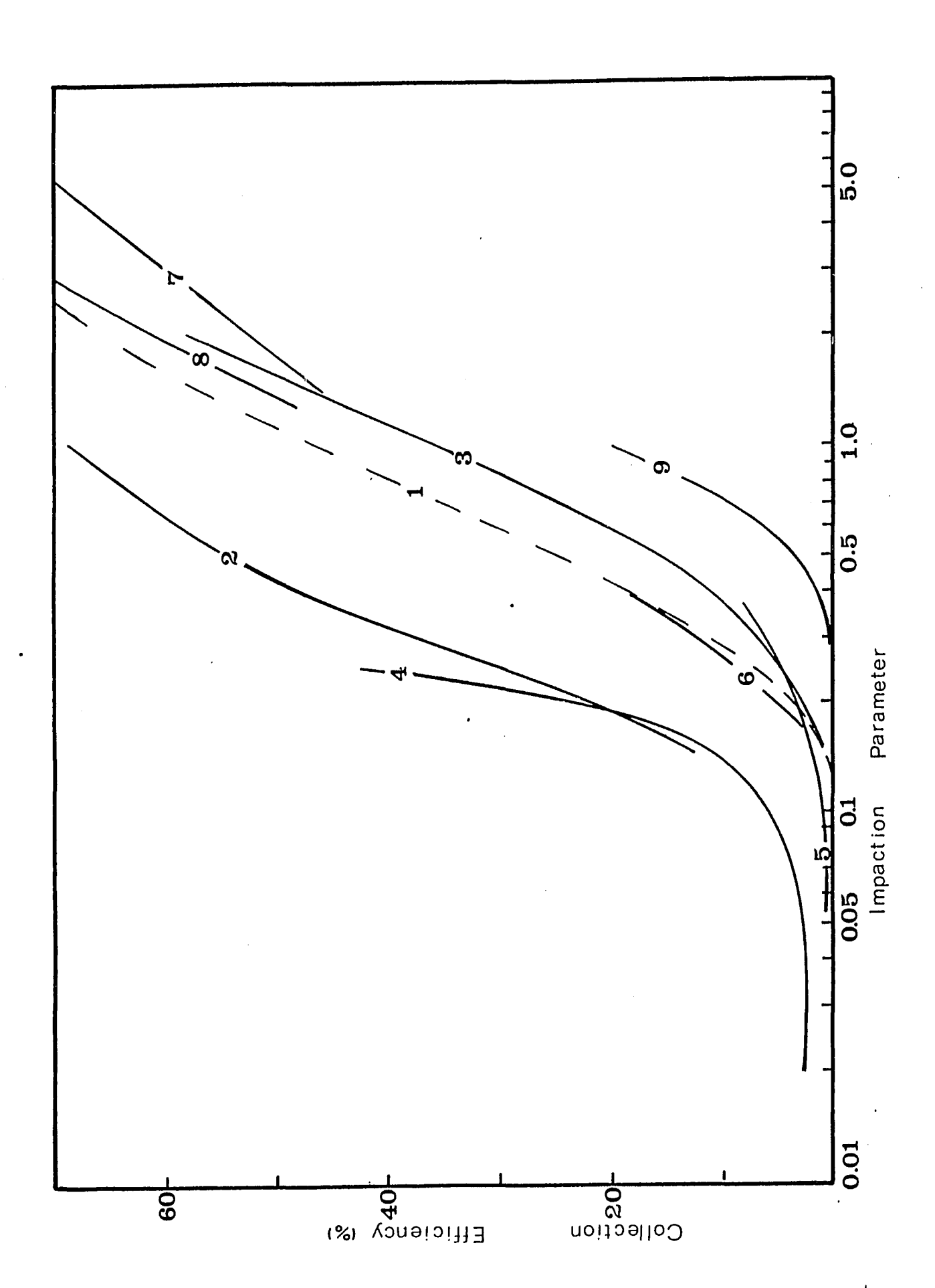
In a recent series of papers, Hampl et al (28, 29, 36) reported measurements for the collection of submicron aerosols by small falling droplets. They found a correlation in their results between the Peclet number and the collision efficiency, suggesting that collection is not by inertial means for these small aerosols. However, in a study of the collection efficiencies of small drops supported by an airstream in the U.C.L.A. wind tunnel, Beard has found results for an indium acetylacetonate aerosol (0.8µ) which agree with his computations for the inertial mechanism at low K (4).

Wherever possible, the experimental results found in the literature have been converted to common units of E'and K and plotted on a single graph to facilitate comparison. Figure 1.4 gives this comparison. Results of all workers appear to show

Figure 1.4

COMPARISON OF PREVIOUS EXPERIMENTAL WORK

- 1. Theoretical curve
- 2. Ranz and Wong (58)
- 3. Walton and Woolcock (70)
- 4. Goldshmid and Calvert (25) (polystyrene)
- 5. Goldshmid and Calvert (25) (sulphur)
- 6. Starr and Mason (68) (lycoperdon and black rust)
- 7. Starr and Mason (68) (paper mulberry)
- 8. Berg et al (6)
- 9. Montagna (49)



approximately the same trend of increasing E with increasing K. However, there is a wide divergence between the various pieces of work. The plot indicates that the results of only three workers agree well with the theoretical curves but that only one of these sets of results covers the entire range 0.1 < K < 3.0. Thus there is still a need for more experimental data on the collection efficiency of hydrophilic particles. Some such further results are presented in this work using the method described in the following chapter.

Chapter 2

EXPERIMENTAL EQUIPMENT AND PROCEDURE

When the literature was reviewed to decide on the method to use for the measurement of collection efficiency, two factors became clear. First, the data for most experiments of this sort are very scattered. Thus meaningful results may only be obtained if large numbers of readings are taken. The method used had therefore to be efficient and simple. Secondly, the majority of workers use one of two general types of analytical method to establish the quantity of aerosol collected by the drop. particles had to be either solid and insoluble so that they could be physically counted, or soluble so that they could be assayed by a procedure linked to the physico-chemical properties of the specific aerosol used. In the latter case, a number of drops are normally collected and analysed by such procedures as titration, conductance measurements, and spectrophotometric This reliance on the physico-chemical properties of analysis. the aerosol did not suit the aim of this work in dealing with a range of aerosols. Consequently, it was decided to develop a new method of measuring the number of particles collected by the drop, designed to be independent of the type of aerosol used.

2.1 Principle of Operation

One further point arose from the preliminary literature survey. All workers in this field expose the drops to the aerosol in one of two ways, either by allowing the drop to fall through a static cloud of aerosol or by supporting the drop and moving the aerosol past it. Both methods have certain disadvantages. For the stationary drop, the effect of the support on the fluid flow in the wake is not known. For the free falling drop, a large apparatus is required to ensure that the droplets are travelling at their terminal velocity. Moreover, the drops in this case tend to sweep the same area of the static aerosol cloud so that the concentration in this region is not necessarily the same for each drop. It was decided to use the static drop method which seems to give better control over the operating variables and to circumvent the limitation on the range of K caused by the terminal velocity in the free falling drop system.

As noted above, the greatest experimental difficulty is encountered in the measurement of the quantity of aerosol collected by the drop. A single droplet of 0.15 cm. diameter sweeps out an area of 1.77 x 10⁻² cm.². At a velocity of 400 cm./sec., in an aerosol of concentration 50 particles/cc., it therefore sweeps 353 particles/sec. If the drop has a collection efficiency as high as 60% and the particles are of 20µ diameter and unit density, this means that the droplet

picks up only 5.33 x 10⁻⁵ gms. of material per minute. gravimetric analysis is not feasible. However, this small weight of material is equivalent to 12,723 particles. clearly advantageous to avoid the use of analytical methods involving the assay of the concentration of aerosol material in the drop and to rely instead on counting methods. One of the most convenient aerosol counting methods available is the forward light scattering particle counter which counts automatically the number of particles in an air sample. present work, such a counter was used to analyse continuously the aerosol collected by drops which were supported on a stainless steel hypodermic needle. The analysis was performed by isokinetically sampling the aerosol from the area immediately behind the droplet. The difference between the particle counts without the droplet and with the droplet was then taken to be the number of particles collected per unit time. only limitation on the type of aerosol used was that it should not corrode the particle counter. The experimental equipment is discussed in greater detail in the next section.

2.2 Experimental Equipment

The aerosol was made using a spinning disc aerosol generator and conducted to a working section where it was formed into a laminar free jet. Its velocity was measured before it was exposed to the droplet which was suspended from the support and sampling probe assembly. The portion of the aerosol immediately behind the drop was then passed through a particle counter. The apparatus is shown schematically in Figure 2.1, and a photograph is given in Plate 1. All electrical power was supplied from a regulated constant voltage source. The experimental equipment has three main sections, the aerosol generator, the droplet support and sampling probe assembly, and the particle counter.

2.2.1 the aerosol generator

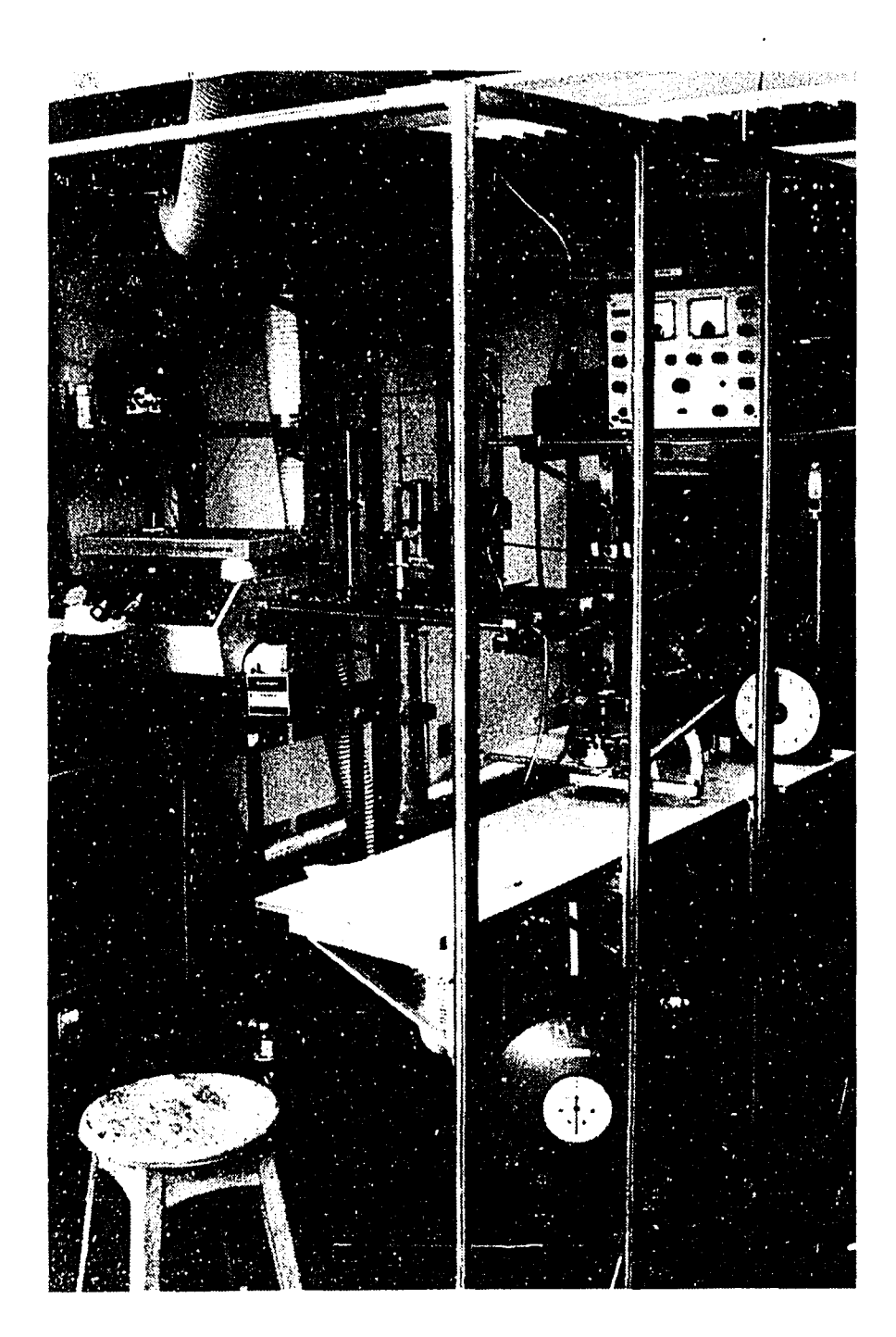
The aerosol was generated using a spinning disc apparatus (Model 8330, Environmental Research Corporation, St. Paul, Minnesota). The generator is shown schematically in Figure 2.2. Its principle of operation is simple. The aerosol material, in a solution or slurry of volatile solvent, is fed to the centre of a smooth, stainless steel disc which is rotating at high speed (60,000 r.p.m.). The liquid spreads on the disc surface and is thrown to the edge where it forms long ligaments of

SCHEMATIC DIAGRAM OF APPARATUS

- 1. Working section
- 2. Droplet holder and sampling probe assembly
- 3. Syringe pump
- 4. Timer
- 5. Hot wire anemometer
- 6. Digital voltmeter
- 7. Contoured nozzle
- 8. Conical section
- 9. Flow divider
- 10. Auxiliary fan for flow divider
- 11. Aerosol generator
- 12. Peristaltic pump
- 13. Stirred holding vessel for aerosol feed
- 14. Camera
- 15. Auxiliary fan
- 16. Calibrated differential pressure type flowmeter
- 17. Air pump
- 18. Particle counter optics
- 19. Particle counter electronics

Plate 1

EXPERIMENTAL APPARATUS

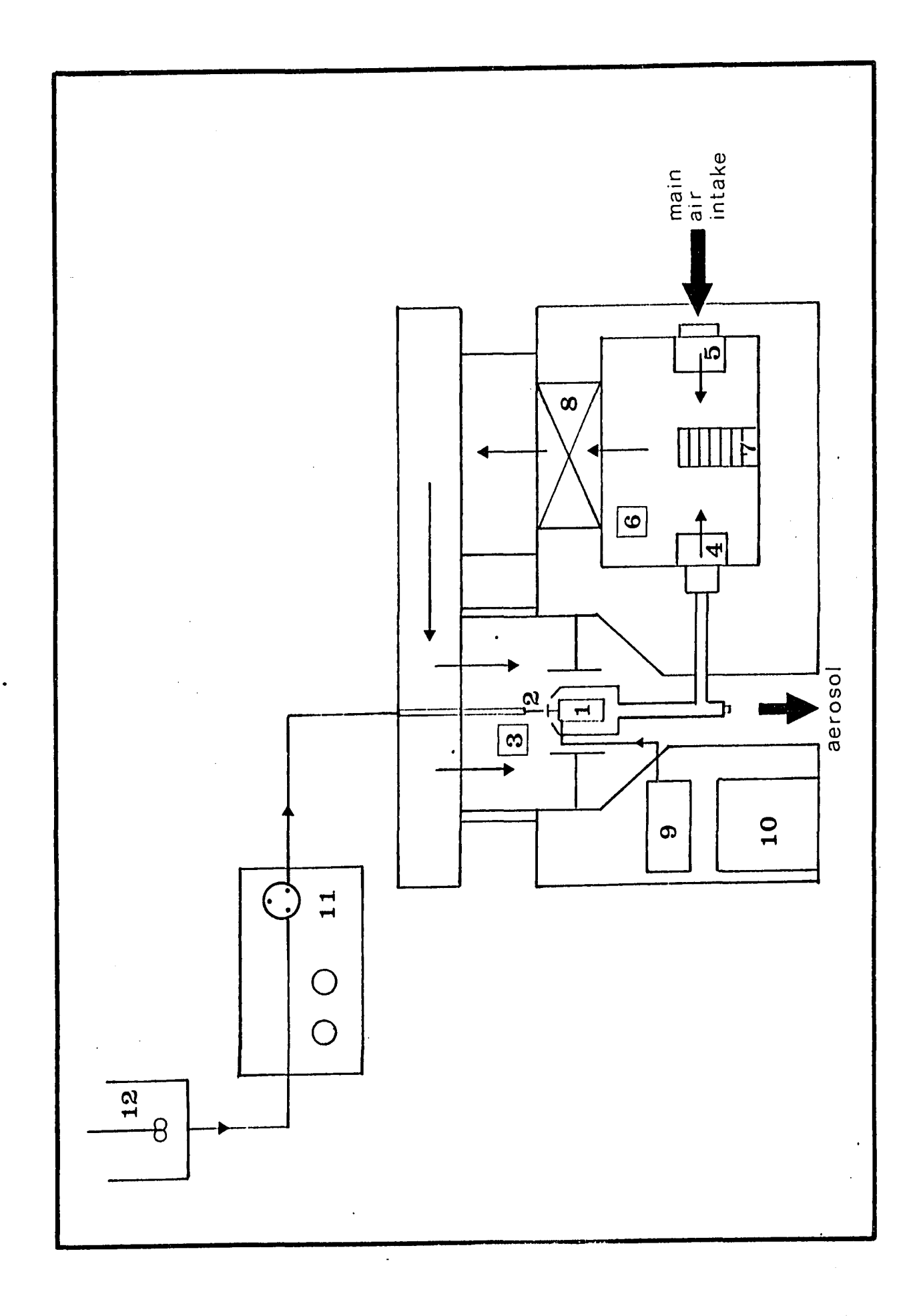


.

SCHEMATIC DIAGRAM OF THE AEROSOL GENERATOR

direction of air flow

- 1. Spinning disc motor
- 2. Feed needle
- 3. Aerosol classifier
- 4. Satellite blower
- 5. Main air blower
- 6. Mixing chamber
- 7. Heater
- 8. Filter
- 9. Small air compressor supply to protect disc motor bearing
- 10. Power supply
- 11. Peristaltic pump
- 12. Feed vessel



fluid (46). These ligaments then break up into two types of particles, the primary particles which are 30 to 50µ in diameter and the secondary 'satellite' particles which are very much smaller. These secondary drops are removed by an air stream which is created by a satellite blower and pass vertically down through an annular gap around the disc. mary drops have sufficient momentum to carry them over this annulus and are thus transported away in the main flow stream. The solvent from the primary droplets evaporates very quickly leaving the non volatile aerosol material as particles. process is aided by a heating unit built into the generator. The diameter of the final particle is thus governed by the size of the primary droplet and the concentration of the aerosol material in the original feed. The primary droplet diameter d_{p} is related to the angular disc speed ω_{d} , the disc diameter $D_{_{\rm S}},$ the fluid surface tension $\sigma,$ and the fluid density $\rho_{_{\rm S}},$ by the expression:

$$d_{p} = k_{1} \left(\frac{\sigma}{\rho_{s} \omega_{d} D_{s}} \right)^{1/2}$$
(2.1)

The constant k_1 is theoretically equal to $(12)^{1/2}$ but is normally found to vary from 2 to 7 depending on the disc speed and on the liquid used (17).

The aerosol material was fed to the disc by a precisely controlled peristaltic pump (The Peri-Pump Company, Trenton,

Ontario) at flow rates of between 4 and 10 cc/min. The flow through this unit was found to be constant during the course of a run, but slightly pulsed at the lower rates. The main blower on the generator had a minimum capacity of 5 to 10 c.f.m. which was in excess of the requirements for these experiments. Provision was therefore made to draw off the surplus aerosol using an auxiliary fan controlled by a variable transformer. The stream was divided at a plexiglass section in the line, the auxiliary portion being taken off through a downwardly inclined arm so that the number of particles carried away in the excess air would be minimised.

Three aerosols were used for the hydrophilic experiments, ferrous sulphate, methylene blue, and water. The ferrous sulphate aerosol was obtained using a 20% aqueous solution with 10% ethanol added. This ethanol lowered the surface tension of the feed so that the disc of the generator was well wetted. The methylene blue aerosol was made from a 1.3% solution of the dye in 50% ethanol. The water aerosol was formed from distilled water with 10% ethanol added since pure water does not wet the disc well. The water aerosol proved to be the most difficult one to work with. The small droplets evaporate very quickly so that the air stream had to be saturated in order to slow this process down. The experiments with this aerosol were performed on a very humid day and steam was injected into the air intake of the generator. The resultant

aerosol proved to be more disperse and less stable than the others used.

2.2.2 the droplet support and sampling probe assembly

After the flow divider, the aerosol was conducted, through a conical section to reduce deposition, into the base of a $1\frac{3}{4}$ " diameter aluminum cylinder. This cylinder contained a contoured nozzle $\frac{3}{4}$ " in diameter which was used to produce a free laminar jet in which the drop was suspended. Turbulence in this jet was damped out by means of a honeycomb of parallel-sided, thinwalled plastic cylinders upstream of the contours to act as flow straighteners. A cross-sectional view of the nozzle and of the whole assembly is shown in Figure 2.3, and a photograph is given in Plate 2.

The sampling probe was made from thin-walled stainless steel tubing. Its leading edge was tapered to a sharp, smooth point at an angle of 30° to reduce turbulence. Furthermore, the first $\frac{3}{4}$ " of the probe was turned down to a wall thickness of 8 thousandths of an inch so that the fluid streamlines would be disturbed as little as possible in the sampling area. Two probe sizes were used in the experiments, 0.135" I.D. and 0.103" I.D. The droplet was supported on either 28 or 30 gauge stainless steel hypodermic needle tubing coaxial with the sampling probe. The droplet support needle was bent through

CROSS-SECTIONAL VIEW OF THE DROPLET HOLDER AND SAMPLING PROBE ASSEMBLY

- 1. Sampling probe
- 2. Probe clamp
- 3. Distilled water feed from syringe pump
- 4. Droplet support needle
- 5. Retractable hot wire anemometer probe
- 6. Protective plexiglass housing for anemometer probe
- .7. Contoured nozzle
- 8. Flow straighteners

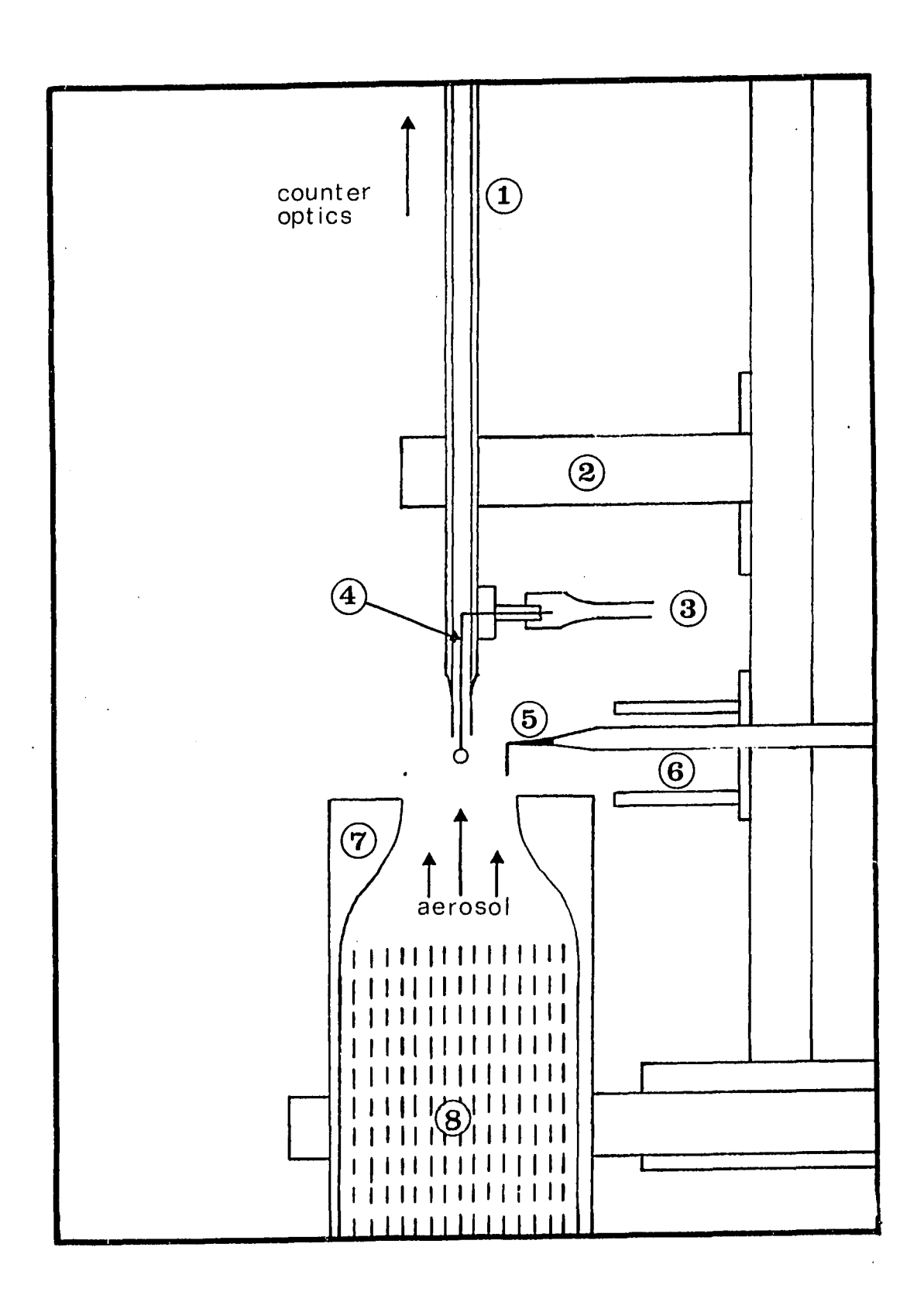
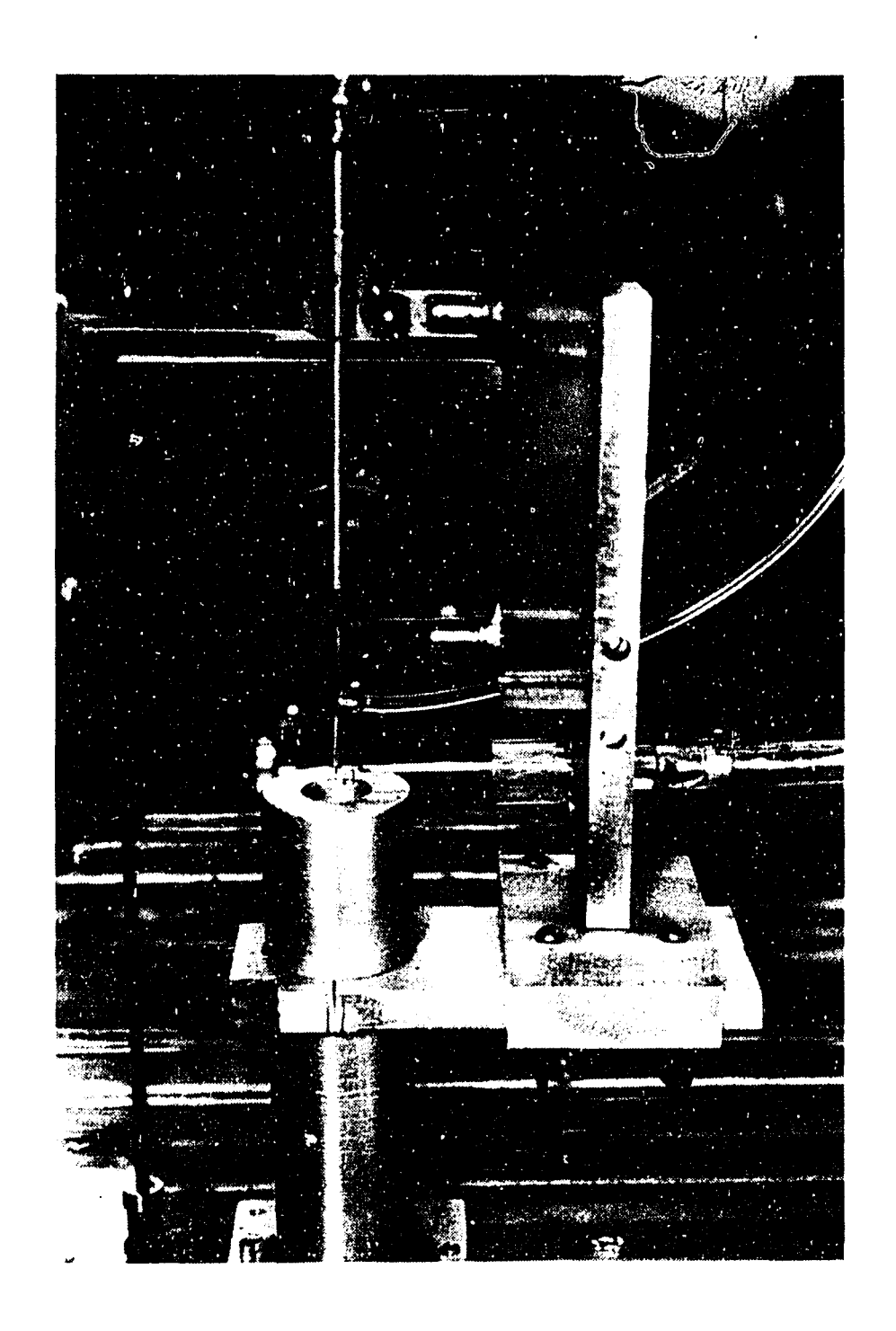


Plate 2

DROPLET HOLDER AND SAMPLING PROBE ASSEMBLY



:

a right angle and entered the side of the probe 1" from the leading edge. It was earthed so as to keep electrical effects to a minimum.

Distilled water to form the droplets was fed to the needle from a continuous syringe pump operated by an electric timer accurate to 0.25 seconds. The support needle was coated with varnish to prevent the drop climbing up the needle. The sampling probe was fixed by quick release clamps to a rigid, vertical, aluminum support which could be moved horizontally by sliding it along a platform attached to the nozzle cylinder. The droplet and probe could thus be positioned in the centre of the jet.

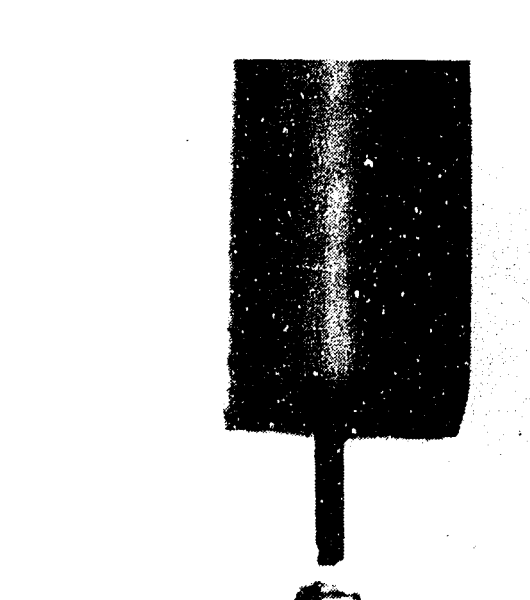
The whole assembly was enclosed in an airtight plexiglass working section. A variable speed fan took the waste aerosol from the top of this section and discarded it to the fume hood. Provision was made to photograph each droplet during the experiment using a 35 mm. Nikon F camera with bellows and a 105 mm. lens. This arrangement gave a subject to image magnification of approximately 1.7. The drop diameter could be measured from these photographs using the droplet support as a scale. A typical drop is shown in Plate 3.

The last feature of the sampling probe assembly was a retractable arm on which the hot wire anemometer probe was mounted for measurement of the velocity and the turbulence of the gas stream. The arm could be moved in order to take

Plate 3

SUSPENDED WATER DROP





:

-

.

readings at the exact position of the drop and then withdrawn into a plexiglass housing when the aerosol was being generated so that the probe would not be contaminated by the aerosol material.

The anemometer (DISA, Herlev, Denmark) works by making the small length of heated wire between the tips of the probe into one resistance in a Wheatstone bridge type circuit. The machine measures the amount of power necessary to keep the wire at a constant temperature and gives as an output a D.C. voltage which is related to the air velocity. This output voltage was measured by a digital voltmeter (DANA, Irvine, California) which could be read to 0.1 mV. The anenometer could also be used to measure the turbulence in the jet. It gave an A.C. voltage from which the percentage turbulence could be found by:

% turbulence = 100 .
$$V_{RMS}$$
 . $\frac{4V}{V^2 - V_O^2}$

where V is the D.C. voltage reading at a particular velocity, V_{RMS} is the A.C. voltage reading, and V_{O} is the D.C. voltage reading at zero gas velocity.

The hot wire probes used in this work were all of the right angle type, that is, the wire supports are bent through 90° from the main probe. The calibration necessary was performed by passing air through a wet test meter (Model AL20,

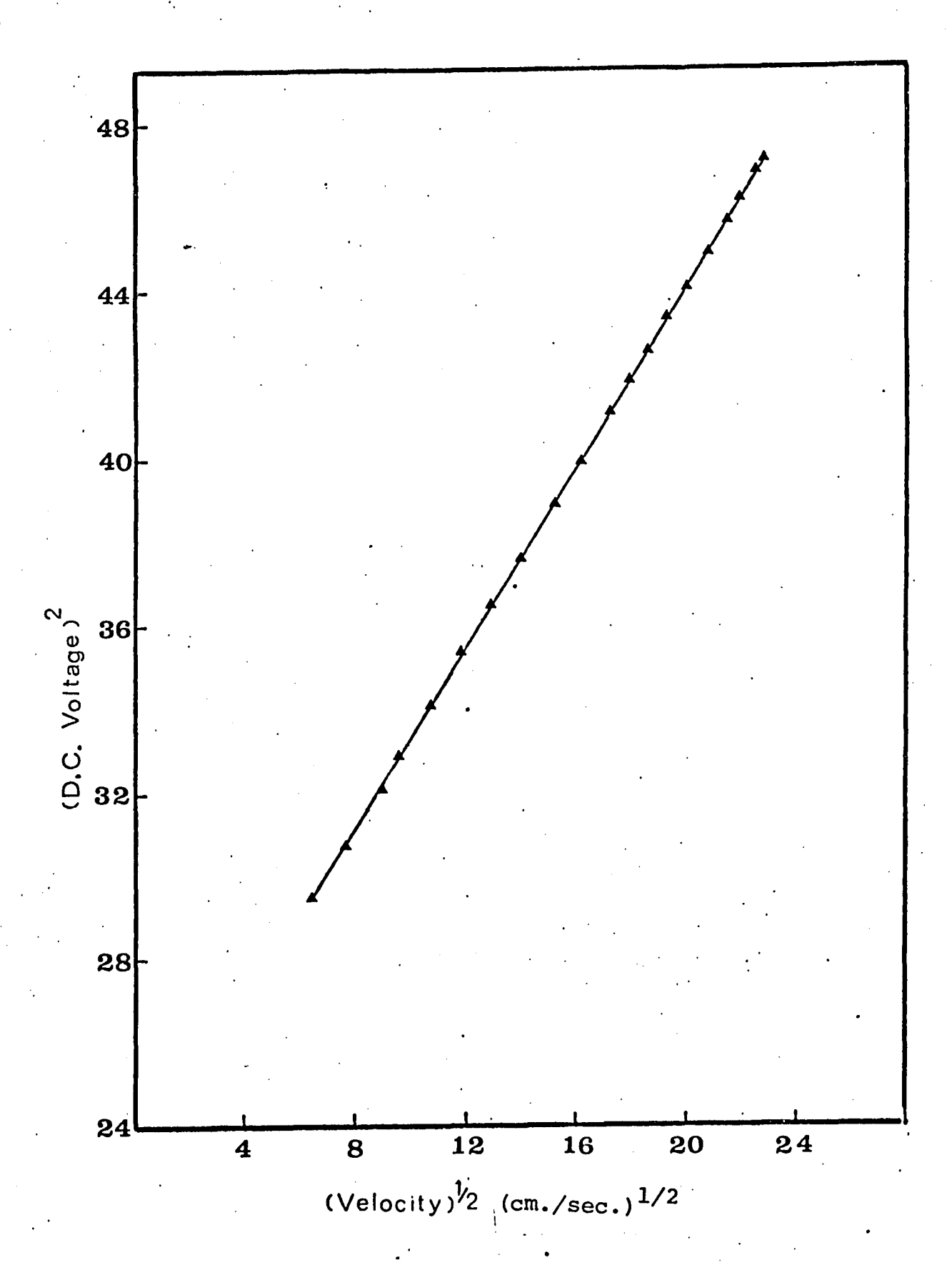
American Meter Company) and through the contoured nozzle. The flow rate could thus be measured using a stopwatch. The hot wire probe to be calibrated was placed in the mouth of the nozzle and the velocity was calculated from the known diameter of the jet and the volumetric flow rate. Results for a typical calibration are shown in Figure 2.4 where the squares of the voltage readings are plotted against the square roots of the air velocity. As may be seen, the result is a straight line, so that velocities intermediate to the measured points could be determined by linear interpolation. Another calibration had to be made each time one of these very fragile probes was broken.

The jet produced a flat velocity profile across its centre region with a very low level of turbulence. A typical traverse across the jet is shown in Figure 2.5. The velocity profile in the jet is clearly flat for 0.5" which is at least 5 times the diameter of the largest drop studied. The turbulence in the jet is confined to its outer region. The droplet holder assembly was placed directly below the optics of the particle counter to minimise deposition in the sampling line.

2.2.3 the particle counter

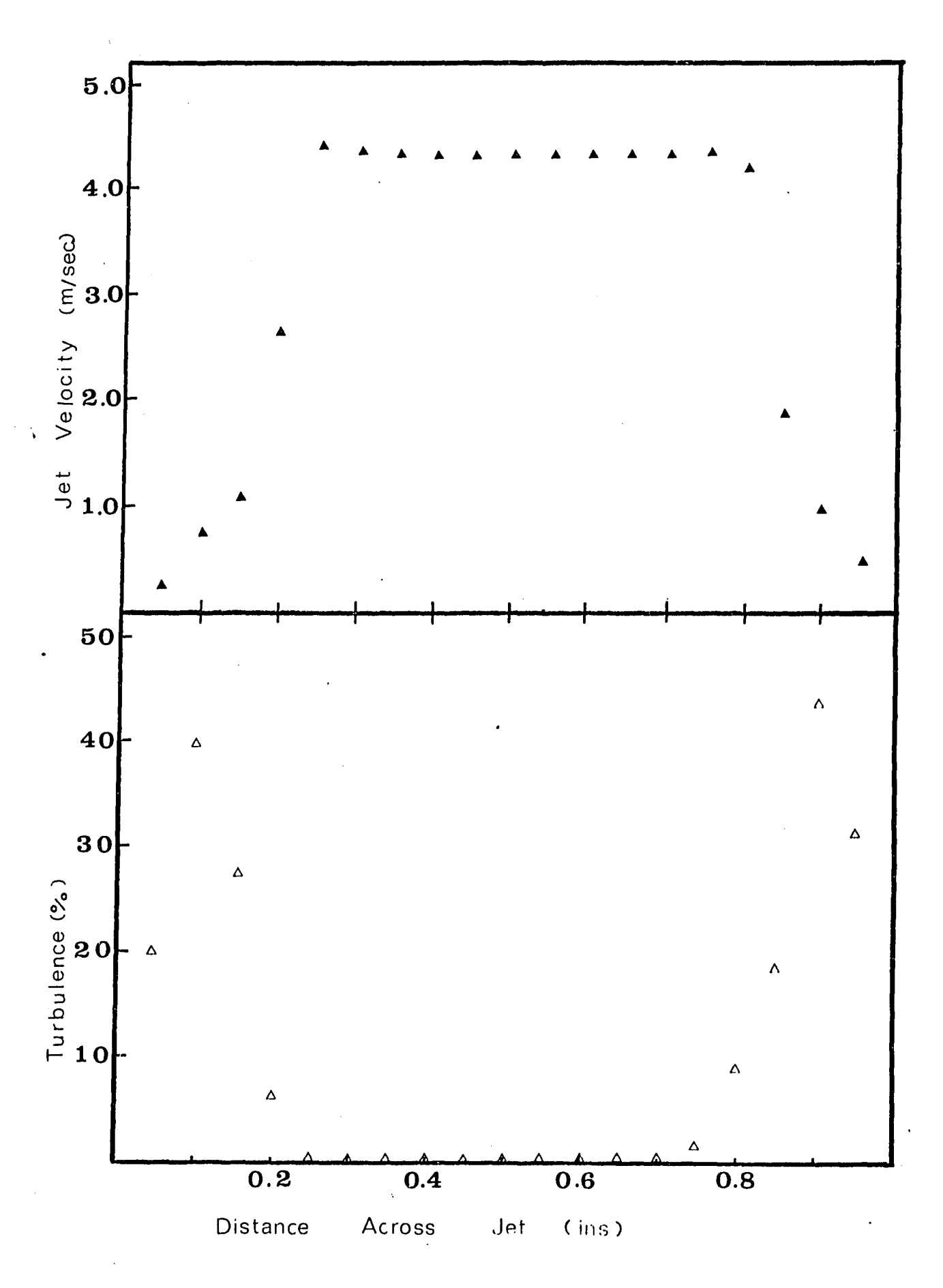
The counter was a forward light scattering particle counter (Model 200A, Royco Ltd., Menlo Park, California).

CALIBRATION CURVE FOR HOT WIRE ANEMOMETER



VELOCITY AND TURBULENCE PROFILES

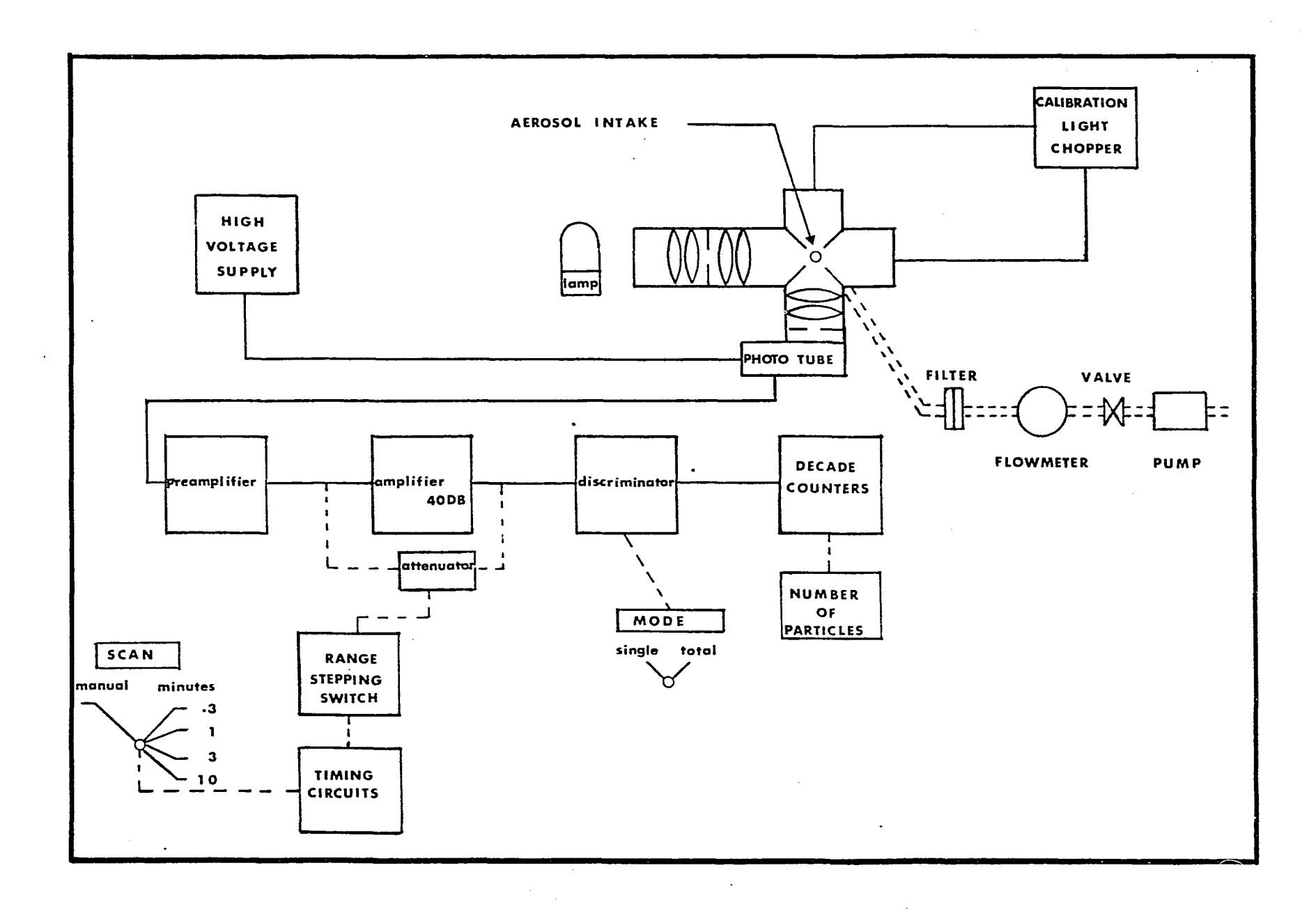
IN THE JET



This machine can be used to count either particles in any one of 15 size ranges from 0.3 µ to 8 µ or all particles greater than a specific size range. It consists of two main units, one of which houses the optics, and the other the electronics. The aerosol sample is passed through an intense beam of light in the optical system. In this beam, the particles scatter light onto a photomultiplier tube which produces a current pulse for each particle. The current pulse is converted to a voltage pulse by a preamplifier and the resulting signal is passed to the electronics section of the counter. Here the voltage pulse is first amplified by a 40 dB. amplifier and the signal then goes through an attenuation circuit to the discriminator. The pulses are sized and, depending upon the counting mode, are ignored or registered on the decade counters. The machine has built-in timing circuits so that samples can be taken for 0.3, 1.0, 3.0, and 10.0 minutes. Provision is made for the counter to be calibrated in the field using pulses of known magnitude created by a light chopper in the optical unit. A block diagram of the counter is shown in Figure 2.6.

A drawback in using this counter is that it is calibrated to operate at a flow rate of only 300 cc/min. As the particle passes through the illuminated section of the optics, the magnitude of the pulse it creates depends not only on its diameter but also on its velocity. Thus as soon as the sample flow rate is changed, there is an error introduced in the

SCHEMATIC DIAGRAM OF THE PARTICLE COUNTER



particle sizing. An increased velocity makes the particles appear smaller. Unfortunately, the requirement for isokinetic sampling from behind the droplet meant that sample flow rates of up to 1200 cc/min. were necessary. During these experiments therefore, the counter was used to obtain only the number and not the size of the particles in the sampled aerosol. It was used exclusively in the total count mode so that every particle which passed through was registered. All of the aerosols used were sufficiently large that their pulses could not be ignored by the discriminator at the higher flow rates.

The sample was drawn through the optics by an air pump (Model 1094, Fisher Scientific) and its flow rate was measured using a calibrated orifice. The pressure drop across this orifice was obtained from an inclined micromanometer (Lambrecht Ltd., Gottingen) which had methanol as the fluid.

The particle size was determined from a sample of the aerosol collected on a 0.8µ membrane Millipore filter. Immediately after the sample was taken it was photographed, using polaroid film, under a microscope (Reichert, Vienna) at 400 times magnification. These photographs were later analysed by comparison with a photograph of a stage micrometer taken at the same magnification. The measurements from the photographs were made on a vertical travelling stage microscope. For the liquid aerosols, the sample was taken on a teflon filter and the same procedure followed. The sizes obtained were corrected

for the deformation of the particle on the filter surface by the method given in Chapter 3. All the particle sizes used were the mean from measurements of 50 particles.

2.3 Experimental Procedure

A typical run was as follows. The aerosol solution was made while the apparatus was warming up. The tip of the feed needle to the spinning disc was adjusted, using a feeler gauge, to be 0.029" from the disc surface, and exactly centred with The value of the anemometer reading at zero respect to it. gas velocity was checked and then the main and satellite air blowers in the generator as well as the two auxiliary blowers were adjusted to obtain the required velocity. through the counter was next regulated to ensure that the sampling was isokinetic. This was checked by traversing across the jet with the hot wire probe. The retractable arm was withdrawn and the system was left for 15 minutes to ensure that the background count of particles was negligible. During this time, the particle counter was field calibrated. motor in the generator was then started and the peristaltic pump switched on. The system was left for a further 5 - 10 minutes so that the aerosol concentration could settle down to a steady state as shown by the readings from the particle Three particle counts were then taken through the sampling probe, each for 0.3 minutes. Immediately after these counts, a droplet was formed at the tip of the needle and three more readings were taken. The droplet was photographed, then discarded, and further readings were taken. The number of particles collected by the droplet was taken to be the difference between the averages of the readings with and without the droplet in position. This process was repeated for the desired number of droplets. Each drop was suspended for approximately two minutes during which time there was no discernable change in diameter. The aerosol was then sampled onto a filter and photographed.

The whole procedure was repeated at various velocities and particle diameters to obtain the required range of impaction parameter. The method used for data reduction and the experimental results are discussed in the following chapter.

Chapter 3

EXPERIMENTAL RESULTS FOR HYDROPHILIC PARTICLES

3.1 Data Reduction

The particles were sized by measuring the photographs of the aerosol on a vertical travelling stage microscope. Measurement could be performed to an accuracy of ± 0.3 thousandths of an inch. An average of 50 readings were taken for each aerosol, and the mean and standard deviation in diameter were calculated. The relative standard deviation of all the aerosols was in the range 7 - 10% except that of water which was 12.3%. The mean particle size was used in all calculations.

When the liquid aerosols were deposited on the teflon filter and sized, the diameter obtained was not the true diameter of the original particle owing to the deformation of the liquid as it lay on the surface. When a volume of liquid is deposited on a surface which it does not wet completely, it spreads out to a certain degree depending on the angle of contact which it makes with that surface. Provided that it is not so large that gravitational effects are significant, the volume and hence the true diameter may be calculated. The geometry for contact angles less than 90° and greater than 90° is shown in Figures 3.1a and 3.1b respectively. It may be seen that:

GEOMETRY OF DROP ON FILTER SURFACE

$$L = a_f Cosec 0 (3.1)$$

$$p = L(1 - \cos \theta) \tag{3.2}$$

where L is the diameter of the sphere of which the drop forms a segment, a_f is the apparent radius of the wetted perimeter of the filter, and b is the height of the spherical cap. The volume V_p of the spherical cap is given by:

$$v_{p} = \pi (Lb^{2} - \frac{b^{3}}{3})$$
 (3.3)

Thus the volume of the liquid on the filter may be expressed in terms of a_f and the angle of contact as:

$$v_{p} = \frac{\pi a_{f}^{3}}{3 \sin^{3} \theta} \left(2 - \cos \theta (2 + \sin^{2} \theta) \right)$$
 (3.4)

The ratio of the true diameter to the apparent diameter is therefore given by:

$$\frac{a}{a_f} = \left(\frac{2 - \cos(2 + \sin^2 \theta)}{4 \sin^3 \theta}\right)$$
 (3.5)

This is the same result as that obtained by Bexon and Ogden (7).

For contact angles of less than 90° , the apparent diameter is 2 $a_{\rm f}$. For contact angles greater than 90° , the apparent diameter of the drop is larger than the diameter of the wetted perimeter and is equivalent to 2L (See Figure 3.1b).

Thus in this situation, a_f may be determined from Equation (3.1) and the true diameter then obtained from Equation (3.3).

The contact angle was measured by dispensing very small drops of the liquid onto the filter and photographing them with a 35 mm. camera by means of a bellows attachment. The contact angle was then measured from the photographs at magnifications of approximately 50 times on a vertical travelling stage microscope which has a vernier scale readable to ± 2 minutes. The results were very reproducible. For water on the teflon filter, the contact angle was found to be 107°36'. This is in good agreement with the value of 108° reported by Fox and Zisman (22).

The densities of the liquid aerosol materials were determined by standard procedures in a pycnometer bottle. The mean of four readings was used as the particle density. The density of the solid particles was determined by similar means but the results were not so consistent. Aerosol material collected from inside the apparatus after a long run was used for the measurements. It was placed in the pycnometer covered with benzene, and subjected to vacuum from a water pump for 1 minute. The density was then determined in the standard way. Since the results varied, the mean of at least 12 readings was taken.

The collection efficiency is defined as the ratio of the number of particles collected to the number of particles in the swept volume. If the sampling rate through the counter is $V_{\rm C}$ cc/sec., the jet velocity U_{∞} cm./sec., and the drop

diameter D cms., then the number of particles N swept by the drop during an 18 second counting period is:

$$N = \frac{\pi D^2}{4} \cdot U_{\infty} \cdot \frac{N_p}{V_c}$$
 (3.6)

where N_p is the number count for 18 seconds. If the number of particles collected by the drop during that time is N_c , then E is given by:

$$E = \frac{N_{C}}{N} = \frac{N_{C}}{N_{p}} \cdot \frac{4V_{C}}{\pi D^{2}U_{m}}$$
 (3.7)

But as the sampling is isokinetic:

$$v_{c} = \frac{\pi D_{p}^{2}}{4} \cdot U_{\infty}$$
 (3.8)

where D_{p} is the diameter of the probe.

$$\therefore E = \frac{N_C}{N_D} \cdot \frac{D_D^2}{D^2}$$
 (3.9)

This equation was used to calculate the collection efficiencies from the experimental data. Provided that the sampling is isokinetic, which can easily be checked by the anemometer, Equation (3.9) has the advantage that, apart from $N_{\rm C}$, $N_{\rm p}$, and D, it depends only on the probe diameter which is precisely measurable. Exact knowledge of the volumetric sampling rate

and of the sampling time is not therefore required.

All the raw data were analysed by means of the computer program listed in Appendix B2. The program calculated the velocity and turbulence directly from the anemometer voltage readings and the calibration data. Provision was made for two types of calibration in the program but, in practice, only the wet test meter type calibration was used. It also calculated the air density and viscosity from the readings of atmospheric pressure and temperature which were taken during the experiments. Two sorts of output variables were generated. The first applied to the conditions prevailing in a complete run and the second referred to those for a particular droplet. The first group of variables was printed at the beginning of each run and the second was printed directly underneath. output of the program is the list of experimental results given in Appendix B3.

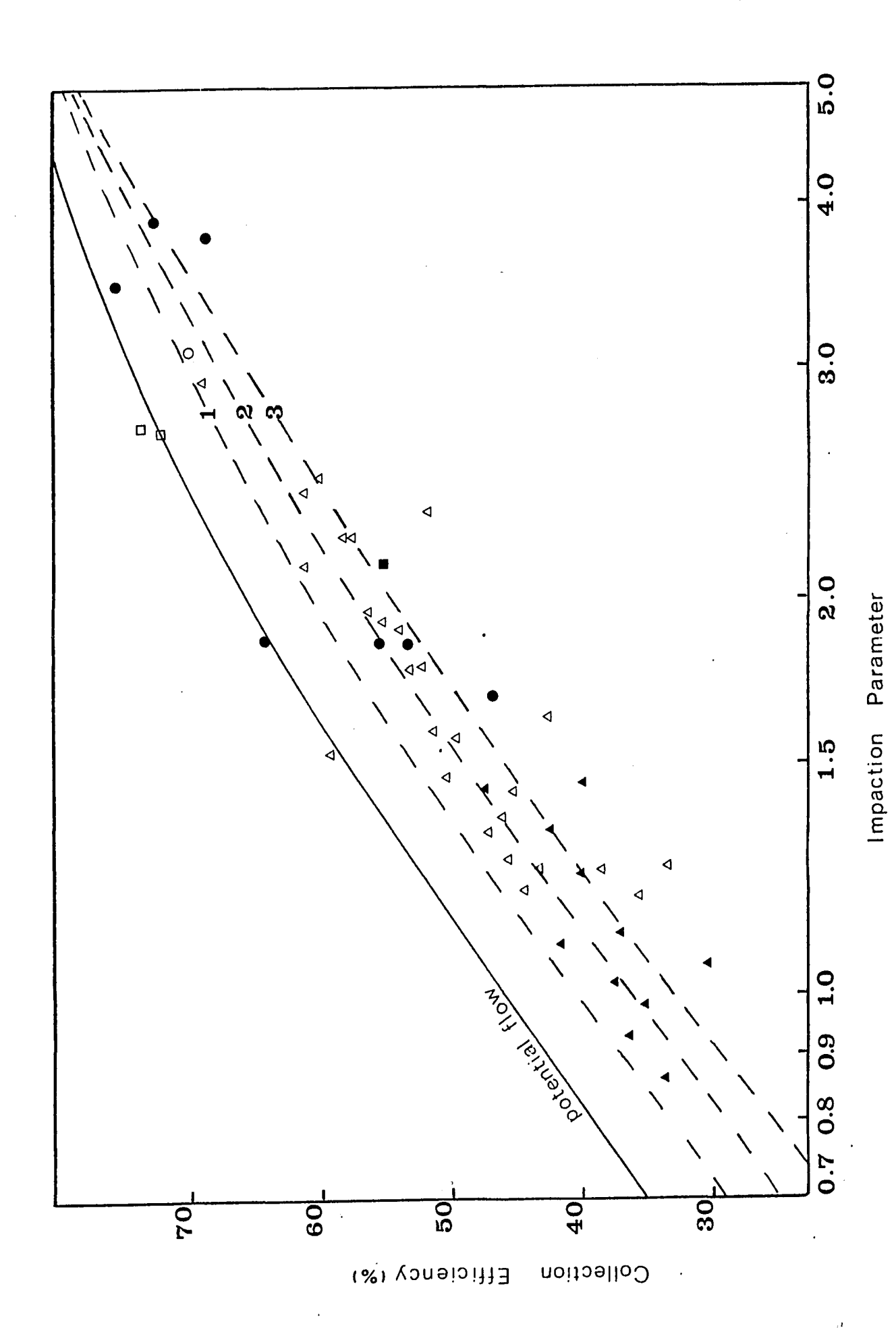
3.2 Experimental Results

The operating conditions for all of the experiments performed in this work are given in Appendix Bl. The results for each run are given in Appendix B3. The hydrophilic aerosols were ferrous sulphate (Runs 100, 101, 102 and 121), methylene blue (Runs 110, 111 and 120), and water (Run 109).

Collection efficiencies of the ferrous sulphate aerosol as a function of the impaction parameter and of the Reynolds number are given in Figure 3.2. The potential flow curve is shown for comparison purposes, and the curves at Re of 400, 200, and 100 taken from Beard and Grover's work (5) are also The average Reynolds number for all the ferrous sulphate experiments was 242. The results correlate well with the Re = 200 line. The average Reynolds number for the experiments with the methylene blue aerosols, shown in Figure 3.3, was 467. The data again correlate well with Beard and Grover's theoretical calculations. The majority of points lie just above the Re = 400 line and below the potential flow The results for the water aerosol run are given in Figure 3.4. The average Re of this run was 494. The agreement with the theoretical lines is quite good but the best fit through the data lies a little below the Re = 200 line. divergence between the experimental results and the theoretical curve may be partially due to the somewhat inferior quality of the water aerosol, but is more likely attributable to instances

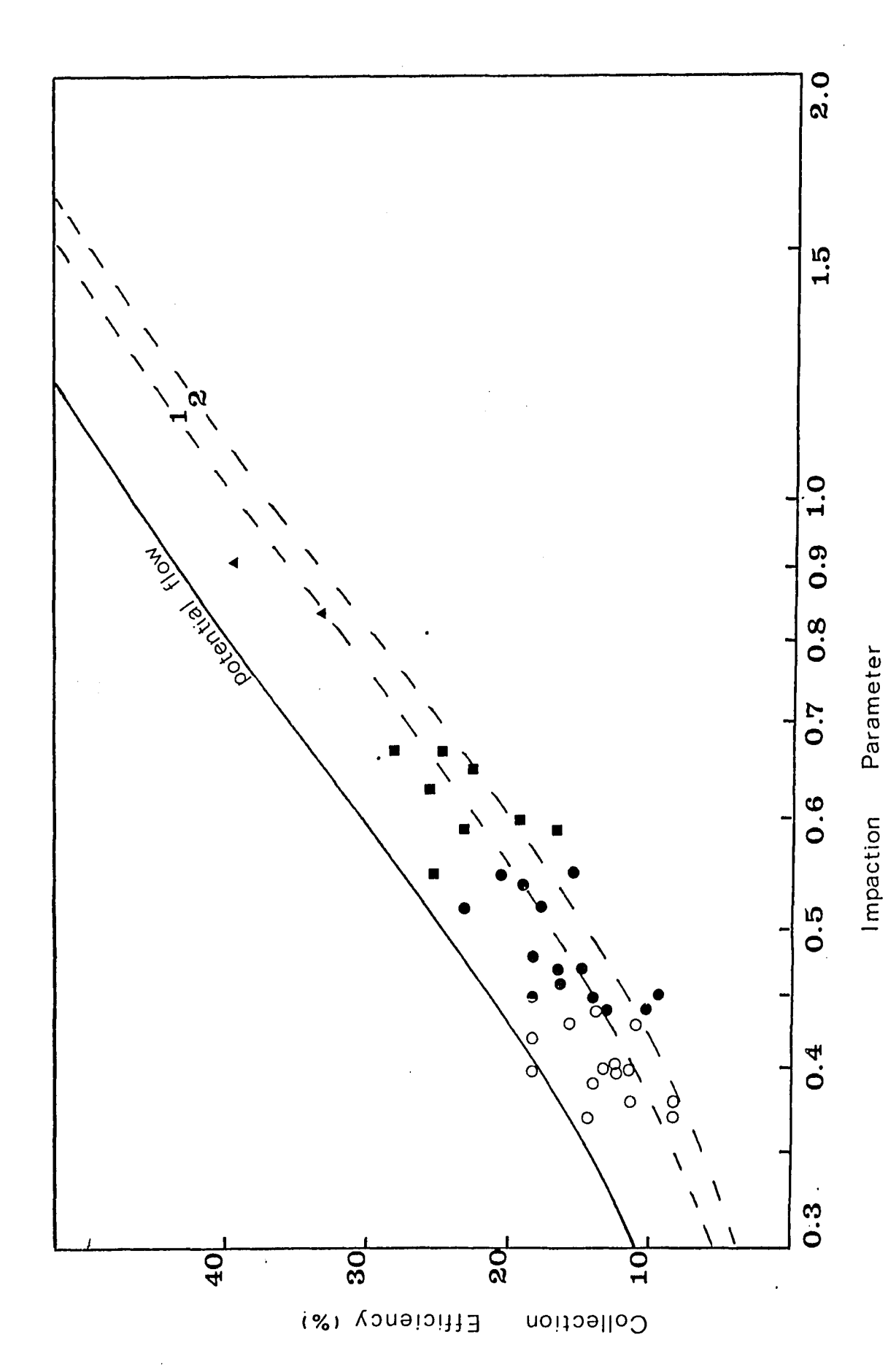
COMPARISON OF EXPERIMENTAL RESULTS WITH THEORY FERROUS SULPHATE AEROSOL

- -1- Re = 400 (Beard and Grover (5))
- -2- Re = 200 (Beard and Grover (5))
- -3- Re = 100 (Beard and Grover (5))
- \triangle 125 < Re < 200
- ▲ 200 < Re < 300
- 300 < Re < 400
- 400 < Re < 500
- O 500 < Re < 600
- □ 600 < Re



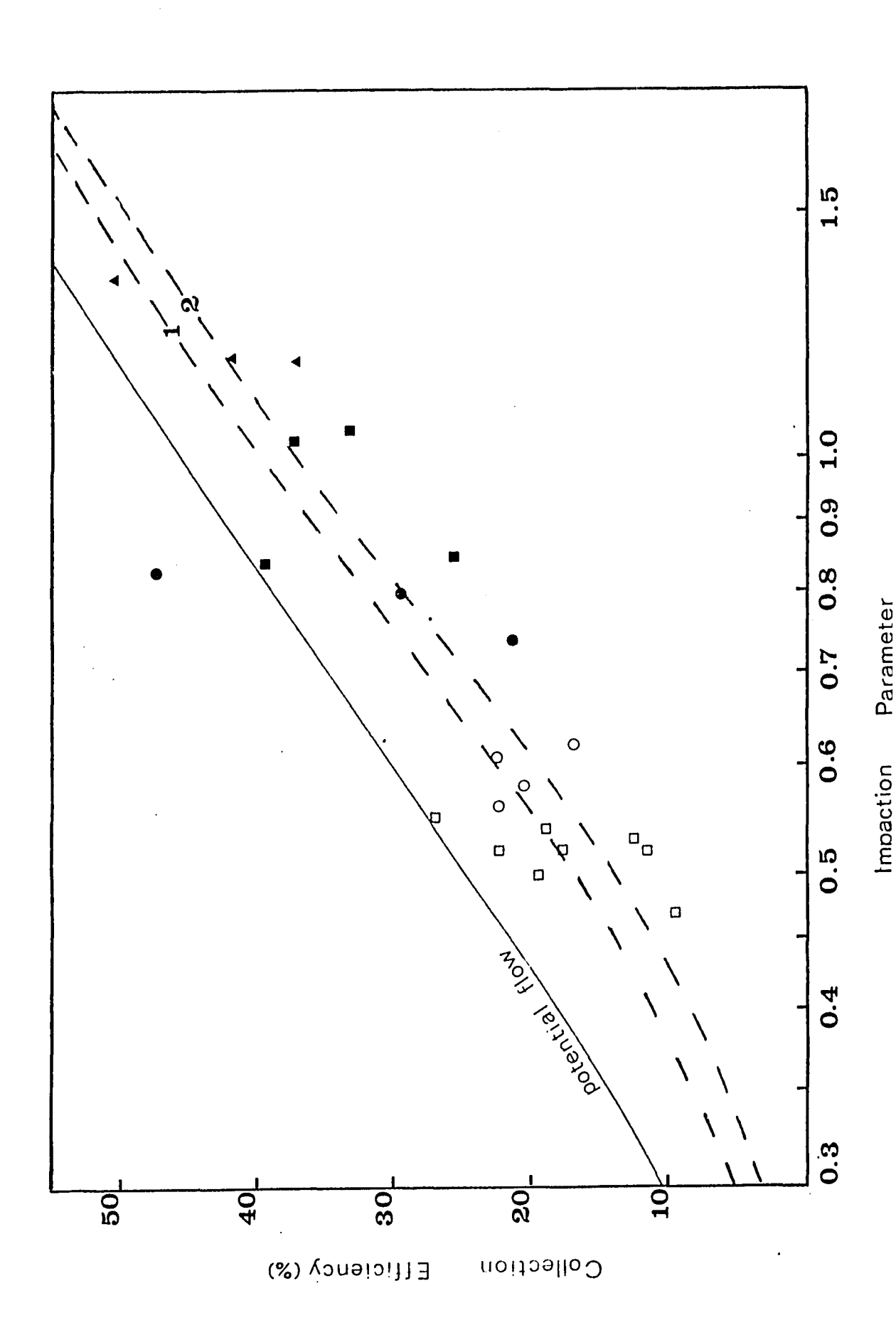
COMPARISON OF EXPERIMENTAL RESULTS WITH THEORY METHYLENE BLUE AEROSOL

- -1- Re = 400 (Beard and Grover (5))
- -2- Re = 200 (Beard and Grover (5))
- ▲ 200 < Re < 300
- 300 < Re < 400
- 400 < Re < 500
- O 500 < Re < 600



COMPARISON OF EXPERIMENTAL RESULTS WITH THEORY WATER AEROSOL

- -1- Re = 400 (Beard and Grover (5))
- -2- Re = 200 (Beard and Grover (5))
 - ▲ 200 < Re < 300
 - \blacksquare 300 < Re < 400.
 - 400 < Re < 500
 - O 500 < Re < 600
- . D 600 < Re



of non-coalescence between the water aerosol and the water droplet. The work of Whelpdale and List (72) shows that, at velocities of 4 m/sec., there can be a small amount of non-coalescence between colliding water drops, especially for particles which impinge upon the collector near to its equator.

On the whole, however, these results are very encouraging. The agreement with the theory, and in the case of methylene blue with the data of Walton and Woolcock, is excellent. It seems that the experimental technique used was successful.

Nevertheless, there remain a few points for further discussion. Whilst the scatter in the data is evidently no greater than that found by other workers, it is still appreciable. It is therefore important to examine the accuracy of the measurements used and the cause of this scatter.

3.3 Discussion of Experimental Method

In general, the experimental technique worked very well. The most common problem encountered during a run was caused by a droplet climbing up the needle and blocking the sampling probe. Such an occurrence required the cleaning of the entire sampling system. Experience showed that, with the sampling probe behind the droplet, larger drops could be held, but the effect of the aspiration through this probe is a little obscure. The distance between the leading edge of the probe and the tip of the needle proved to be important. If there was too large a gap, the droplet was found to be less stable but, if the gap was too small, the drop tended to climb up the needle so blocking the sampling system. An optimum distance of approximately one probe diameter was reached. Some of the larger drops were found to vibrate at the higher air velocities but no difference could be perceived between the results obtained from vibrating as opposed to static drops. This finding is in agreement with the experiments of Goldshmid and Calvert (25) using oscillating glass spheres. Nevertheless, owing to the difficulty involved in determining the diameter of a deformed drop from the negatives, vibration was avoided wherever possible. The larger drops were found to be slightly prolate with a ratio of major to minor axes of approximately 1.05. The horizontal diameter was used in the calculations. Both the drop support needle and the aspiration of air from behind the droplet

obviously affect the flow in the wake, but it is reasonable to assume that the flow conditions over the forward half of the collector are undisturbed by the sampling probe and that they approximate those of the potential flow theory. This assumption is supported by the fact that a traverse across the jet with the hot wire anemometer showed a flat velocity profile when the probe was aspirating isokinetically.

One effect which has been ignored up until this point is that of electrostatic charge on the particles. The original generator was supplied with a radioactive ioniser to neutralise the charge on the aerosol. However, it was found that the large particles required for these experiments were too easily deposited in the horizontal section of this ioniser. Consequently, the generator was modified so that the aerosol travelled vertically out of the machine. This meant, however, that the charge on the particles could not be neutralised. In order to keep the elatrical effects to a minimum, the droplet holder was earthed. Nevertheless, it is desirable to form some estimate of how much these charges may affect the collection efficiency. Whilst it was not possible to measure the charge on an individual particle, a useful estimate of its order of magnitude can be made.

When the aerosol is generated, all the charges on the primary drops remain on the final particles. Liu and Pui (42) show that the maximum charge which can be encountered on

atomized droplets of 50μ diameter is in the region of 100 electrons. Kraemer and Johnstone (37) have developed an expression for the force F_e on an aerosol particle near an earthed spherical collector as:

$$F_{e} = Q_{p}^{2} \left(\frac{D}{8\pi \epsilon_{o} H^{3}} - \frac{2DH}{\pi \epsilon_{o} (4H^{2} - D^{2})^{2}} \right) - Q_{p}^{2} \frac{DC_{p}}{24\epsilon_{o} H^{2}}$$

$$- Q_{p}^{2} \frac{D^{2}C_{p}R_{j}}{8\epsilon_{o} H^{2}}) \qquad (3.10)$$

where Q_p is the charge on the particle in coulombs, ε_o is the permittivity of free space (8.85 x 10^{-21} coulombs²/dyne cm.²), H is the surface to surface separation, C_p is the particle concentration, and R_j is the radius of the aerosol jet. The first term in this equation represents the force on a particle owing to the attraction between itself and its image in the collector. Under these circumstances, it is dominant. The second term is due to the repulsion of the surrounding aerosol, and the third is the force on the particle arising from the total charge induced in the collector by all the other particles in the jet. For C_p = 50 particles/cc., Q_p = 1.602 c 10^{-17} , and D = 0.2. Equation (3.10) reduces to:

$$F_{e} = \frac{2.31 \times 10^{-16}}{H^{3}} - \frac{3.69 \times 10^{-15} H}{(4H^{2}-D^{2})^{2}} - \frac{7.41 \times 10^{-15}}{H^{2}}$$
(3.11)

Thus this force can only become appreciable when the particle is close to the collector. The electrical effects are therefore confined to an area very near the drop and consequently cannot modify the collection efficiency to any significant degree.

Kraemer and Johnstone also defined a dimensionless parameter $K_{\mathbf{G}}$ to describe the ratio of electrical forces to viscous forces for a charged particle in the vicinity of an earthed collecting sphere:

$$K_{G} = \frac{C Q_{p}^{2} C_{p} R_{j}}{3\pi\mu \ d \ U_{\infty} \epsilon_{O}^{D}}$$

They found that collection due to electrical effects varied with K_G . They showed experimentally that, for $K_G = 10^{-3}$, the collection efficiency was around 1%. The largest value of K_G that was encountered in the present experiments was of order 10^{-8} . It may be concluded that electrostatic effects are not important under the experimental conditions.

Although every attempt was made to measure each variable as precisely as possible, the data were still found to be scattered. It is pertinent therefore to analyse what errors were involved in the experimental technique.

The air velocity was measured with a high precision anemometer calibrated in situ against a wet test meter accurate to ± 1%. The velocity readings were thus accurate to ± 0.5%.

They were found to remain constant to ± 0.6% during the course The drop diameter could be measured from the negatives to ± 0.3 thousandths of an inch which, at a magnification of 1.7, means that the drop diameter was measurable to $\pm 8 \times 10^{-4} \text{cm}$. The particle density was measured reproducibly to within ± 0.4% for the liquids. For the solid particles, a larger error is possible due to the variations found in the results. However, the values obtained are in good agreement with others found in the literature (70). The particle size was determined microscopically by photographing the aerosol at 400 x magnification. Each particle could be measured to an accuracy of ± 0.1µ. The arithmetic mean of about 50 particles was taken as the average diameter for the aerosol in each Except for water, the aerosols were found to be monodisperse with a relative standard deviation of 7 - 10%. contact angle measurements gave reproducible values which were in good agreement with those of other workers.

All the errors were thus relatively small and not enough to explain the scatter in the data. It therefore seems that the extent of the scatter is mainly attributable to statistical error in the sampling and counting technique. The statistical error involved in counting $N_{\rm p}$ particles is (75):

Fractional Error =
$$\frac{1}{\sqrt{N_p}}$$
 (3.13)

It is clearly desirable to register as large a number of particles as possible. From Equation (3.13) the count is accurate to $\pm \sqrt{N_p}$ particles. Thus the error involved in the measurement of collection efficiency is given by:

$$Error = \frac{\sqrt{N_D}}{N_C}$$
 (3.14)

Experimental conditions were chosen so as to keep this error value to less than 10%. This was not always possible, and for some droplets the value rose as high as 12.5%. for droplets having more error than this were discarded. third order polynomial regressions were made through the data, the standard error of the estimate for E for ferrous sulphate was found to be 4.59. Using a median E reading of 51, this amounts to an average of 8.3% error. For methylene blue, the standard error was calculated to be 2.98, giving an average of The average experimental error for water was found in the same way to be 20.3%. The scatter in the data for ferrous sulphate and methylene blue is therefore approximately what The fact that the water aerosol was more would be expected. polydisperse may be the reason for the extra scatter in this run.

It seems that the technique proposed has been reasonably successful. It can measure collection efficiencies within a maximum random error of 10 - 12%, as demonstrated for the

hydrophilic aerosols. It remains to apply this method to the study of the collection efficiency of hydrophobic particles.

This is the concern of the second part of this work.

PART II

COLLECTION OF HYDROPHOBIC PARTICLES BY WATER DROPLETS

Introduction

One of the basic assumptions inherent in the theory presented in the first part of this work has been that every particle which is transported to the surface of the collector drop is captured. It has been shown experimentally in Part I that, for hydrophilic aerosols such as methylene blue and ferrous sulphate, this assumption holds true. However, in recent years, its validity with regard to all aerosol particles has been increasingly challenged. There has been a growth of experimental and theoretical evidence to suggest that there may be sufficient rebound of hydrophobic particles from the surface of a collecting water drop that the overall collection efficiency may be reduced. This idea is in opposition to the persistent and widely maintained viewpoint that wettability effects are not very important. Several authors (70, 23, 71) have effectively dismissed this factor, and Beard and Grover have recently stated that as long as a particle, whether wettable or non wettable, is transported to a droplet surface, it will stick there by the action of van der Waals forces (5). Such a statement is erroneous as will be shown in Chapters 5 and 6. The only way that this debate over wettability can be resolved is by good experimental evidence to prove conclusively whether non wettable particles are collected less efficiently. The major thrust of the work presented in the second part of this thesis is to provide and

analyse such data for certain solid non wettable aerosols and also for aerosols of hydrophobic oils.

Chapter 4

DEFINITION OF THE PROBLEM

It has become very fashionable in recent years to include in papers on the subject of aerosol impaction phenomena an acknowledgement that not every particle that reaches the surface of a collector necessarily sticks to it. Some authors have gone so far as to define a capture efficiency or sticking probability (62) or, in the case of colliding droplets, a coalescence efficiency (50). In general terms, such efficiencies are defined by:

$$E = E_C \times E_A$$

where E is the total collection efficiency; E_{C} is the capture efficiency defined as the ratio of particles which are actually captured by the collector to the number which are brought to its surface; and E_{A} is the aerodynamic collection efficiency as used in the first part of this work. However, very few authors have made more than a gesture in this direction and the problem, both in theoretical and experimental terms, remains substantially unsolved.

4.1 Literature Review

The first workers who seem to have considered theoretically the idea of a non wettable particle impacting with a droplet were McCully et al (47). They noted that a head-on collision of a particle into the forward stagnation point of the collector would maximise the chances of collection and that a glancing collision would lessen those chances. They derived an expression for the minimum kinetic energy that a particle must possess if it is to penetrate into the drop during a head-on collision:

$$KE_{min} = \sigma \pi^2 a^2$$

This is fundamentally the same equation that was derived by Evans (19) two years previously in connection with the flotation of suspended particles in water.

These rather superficial analyses were improved upon by Pemberton (54) who calculated the energy required to penetrate the surface tension barrier for completely non wettable particles during glancing collisions. Pemberton was very concerned with the problem of 'shoot through' of the particle whereby it travels so fast that it can pass completely through the collector. This is theoretically possible but it can be argued that the effect is more likely to be evident for wettable particles than for non wettable particles. Pemberton defined a parameter M which is the ratio of the normal velocity required for

penetration to the free stream velocity. He computed collection efficiencies as a function of this parameter and of K.

In so doing, he implicitly assumed that penetration and collection are equivalent. His results for several values of M are shown in Figure 4.1.

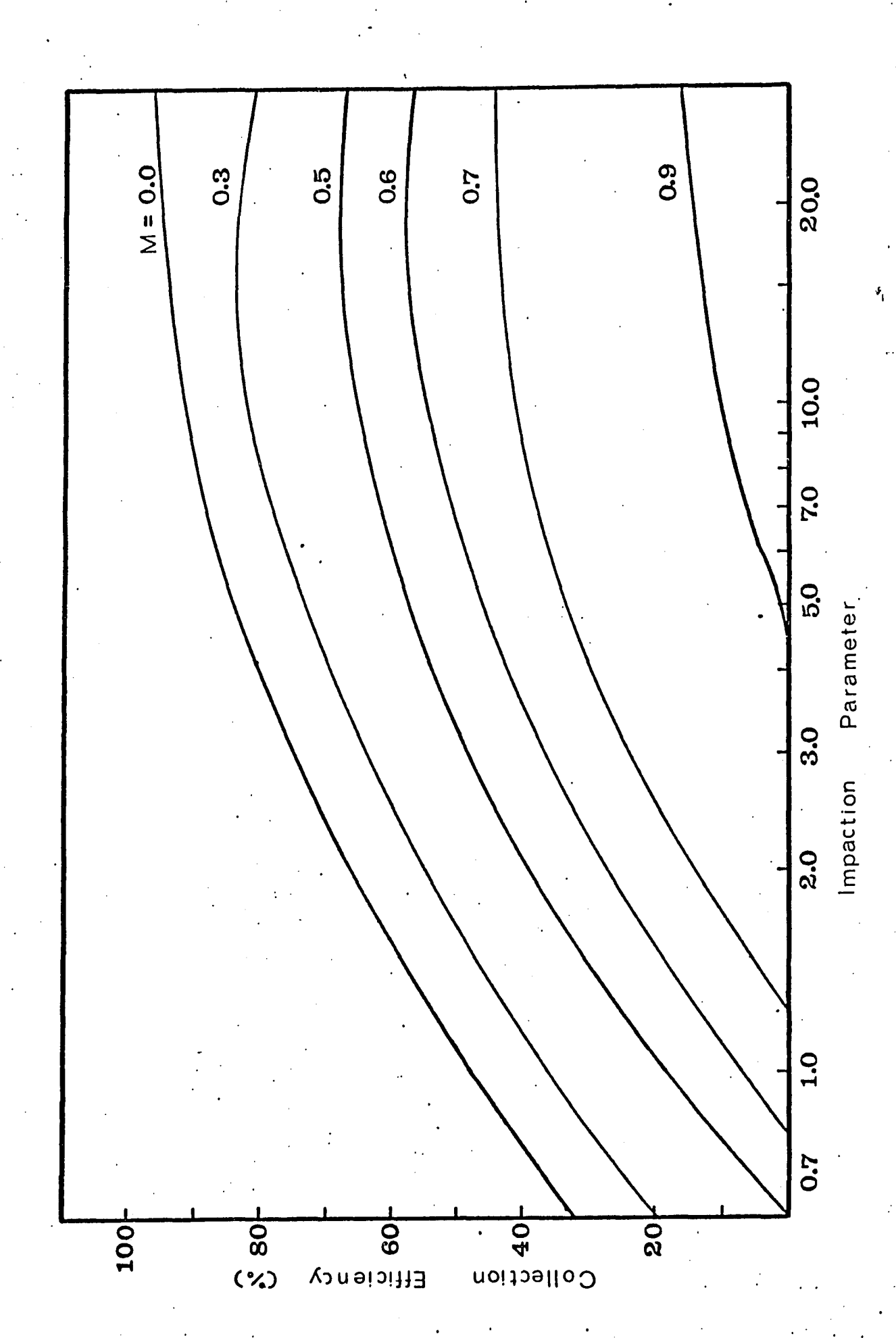
This analysis was extended by MacDonald (43) to situations for $90^{\circ} < 0 < 180^{\circ}$. He considered that the only forces on the particle were due to the surface tension of the drop and that these forces acted in a direction tangential to the water surface at the point of contact. He derived an expression for the resistive force during penetration which he then integrated to produce an equation for the entry work of the particle. His final expression was the same as Pemberton's except that it differed by a factor of Cos 9. M is thus defined as:

$$M = \frac{\left[\frac{-8\sigma\cos\theta}{\rho_{\rho}d}\right]^{1/2}}{U_{\infty}} \tag{4.1}$$

Pemberton's original calculations could therefore be used in conjunction with this newly defined parameter to predict E for any system.

MacDonald made one particularly important prediction. He showed that a water surface will do work upon a particle to make it penetrate if it has a contact angle of less than 90° with the aerosol material so that it is only for situations where 0 > 90°

Figure 4.1 VARIATION OF COLLECTION EFFICIENCY WITH IMPACTION PARAMETER AT VARIOUS VALUES OF M ACCORDING TO PEMBERTON (54)



that capture efficiency is reduced. However, his approach was conceptually wrong in that he considered only the interfacial tension forces due to the liquid-vapour interface. There are two other interfaces present, the surface energies of which play a part in the penetration process. Although MacDonald's work is thus inexact, it remains, along with the paper by Pemberton, one of the only published theoretical analyses of the situation. Other discussions of the effect of wettability have been either qualitative or experimental.

Experimentally, the question of whether non wettable particles may bounce off a collector has also been open to debate. However, it seems that this can be the case since it has been observed by McCully et al (47). They used aerosols of wettable and non wettable glass beads of 5-50µ diameter issuing from a hypodermic needle surrounded by an air stream, and they photographed what happened when the particles impinged upon the drop at air velocities of 3 m/sec. They actually observed particles bouncing off the drop, but their observations were only qualitative. They also measured collection efficiencies of drops falling through columns of aerosols and found that the non wettable material gave a reduction in collection efficiency of approximately 12% for particles greater than 18µ. The authors did not attempt to define their 'non wettability' nor did they give details of how it was achieved.

Chronologically, the next definite statement to be found in the literature is by Walton and Woolcock (70), who concluded

that surface tension effects were irrelevant in their experiments. They deduced this from the fact that there was no significant variation in collection efficiency when surfactant was added to their drops. In view of the fact that their aerosol was methylene blue, which is water wettable, this is not surprising.

Oakes (51) did some laboratory experiments to determine whether non wettable material was scavanged more slowly by rainfall than was wettable aerosol. He used two chambers in which he generated an artificial rain and recorded photometrically the change in aerosol concentration with time during the course of a shower. The wettable aerosol that he used was ammonium chloride (0.6μ) and the non wettable particles were oil (0.8μ) , paraffin wax (0.8μ) , and ammonium salicyclate (2μ) . The data obtained are very inconclusive and differ considerably between the small chamber (0.134m^3) and the room which served as the large chamber. In the small scale experiments, he found that readings of light extinction were lower at a given time for ammonium chloride than for the oil cloud. He therefore concluded that the non wettable particles are less easily scavenged.

In a quite comprehensive piece of work, Goldshmid and Calvert (25) investigated collection efficiencies of supported drops. They used five different liquids as collectors; water, glycerol, phenol-m-methoxy formamide, and n-hexadecane; and two different aerosols, polystyrene (0.8-2.85µ) and sulphur

(0.6-2.65μ). They suggested that mutually non wetting pairs gave a lower collection efficiency than wetting pairs. However, there is much confusion in their data. Whilst there appears to be a lowering of the value of E with increase in θ from 20° to 87°, their results for wettable aerosols seem to exhibit exactly the same variation. They do not consider contact angles greater than 90°, which is the normal limit for non wettable behaviour. Moreover, their results for hydrophilic aerosols do not consistently agree with those presented in Part I of this work. On the whole, their findings seem inconclusive.

Rosinski et al (62) conducted an experimental study of the capture of hydrophilic and hydrophobic particles by condensing and evaporating water drops. They used zinc sulphide powder (1.14µ) as their aerosol and made it hydrophilic by exposing it to a surfactant solution. Unfortunately, they did not undertake a series of experiments at zero droplet growth rate which could be used for comparison. For a growing droplet, they found that hydrophilic particles exhibit a greater collection efficiency than hydrophobic particles but, again, those conclusions were qualitative since no attempt was made to define the degree of wettability of their aerosol.

A meteorological study of particle retention under field conditions was conducted by Esman (18) who investigated the capture of particles by rainfall as a function of wettability. Starting from the assumption that the capture efficiency of soluble particles is 1, he went on to draw some conclusions

about the retention efficiencies of insoluble (and by implication non wettable) particles based on analyses of the atmospheric aerosol immediately before and after rainstorms in Pittsburgh. He concluded that the capture efficiency for insoluble particles could be taken as approximately 67% independent of rainfall intensity and aerosol concentration. His figure of 67% was the average of 6 values ranging from 52% to 85%.

The most recent piece of work on the effect of particle wettability on collection efficiency is by Montagna (49). studied the effect on collection of adding surfactant to a suspended drop. The aerosol consisted of sulphur particles up to 5µ in diameter, at velocities of 625 cm/sec. He found an increase in collection with increasing concentration of surfactant or decreasing angle of contact. The major deficiency in this work is the lack of definition and control of the wettability aspects of the experiments. The method used to obtain 0 was inaccurate in that the contact angle was measured from an advancing interface travelling at 5 cm/sec. well known that measurements of θ for moving interfaces give results which are heavily dependent on the velocity. Phillips and Reddiford (56) have shown that velocities of up to 0.1 cm/min. can produce a 72% increase in 0 for water on a dimethyl silicone surface. Thus correlation of Montagna's experiments with other work is very difficult. The normally accepted figure of 0 for an air-water-sulphur interface is about 60°

(25). If this is so, it means that Montagna found a decrease in E for contact angles of less than 90°. This is in agreement with the rather dubious data of Goldshmid and Calvert but in contradiction to the theoretical predictions of MacDonald.

It is therefore evident that there is a great deal of confusion in this particular area. A review of the literature indicates that there are three basic requirements for further study. First, there is a need for experimental data on solid, hydrophobic particles for which the wettability parameters are well defined and for which direct comparison with wettable aerosols can be made in order to resolve the question of whether non wettable particles are collected less efficiently. A second requirement is for an experimental investigation of the collection efficiencies for hydrophobic liquids such as oils for which there are no experimental data available. Finally, there exists a need for further theoretical analysis of at least two aspects of the problem. The first of these involves the interfacial energies of the colliding system and their effect on penetration into the droplet. The second aspect concerns the relationship between penetration and collection.

The aim of the work presented in the remainder of this thesis is to fulfill these three objectives.

4.2 Experimental Procedure

Of the three objectives outlined above two are experimental, the gathering of data for solid and for liquid hydrophobic acrosols. The objective of using liquid acrosols stems from the lack of any experimental data for this relatively common situation. This lack of data has been caused in large part by the absence of an accurate method to analyse the quantity of acrosol collected by the water drop. The new method, outlined in Part I, for the measurement of the number of particles collected by the droplet overcomes this difficulty and results are now attainable.

In order to fulfill the two objectives, experiments were undertaken with 4 different hydrophobic aerosols; paraffin wax and talc for solid particles, and paraffin oil and dioctyl phthalate (D.O.P.) for liquid particles. The experimental procedure and equipment were exactly the same as reported in Chapter 2 with the exception of the conditions for the generation of the aerosols and the measurement of the size of the liquid particles.

All four of the aerosols were generated using the spinning disc generator described in Chapter 2. For the talc runs,
depending on the particle size obtained, either 100 gms. or
175 gms. of talc powder was slurried in 400 ccs. of distilled
water to which 100 ccs. of 95% ethanol was added. This slurry
was agitated in a holding vessel from where it was fed to the

disc by the peristaltic pump at flow rates from 4 to 10 ccs/min. The aerosols produced were collected isokinetically onto a filter and analysed in exactly the same way as for the solid aerosols described in Part I. Under microscopic examination, it was found that the particles were not perfectly spherical but were composed of aggregates of the original talc fragments in the slurry. Nevertheless, they were quite monodisperse, having a relative standard deviation in measured diameter of 0.072.

Paraffin wax aerosols were obtained by making up a 25% solution of the wax in benzene. This solution was maintained above the melting point of the solid by immersion in a hot water bath. A spherical particle of rough surface texture was obtained with an average of 0.084 for the relative standard deviation in diameter.

Paraffin oil aerosols were generated using a 30% solution of paraffin oil in benzene. They were collected, in the same way as were the water aerosols in Part I, on a teflon filter and photographed immediately under a microscope. The photographs were later analysed on a vertical travelling stage microscope to determine the apparent diameter of the particles. The true diameter was then obtained using the contact angle between the teflon and the oil in conjunction with Equation (3.5). The contact angle was measured using the method proposed in Section 3.1 and was found to be 58°27'. The relative standard deviation of the particle size was 0.079.

Three different D.O.P. aerosols were generated using three concentrations of D.O.P. solution, 10%, 15%, and 30%, in 95% ethyl alcohol. The aerosols produced were measured by the same method as for paraffin oil. They were sized at 9.8 μ , 11.4 μ , and 15.7 μ , with an average relative standard deviation of 0.091. The contact angle of the liquid on the filter was found to be 63°49'.

Each material was analysed in order to determine its degree of hydrophobicity. The contact angle between the paraffin wax and water was measured at 102°17' from 12 readings, with a relative standard deviation of 0.0118. A similar technique was used for a compressed tablet of talc powder but with far less consistent results. The average reading of 63°42' was comparable to the figure found by Rebinder et al (60) but completely at variance with the values of around 90° quoted by McHardy (48) for freshly cleaved talc surfaces.

The surface and interfacial tensions of the two liquids were obtained using a Fisher Tensiomat. This device uses a torsion balance to measure the force on a platinum ring which is pulled through the interface. The measured force must be adjusted to account for the weight of the film in the ring and the dimensions of the ring. The adjustment factor F' may be calculated from:

$$F' = 0.725 + \left[\frac{0.01452 \text{ P}}{c^2 (\rho_1 - \rho_2)} + 0.04534 - \frac{1.679}{k} \right]^{1/2}$$
 (4.2)

Table 4.1

	^P sv	F'	$^{\gamma}$ sv	^P sL	F'	Υ _{SL}
	dynes/cm.		dynes/cm.	dynes/cm.		dynes/cm.
D.O.P.	36.22	0.9002	32.61	26.65	1.4200	37.84
			•			
Paraffin .	34.92	0.9032	31.54	32.97	1.0807	35.63

α ο

where c is the circumference of the ring, P is the dial reading, ρ_1 is the density of the lower phase, ρ_2 is the density of the upper phase, and k is the ratio of the ring diameter to the diameter of the wire. The results for both paraffin oil and D.O.P. are shown in Table 4.1 in which $\gamma_{\rm SV}$ is the surface tension of the liquid, and $\gamma_{\rm SL}$ is the interfacial tension between the liquid and the water.

A total of 14 runs were performed with the hydrophobic aerosol materials. During these, it was observed that the solid aerosols collect on the outside of the water surface and eventually form a thin crust if the drop is left exposed to the stream for over 5 minutes. The two liquid aerosols were found to affect adversely the adhesion of the droplet to the support such that it would fall off the needle prematurely at velocities lower than those used. The experimental operating conditions and the results are given in Appendix B. In order to complete the two objectives, the data must now be compared with those obtained for hydrophilic particles.

4.3 Comparison of Results for Hydrophobic and Hydrophilic Aerosols

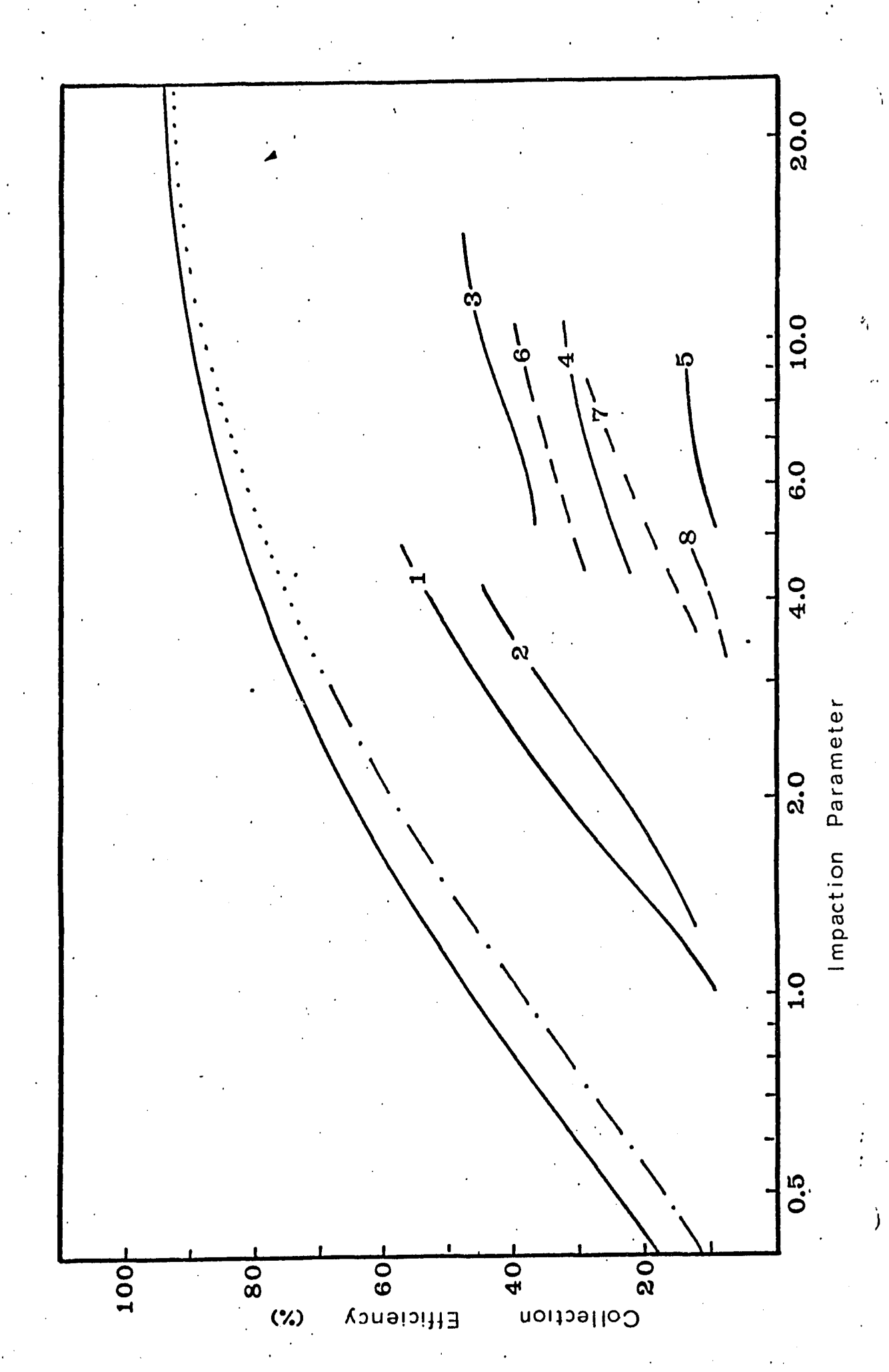
In this section, the experimental results for hydrophobic particles will be compared to those obtained for the hydrophilic particles in Part I. It will be shown that all four hydrophobic aerosols are collected less efficiently, and that E cannot be predicted using either potential flow theory or the more accurate computations of Beard and Grover.

It was found that the results for any aerosol varied according to the size of the particle and the velocity at which the experiments were conducted. The 14 runs performed thus grouped themselves naturally into 8 different sets of results, 3 for paraffin wax, 3 for talc, and 1 each for D.O.P. and paraf-A third order polynomial was fitted to each set of data points using the 'STATPAK' routine from the McGill 'MUSIC' program library. For the sake of clarity when comparing the experimental results, the smoothed best fit lines from these polynomials, rather than the points themselves, have been plotted. Graphs showing individual experimental points may be found in Chapter 6. Figure 4.2 compares the experimental results for the eight hydrophobic aerosol data sets with the results obtained for wettable particles, as well as with the computations of Beard and Grover and with the collection efficiencies calculated from potential flow assumptions. Beard and Grover results are not plotted for K < 3.0 because

Figure 4.2

COMPARISON OF THE BEST FIT LINES FOR THE EXPERIMENTAL DATA

	POTENTIAL FLOW THEORY
• • • • • • • • • • • • • • • • • • • •	BEARD AND GROVER
	WETTABLE RESULTS
-1-	PARAFFIN OIL
-2-	D.O.P.
-3-	•
-4-	PARAFFIN WAX
- 5-	
-6-	
-7-	TALC
-8-	



<u>.</u>

they are indistinguishable from the line for the wettable data. Curves 3, 4, and 5 are for paraffin wax at three different, successively lower velocities, and curves 6, 7, and 8 are for talc again at descending velocities.

It is immediately apparent from the data obtained that, under the same experimental conditions, the hydrophobic particles are collected less efficiently. For example, at an impaction parameter of 2.0, collection efficiencies of around 59% were found for wettable aerosols while efficiencies of only 33% were found for paraffin oil and 23% for D.O.P. At K = 8.0, paraffin wax gave a collection efficiency of only 14%. Clearly, the theoretical values calculated using either potential flow assumptions or Beard and Grover's computations are inadequate for predictions of the true collection efficiency of the hydrophobic aerosols.

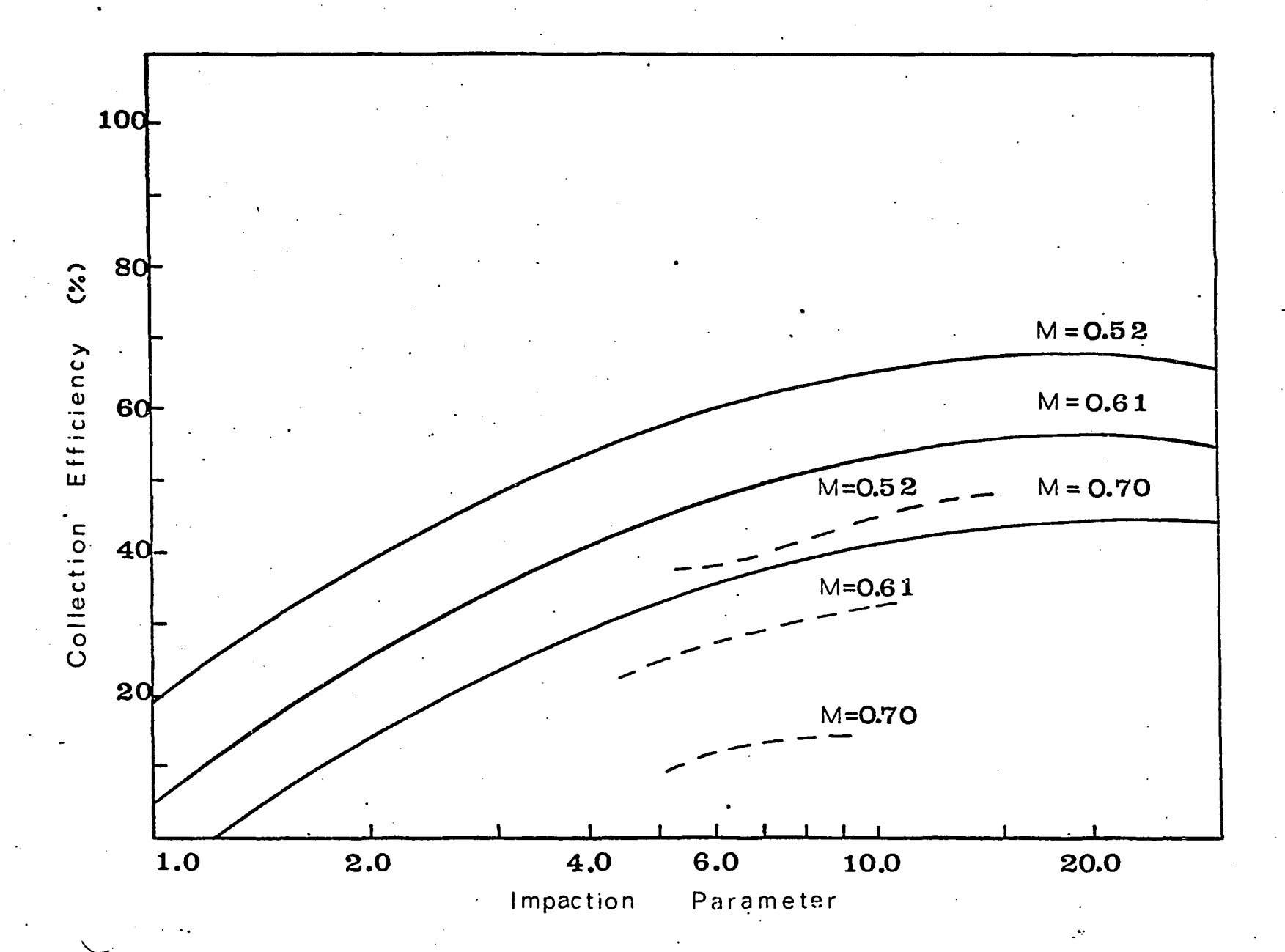
In addition to this important finding, the experimental data also show that the collection efficiency varies according to the velocity at which the experiments were conducted. This effect was predicted by MacDonald but has never before been experimentally verified. However, whilst his predictions were qualitatively correct, his theory is not adequate to describe quantitatively the experimental data. Figure 4.3 shows the results for paraffin wax and his corresponding theoretical lines obtained by interpolation. There is a large divergence between his theory and the present data.

Figure 4.3

COMPARISON OF THE BEST FIT LINES FOR THE PARAFFIN WAX DATA WITH MACDONALD'S THEORY

MACDONALD'S THEORY

— — — EXPERIMENTAL RESULTS



The two experimental objectives have therefore been fulfilled. Experiments have shown that both solid and liquid hydrophobic particles are collected less efficiently than the hydrophilic particles discussed in Part I. The third objective, however, is more complex. The collision process has proved very difficult to study theoretically, and the mechanisms which influence a particle close to a collecting surface are not completely understood. This must largely explain why a complete discussion of the collision of hydrophobic aerosols and water surfaces has never appeared in the literature. However, in the next two chapters, the theoretical background necessary to an understanding of the collision process will be outlined and the problem will be discussed in terms of the prevailing conditions in the experiments summarized above.

Chapter 5

COLLISION DYNAMICS FOR HYDROPHOBIC PARTICLES

This chapter will introduce and review the theoretical background to the discussion of the experimental results in chapter 6. There are three principal sections. First, an analysis of the collision process is presented in terms of a unified concept which links the outcome of the collision with the magnitude of the various mechanisms involved. A criterion is developed for the rebound of an aerosol particle from the droplet. In the second section, a new theory is introduced which predicts the circumstances under which a particle will penetrate the droplet surface.

The last section reviews the complex areas of van der Waals forces, electrostatic forces, and viscous forces. Since methods adequate for the exact calculation of each of these forces do not exist, the work presented here is approximate. Consequently, the discussion is limited to situations which are pertinent to the experiments described above. This restriction allows calculation of the order of magnitude of the various forces such that the important factors may be isolated. An experimental situation has been introduced as an illustrative example to provide a handle on the mechanisms involved. A 20µ paraffin wax particle is the case used. However, before considering this specific example, it is first necessary to look more closely at the collision process in general.

5.1 Energy Considerations in the Collision Process

Consider a particle approaching a water droplet in potential flow. At large distances its motion is parallel to the axis of the drop. As the separation decreases, however, the fluid drag tends to pull the particle around the droplet whilst the particle's inertia acts to maintain its instantaneous Thus, depending upon its initial distance from the axis, ym, which determines the aerodynamic collision efficiency as calculated in Part I, the particle may or may not collide with the droplet. These aerodynamic considerations dictate at what point a particle which started at a given y_{∞} will reach the surface of the drop. For hydrophobic aerosols, however, it seems certain that, once the droplet to particle separation becomes very small, surface to surface interactions will determine whether or not a specific particle is actually captured by the droplet. If this particle is approaching a liquid spherical collector such that a << R, the droplet surface will appear to the particle as a flat wall. The ensuing discussion will therefore deal with collisions between particles and flat surfaces. Suppose that the particle has approached sufficiently near the drop that surface to surface interactions are significant. From this point on, the particle is acted upon by several forces: viscous drag in the draining film between it and the collector; surface forces of the van der Waals type; electrostatic forces; and the surface tension forces which

resist the motion of the particle through the surface of the drop itself.

Assume that the particles are perfectly smooth, solid, non rotating spheres. Assume that the tangential component of the velocity of the particle is conserved throughout the collision process such that the dynamics of the collision are determined by the particle motion normal to the drop surface. There are then two basic possibilities which can result from a collision:

- a) the particle does not enter the droplet, in which case it either rebounds from the drop surface into the free gas stream and is not captured, or it is brought to rest on the outside surface of the drop where it remains and is so captured.
- b) the particle enters the droplet despite its hydrophobicity.

5.1.1 collisions where complete penetration does not occur

The ultimate aim of an analysis of a collision process such as this is to develop criteria to predict when a particle will bounce from or adhere to the surface. Although this problem has been subjected to much study by surface scientists, it is still not possible to predict accurately the conditions

under which the rebound will take place, especially since there is no exact knowledge of the van der Waals (V.D.W.), electrostatic, and film drainage mechanisms involved. However, these are the forces which must be discussed in any study of the collision process. What is required in order to simplify the analysis is a line of approach which will allow the calculation of the relative effects of these various forces such that their magnitude may be estimated. For surface forces, Dahneke (11) proposes the concept of a particle-surface potential well, and analyses collisions between solid surfaces in terms of this and other derived parameters. Since the approach suggested by his method is useful here, the collision process will be discussed in terms of the effect of the various surface forces on the kinetic energy of the particle.

The particle on approach has a certain kinetic energy due to its normal velocity \mathbf{U}_R . Consider the particle to have reached a sufficiently small distance from the collector surface for any of the surface forces outlined above to be effective. The kinetic energy at this point will be referred to as the approach energy \mathbf{I}_{na} . Define the following energy potentials as:

 I_{vi} = energy given up to viscous effects on the way in

 I_{vr} = energy given up to viscous effects on the way out

I_e = energy of electrostatic interaction, assumed
 negligible on rebound

 $I_s = energy of VDW interaction$

f = fraction of the particle's energy dissipated during the contact period.

Then the kinetic energy at the instant of impact is given by:

$$I_{ni} = I_{na} - I_{vi} + I_{e} - I_{s}$$
 (5.1)

and the kinetic energy at the instant of rebound is given by:

$$I_{nr} = I_{ni} (1-f)$$
 (5.2)

When the particle rebounds it must do work to escape the influence of the drop. Consider a particle which has just succeeded in escaping. Its kinetic energy is given by:

$$I_{np} = I_{nr} - I_{vr} + I_{s}$$
 (5.3)

The particle will be captured when:

$$I_{np} = 0$$

that is, when:

$$I_{nr} = I_{vr} - I_{s}$$

and:

$$I_{ni} = \frac{I_{vr} - I_{s}}{(1-f)} = I_{na} - I_{vi} + I_{e} - I_{s}$$
 (5.4)

Thus for a rebounding particle to escape, its approach energy

must obey the inequality:

$$I_{na} \ge \frac{(I_{vr} - I_s)}{(1-f)} + I_{vi} - I_e + I_s$$
 (5.5)

where the term on the right hand side represents the total energy lost during the entire collision process.

It is pertinent to discuss the quantity f which is analgous to the coefficient of restitution between solid surfaces. It has been included in this formulation to cover such aspects as viscous dissipation in the droplet, heat losses, and energy dissipated due to the creation of surface waves. Recent computations, such as those by Foote (21) of the internal momentum transfer in large drops bouncing on flat surfaces, show that the exact calculation of a quantity such as f is feasible. However, the difficulties involved in this type of calculation suggest that it would be easier to use typical measured values such as those given by Whelpdale and List (72). If f were zero the droplet surface would behave like a perfectly elastic skin as suggested by Philipoff (55). In this case, the drop surface would return all kinetic energy to the particle upon rebound. If:

$$I_{na} \ge I_e + I_s$$

then inequality (5.5) reduces to:

$$I_{na} \ge I_{vr} + I_{vi} - I_{e}$$
 (5.6)

for a successful bounce.

However, it does not appear that f is negligible in reality. The experiments of Whelpdale and List show very clearly that this quantity is significant. They conclude that the energy losses of the particle depend on the incident angle, the incident velocity, and the collector droplet size. The energy loss increases at lower incidence angles and higher velocities, and decreases with increasing drop size. Their experiments were conducted with a 70 μ water aerosol with a 1 mm. diameter collector. It could be expected that the dependence on collector size would be less significant in the present experiments owing to the increased relative curvature. For the angles with which we are primarily concerned here, between 50° and 90° , the fractional energy loss was found to vary between 0.4 and 0.1.

5.1.2 collisions for which the particle penetrates the droplet

In this case, the particle arrives at the drop surface with sufficient normal momentum to punch through the surface of the liquid, thus doing work against the droplet surface energy. If $\mathbf{I}_{\mathbf{T}}$ is the energy required for the particle to penetrate the surface tension 'barrier' then penetration is achieved when:

$$I_{na} > I_{vi} - I_{e} + I_{s} + I_{T}$$
 (5.7)

Thus the particle only penetrates if it has enough kinetic energy to overcome the combined resistance and attraction of the viscous, VDW, electrostatic and surface tension forces.

From this conceptualization of the collision process, two criteria have thus been developed to predict when a particle will bounce from a drop surface and when it will penetrate. In order to apply these models to a specific situation, it is necessary to examine the theoretical bases for the estimation of the interaction potentials of the various forces at work during collision.

5.1.3 the approach energy I na

The kinetic energy of a particle due to its motion in a radial direction relative to the droplet is given by:

$$I_{na} = \frac{1}{2} m U_R^2$$
 (5.8)

where U_R is the normal approach velocity which, with the nomenclature defined in Chapter 1, is given by:

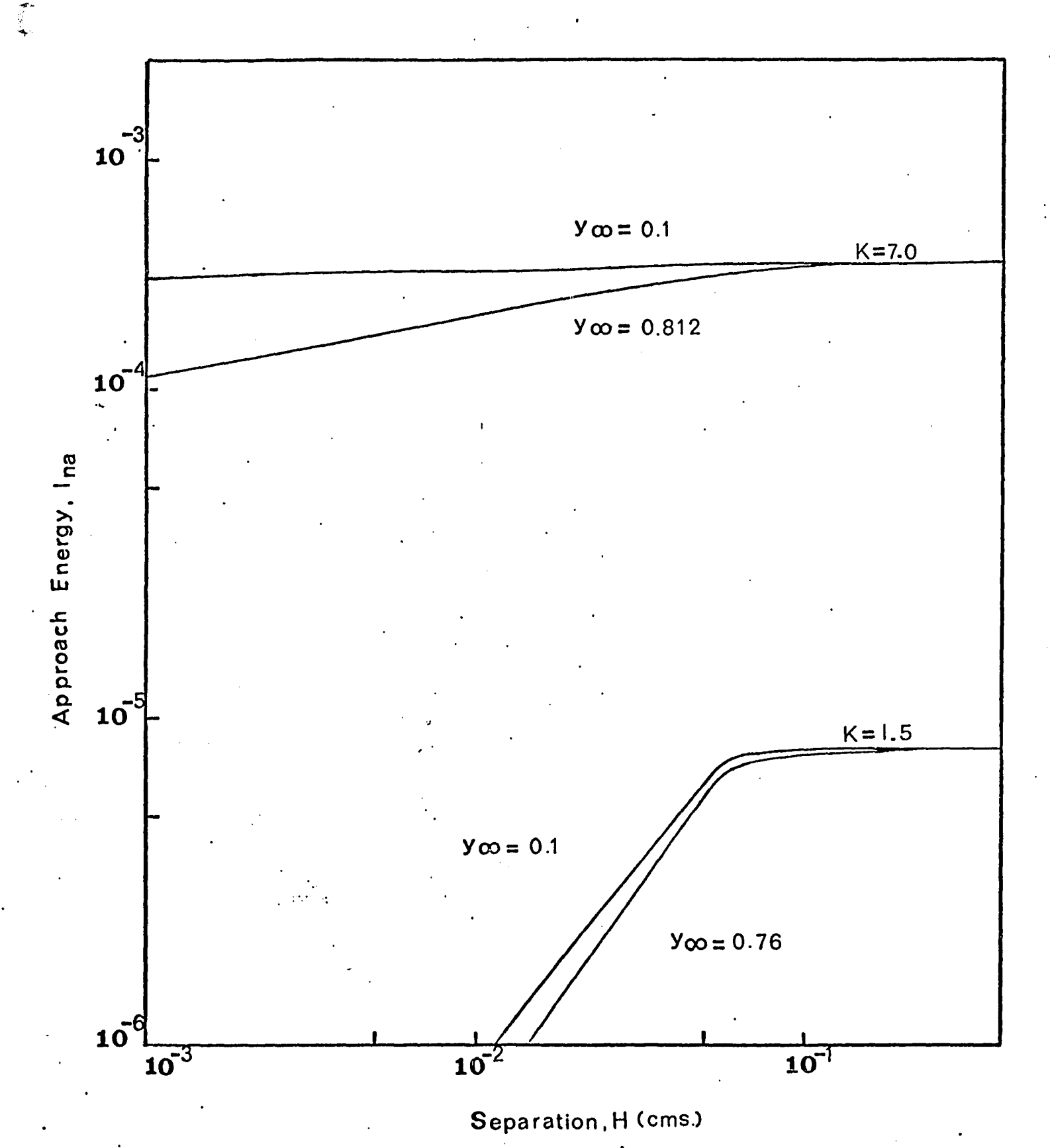
$$\frac{U_R}{U_m} = U_X^{\dagger} \frac{X^{\dagger}}{B^{\dagger}} - U_Y^{\dagger} \frac{Y^{\dagger}}{B^{\dagger}}$$
 (5.9)

It is obvious that for high values of the angle of incidence α

the normal velocity falls very rapidly when the separation becomes small. Thus the approach energy depends on the initial horizontal distance of the particle from the drop's axis, y, and on the impaction parameter. Figure 5.1 is an example of how the approach energy changes with separation for 2 values The first value, chosen to be typical of the experiments which have been performed for paraffin wax, represents a 20µ particle travelling towards a 0.1 cm. drop at a velocity of 354.4 cm/sec. such that K = 7.0. The other value is representative of a lower energy of approach and corresponds to a -12.5µ particle approaching the same drop at 194.4 cm/sec. such The curves shown in Figure 5.1 are typical of that K = 1.5. the sort of situations that have been encountered in the experiments, and have both been computed from particle trajectories calculated assuming potential flow around the collector.

Figure 5.1

VARIATION OF APPROACH ENERGY WITH SEPARATION AT K = 7.0 AND K = 1.5



5.2 Penetration of the Droplet Surface

It has been suggested that a collision between an aerosol particle and a droplet may or may not result in the particle overcoming the surface energy of the drop and entering the bulk of the liquid. In order to substantiate this assertion, it is necessary to calculate the circumstances under which this penetration may take place. It is first important to review the nature of the contact between a solid and a liquid in the presence of air as the third phase.

In many instances, a liquid placed on a solid will not wet it but remain as a drop having a definite angle of contact between the liquid and solid phases. The situation is illustrated in Figure 5.2 Adamson (1) has reviewed the background to this phenomenon and gives a simple derivation of a useful relationship known as the Young-Dupré equation. The change in surface free energy, ΔI , accompanying a small displacement of the liquid such that the change in area of solid covered is ΔA , is given by:

$$\Delta I = \Delta A.\gamma_{SL} - \Delta A.\gamma_{SV} + \Delta A.\gamma_{LV}.Cos(\Theta - \Delta\Theta)$$
 (5.10)

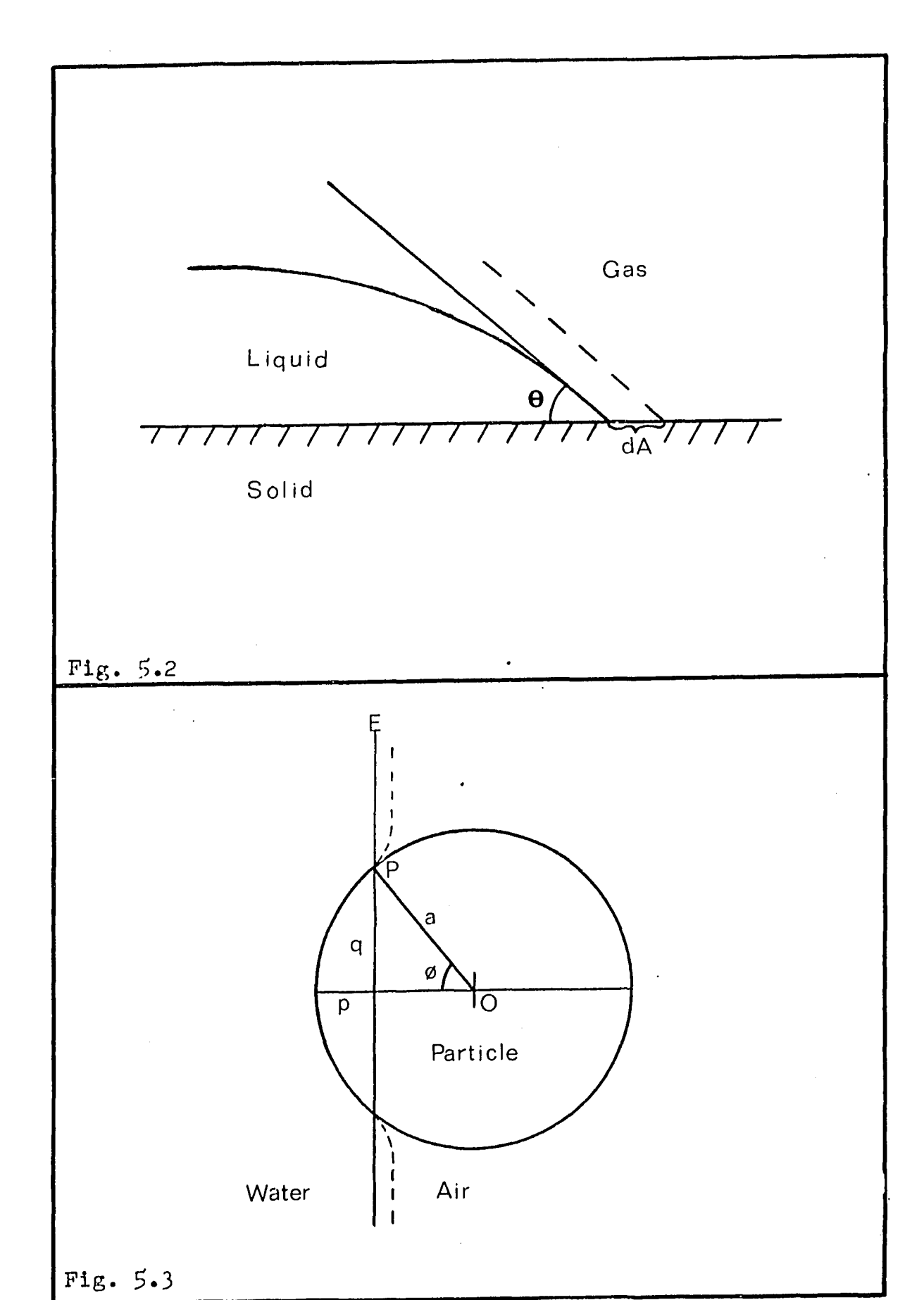
where $\gamma_{\rm SL}$ is the interfacial energy per unit area of the solid to liquid interface, $\gamma_{\rm SV}$ is the interfacial energy per unit area of the solid to vapour interface, and $\gamma_{\rm LV}$ is the surface free energy per unit area of the liquid phase. At equilibrium:

Figure 5.2

SESSILE DROP ON A SOLID SURFACE

Figure 5.3

PENETRATION OF THE PARTICLE INTO
THE DROPLET SURFACE



.

and

$$\gamma_{LV} \cos \Theta = \gamma_{SV} - \gamma_{SL}$$
 (5.12)

Equation (5.10) makes use of the fact that the total change in energy during a movement of the line of three phase contact is the sum of the changes in energies of the three interfaces involved. A similar procedure may be used for a particle penetrating a liquid surface although in this case the geometry of the system is different (see Figure 5.3).

Assume for simplicity that the droplet surface does not deform until the particle is actually in contact with it and that when deformation does occur the surface takes on the exact shape of the particle. The energy change of the particle-liquid interface system, and hence the work done on the particle during its penetration to a depth p may be calculated from the total interfacial energies before and after penetration. Before contact between the particle and the droplet, the interfacial energy is given by:

$$I = 4 \pi R^2 \gamma_{LV} + 4 \pi a^2 \gamma_{SV}$$
 (5.13)

After penetration to a depth p the energy of the system may be estimated if it is assumed that the interfacial energies do not

change throughout the collision process. The total surface energy is then given by:

$$I = \gamma_{SL}(2\pi ap) + \gamma_{SV}(4\pi a^2 - 2\pi ap) + \gamma_{LV}(4\pi R^2 - \pi q^2) \quad (5.14)$$

where $2\pi ap$ is the wetted area of the particle and q is the radius of the wetted perimeter (see Figure 5.3). The energy change during penetration is thus given by:

$$I_{T} = 2\pi a p (\gamma_{SL} - \gamma_{SV}) - \pi \gamma_{LV} (2ap - p^{2})$$
 (5.15)

For full penetration, p = 2a and the work done by the particle is given by:

$$I_{T} = -4\pi a^{2} (\gamma_{SV} - \gamma_{SL}) \qquad (5.16)$$

This work must be done at the expense of the kinetic energy of the particle which, for complete penetration, must be greater than $I_{\mathbf{m}}$ and so:

$$\frac{1}{2} m U^{2} \ge -4 \pi a^{2} (\gamma_{SV} - \gamma_{SL})$$
 (5.17)

i.e.
$$v^2 \ge -\frac{12}{\rho_{p}d} (\gamma_{SV} - \gamma_{SL})$$
 (5.18)

It has been assumed that the interfacial energies are not functions of the depth of penetration or of the velocity of penetration. Such an assumption is not strictly true. The movement of the line of contact between the three phases is not a quasistatic process. Equilibrium assumptions cannot therefore

be used to calculate exact values of the interfacial energies since these change during penetration owing to the reordering of the molecules at the interfaces. Moreover, whilst it is possible to obtain values of γ_{SV} from the experimental work of El Shimi and Goddard (65) and to calculate values of γ_{ST} from the equations proposed by Wu (74) and amplified by Good (26), the figures so obtained cannot be used in Equation (5.18) without introducing error. In fact, there are no reliable ways of predicting γ_{SV} and γ_{SL} under non equilibrium conditions. Phillips and Reddiford (56) have studied moving interfaces experimentally. Quy (69) has made a theoretical hydrodynamic study of liquid flow between two parallel plates and has related the changes in contact angle to the flow velocity. However, such attempts as these have only been concerned with very slow movements of the interface and do not therefore correspond to the present experimental conditions where the velocity of penetration is high.

When the particle begins to penetrate, the liquid surface will exhibit the same characteristics as the receding edge of a droplet moving on a hydrophobic surface. The work done on the particle by the drop surface during this time will thus be greater than that which would be predicted if quasistatic theory were used. After a certain amount of penetration, the line of three phase contact will form an effective "advancing contact angle" and the work done by the particle will be greater than

that which would be predicted using equilibrium assumptions.

Over the whole penetration process the two errors are cancelled out to some undefinable degree. Under these circumstances, it is convenient, despite the reservations outlined above, to use the Young-Dupré equation in order to correlate the interfacial energies such that:

$$\gamma_{SL} = \gamma_{SV} - \gamma_{LV} \cos \theta \qquad (5.12)$$

where 0 is the equilibrium contact angle between the three phases. Thus for full penetration, Equation (5.18) reduces to:

$$v^2 \ge -\frac{12\gamma_{LV}}{\rho_{\rho}d} \cos \theta \tag{5.19}$$

This is similar to the result proposed by Pemberton (54) for $0=180^{\circ}$. The right hand side is negative because, for $0>\pi/2$, Cos 0 is negative and hence work must be done by the particle to penetrate. However, for $0<\pi/2$, the work done is positive, signifying that the surface of the drop will do work upon the particle to make it penetrate. Therefore, a particle which has an air-water-particle contact angle of less than $\pi/2$ has only to touch the surface of the droplet in order to be captured by it. This is a possible explanation of why so many doubts have been expressed in the literature as to whether or not the capture efficiency of aerosol particles can be less than unity. If contact between the particle and the water may be assumed at all stages of the collision then it is only for materials for

which θ is less than $\pi/2$ that the capture efficiency will be decreased.

Equation (5.19) may be expressed in dimensionless terms as:

$$\frac{U_{R}^{2}}{U_{\infty}^{2}} = -\frac{12 \cos \theta}{We}$$
 (5.20)

where We is the Weber number of the system given by:

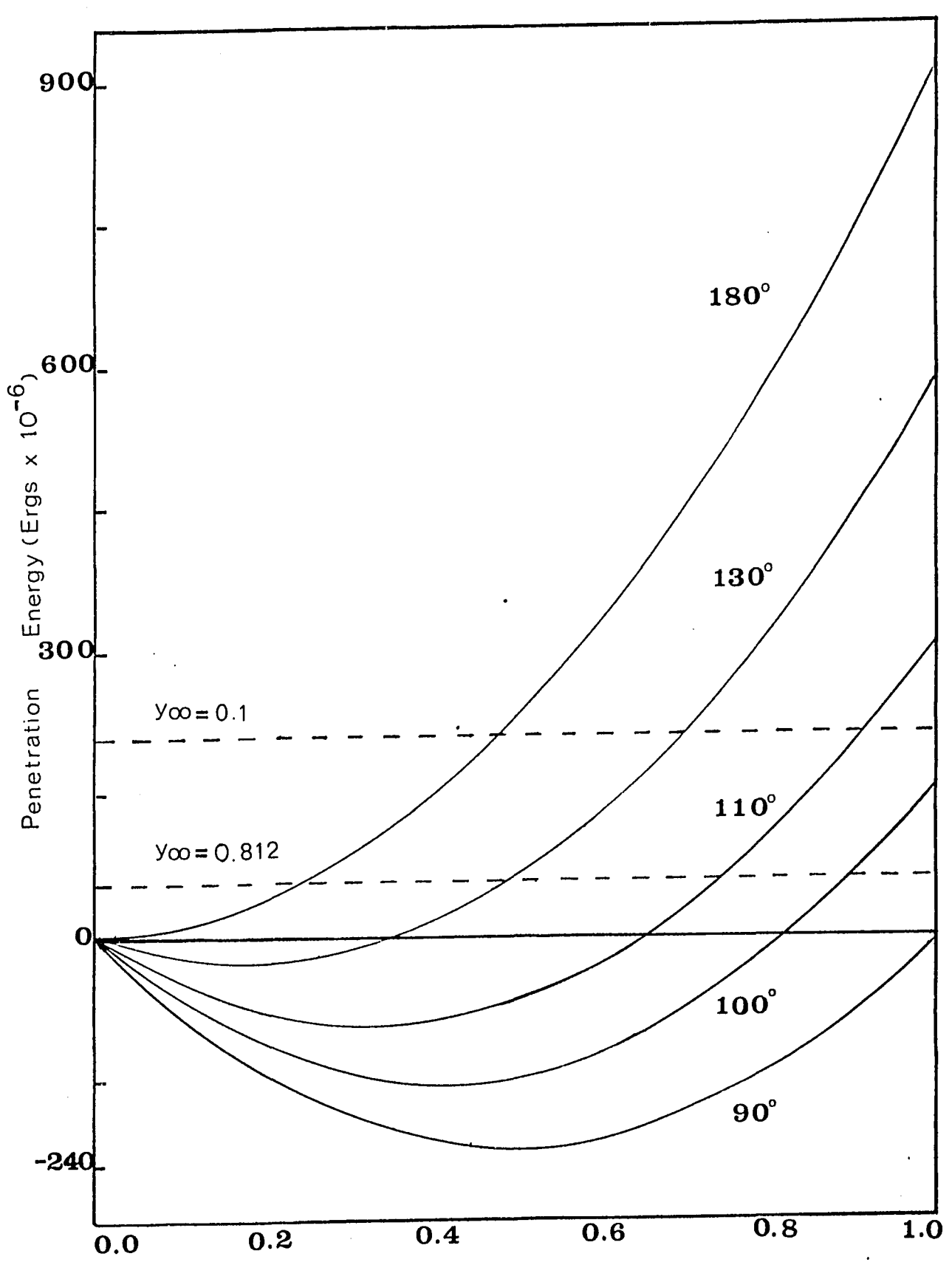
$$We = \frac{\rho_{\rho} dU_{\infty}^{2}}{\gamma_{LV}}$$

Thus the minimum velocity for penetration is shown to be governed by two system parameters, the Weber number, and the contact angle.

Equations (5.12 and 5.15) may be evaluated as a function of p. The results for a 20µ particle, for contact angles of 90° , 100° , 110° , 130° and 180° , are shown in Figure 5.4. As may be seen, the penetration energy is negative for the initial part of the penetration and never becomes positive for $0 = 90^{\circ}$. For $0 > 90^{\circ}$, the energy function passes through a minimum and then rises to the value necessary for complete penetration of the particle. For $0 = 180^{\circ}$, there is no minimum in the energy function which is never less than zero. The negative values of $\mathbf{I_T}$ occur when the change in area of the liquid-vapour interface produces more energy than is used up by the formation of the

Figure 5.4

CORRELATION OF PENETRATION ENERGY
WITH PENETRATION



Penetration (Particle Diams.)

solid-liquid interface. The practical significance of these minima is that the surface of the droplet does work upon the particle to make it penetrate to the position, p, where the minimum occurs. Thus the fact that I_T never becomes positive for $\theta=90^\circ$ means that no penetration energy is required and that the particle will behave as a completely wettable particle.

Values of the approach energy of a particle as it arrives at the droplet surface, for two values of y_{∞} and for K = 7.0, are also drawn and are shown as horizontal, dotted lines on the graph. As may be seen, the particle trajectory which begins at $y_{\infty} = 0.1$ has sufficient energy to penetrate the surface for an aerosol material whose contact angle is 100° . However, if 0 is 110° , this particle would not penetrate. For $y_{\infty} = 0.812$, the particle could not pass through the drop surface completely even for $0 = 100^{\circ}$. In this case, the particle would penetrate up to 0.89 diameters and then be stopped, all of its kinetic energy being expended in overcoming the surface tension forces.

5.3 Interactive Forces

Before the particle reaches the surface of the drop, it will be subject to surface to surface interactive forces which are effective over very small separations. These forces are notable for the lack of accuracy with which they can be predicted. In real situations, they will be modified as a result of contamination of the air-water interface both by foreign matter and the presence of aerosol particles which have already been captured. However, in an ideal situation, there are 3 main types of forces acting on the particle, van der Waals forces, electrostatic forces, and viscous forces.

5.3.1 van der Waals forces

There has been much work published on the forces between a collecting surface and an approaching particle and most workers agree that, whilst small and difficult to calculate, van der Waals (VDW) forces can constitute, under some circumstances, an important parameter in collision dynamics. As early as 1954, Jordan attempted to assess the role of VDW forces in the adhesion of particles within dust sampling instruments (35) and, in 1955, Gillespie considered the problem of the attachment of small particles to filter fibres (24). A recent series of papers by Dahneke (11, 12, 13) has made considerable

progress in formulating the solution to the dynamics of the impact between latex particles and solid plates. Spielman (66, 67), and Derjaguin and Smirnov (15) have independently developed theories to describe the deposition of particles by VDW forces onto a sphere in Stokes flow. It seems desirable, therefore, to examine the effects of VDW forces.

It has been known for many years (27) that VDW forces exist between a macroscopic sphere and a plane surface or half space. However, it has become possible only very recently to estimate with any certainty the order of magnitude of these forces, and even then only in the case of specific systems for which values of the fundamental constants have been published. A good summary of the theory of VDW forces and a review of the present state of knowledge on them has been given by Israelachvili and Tabor (34).

For non-polar substances such as paraffin wax, the forces result from the instantaneous dipoles caused by the changes in relative positions of the electrons in the molecules of the materials involved. The dipole generates an electric field which polarises a nearby molecule thereby inducing in it another dipole moment. The resulting interaction between the two dipoles creates an instantaneous attractive force between the two molecules, and the time average of this force is finite. These forces between neutral atoms are generally referred to as dispersion forces or London forces and are one component of the

total van der Waals force. The other two components are orientation forces, which are caused by the alignment and subsequent attraction of two polar molecules, and induction forces, which are caused by a polar molecule inducing a dipole moment in a nearby neutral molecule. For the highly polar material of water, the ratio of the dispersion, orientation, and induction forces is 4:20:1 (34).

When two molecules are an appreciable distance apart, the time taken for the electrostatic field from the first molecule to reach the second and then return may be comparable with the fluctuating period itself. In this case, the dipole of the first molecule is no longer in phase with that of its neighbours and the laws of force change. The interaction is referred to as the retarded van der Waals force and was first proposed by Casimir and Polder (10). In general, less is known of the magnitude of retarded forces than is known about non-retarded forces, especially concerning the range of distances of separation over which the retarded forces operate. It is normally accepted that the retardation effects start at distances of about 0.1λ (where λ is the wave length of the intrinsic electronic oscillations of the molecules) but that the forces are not fully retarded until the separation is of the order of Theoretical predictions of VDW forces are available only for fully retarded and fully non-retarded interactions.

The forces between large bodies can be obtained by one of two methods, the microscopic approach which considers all

the atoms within the body, or the macroscopic approach where the large bodies are treated as continuous media and the forces are drived in terms of their bulk properties. In the microscopic approach, the force between the bodies is determined by integration of the interactions between all the atoms within the two bodies (27). Israelachvili and Tabor give expressions for the interactive force between a sphere and a half space as follows:

For non-retarded forces:

$$F_1 = \frac{A'a}{6H^2}$$
 (5.21)

For retarded forces:

$$F_2 = \frac{2\pi A''a}{3H^3}$$
 (5.22)

where H is the gap between the two surfaces, and A' and A" are the Hamaker constants for the non-retarded and retarded VDW forces respectively.

- estimation of the Hamaker constant

The equations for the magnitude of the VDW forces have always been expressed in terms of constants such as the Hamaker constant whose value was very difficult to predict. However, as a result of recent research, it is now possible to calculate these constants, and hence the forces involved, in a more precise

way. Krupp et al (39) have recently published a set of computations of the 'Lifshitz-van der Waals constant' $(h\overline{\omega})$ which is related to the Hamaker constant as follows:

$$h\,\bar{\omega} = \frac{4}{3}\pi A^{\dagger} \tag{5.23}$$

For non-retarded forces between two dissimilar materials 1 and 2 interacting through a medium 3, their results were calculated from the equations:

$$h\bar{\omega} = h \int_{0}^{\infty} \frac{\varepsilon_{1}(i\xi) - \varepsilon_{3}(i\xi)}{\varepsilon_{1}(i\xi) + \varepsilon_{3}(i\xi)} \cdot \frac{\varepsilon_{2}(i\xi) - \varepsilon_{3}(i\xi)}{\varepsilon_{2}(i\xi) + \varepsilon_{3}(i\xi)} d\xi \qquad (5.24)$$

with

$$\varepsilon_{j}(i\xi) = 1 + \frac{2}{\pi} \int_{0}^{\infty} \int_{\xi^{2} + \omega^{2}}^{\varepsilon_{j}''(\omega)\omega} d\omega$$
 (5.25)

where ε_{j} (iξ) is the dielectric permittivity of medium, j, at imaginary frequency, (iξ); h is Planck's constant (= 1.054 x 10^{-27} erg-sec.); ω is the angular frequency of photon energy: and ε_{j} "(ω) is the imaginary part of the complex dielectric constant of medium j. Values of $h\overline{\omega}$ were calculated by numerical analysis of ε_{j} " determined from optical reflection measurements. Such calculations as these are beyond the scope of this work.

A review of the literature shows that there is insufficient information available to estimate A' for either D.O.P. or talc. However, solid alkanes such as paraffin wax and, to a lesser degree, liquid alkanes such as paraffin oil have been studied

and it is possible to proceed with an estimation of their properties.

As Krupp et al did not calculate a value for a paraffin wax-water-air system, a simple way must be found to estimate the Hamaker constant. Israelachvili and Tabor examine the accuracy of a variant of the Berthelot relationship:

$$A'_{132} = (A'_{132} \cdot A'_{232})^{1/2}$$
 (5.26)

where the subscripts refer to medium 1 acting on medium 2 through medium 3. They find that the relationship always gives an overestimate for A_{132} but is accurate to within 1-3%. the case of the experiments presented in this work, medium 1 is paraffin wax, medium 2 is water, and medium 3 is air. estimate of the Hamaker value for this system has ever been Furthermore, compared with the intensively studied ideal case of interactions across a vacuum. little is known about the effects of air as the third medium. However, it can be seen from Equation (5.24) that the effect of the medium is related to its dielectric constant, the higher the dielectric constant the lower the VDW forces. As the difference between the dielectric constant of vacuum (1.0) and the dielectric constant of air (1.000536 at 20°C and 1 atm.) is small, the Hamaker constant in air will be assumed, in the absence of information to the contrary, to be approximated by the Hamaker constant in vacuum (A!;). Krupp et al (39) calculated the

Lifshitz-van der Waals constant for water-water interaction to be 1.14 eV. From Equation (5.23), this yields a value for A_{22} of 4.35 x 10^{-13} ergs. Israelachvili and Tabor quote a value of A_{11} for solid n-alkanes of 8.8 x 10^{-13} ergs. Substitution in Equation (5.26) gives:

$$A'_{132} = A'_{12} = +6.19 \times 10^{-13}$$
 ergs.

where the positive sign signifies, using the normal surface force notation, that the force is repulsive. For liquid nalkanes a value of 6.3×10^{-13} is quoted. This yields:

$$A'_{12} \approx 5.12 \times 10^{-13} \text{ ergs.}$$

These are approximate figures but, since they are probably accurate to at least a factor of 2, they are useful for the analysis of the experimental results in the present work.

There are no reliable, simple ways of estimating the Hamaker constant for retarded forces. Even the concept of a single valued Hamaker constant for retarded forces is rather dubious and suggestions have been made for replacing it with a Hamaker function, the value of which would depend on the size of the particle and the gap width (53). In general, however, the longer range retarded forces appear to be less important than the shorter range non-retarded forces, Parsegian and Ninham (53) have calculated, for example, that lipid waxes in a water system exhibit only very weak retardation effects.

These forces will, therefore, be ignored in the following discussion.

- energy losses and surface deformation

For the purpose of this analysis it is necessary to estimate the energy loss due to repulsive surface forces. The normal force between the surfaces is approximated by:

$$F = \frac{A'_a}{6H^2} \tag{5.27}$$

$$I = \int_{H_0}^{H_1} F dH = -\frac{A'a}{6} \left[\frac{1}{H}\right]_{H_0}^{H_1}$$
 (5.28)

 H_{0} can be assumed to be ∞ . At $H_{1}=0$, the force appears to become infinite. However, Krupp (38) suggests that the maximum VDW pressure between interacting surfaces occurs at separations of approximately 4°A because bonds of a chemical nature tend to predominate below this gap width. This figure can thus be used as a value for H_{1} . Therefore, for a 20 μ particle of paraffin wax approaching a water droplet, the normal energy change is given by:

$$I_s = -2.58 \times 10^{-9} \text{ ergs.}$$

For a paraffin wax particle travelling towards a 0.1 cm drop at a velocity of 354.4 cm/sec. such that K = 1.5, the normal

kinetic energy has been shown to vary between 1.1 and 2.2 x 10^{-4} ergs depending on the value of y and the separation of the particle. Since, in this case, the energy lost in overcoming VDW repulsive forces is only 0.002% of the approach energy, it can be neglected. However, for particles travelling at a smaller speed, as low as 2 cm/sec. for example, the VDW energy losses would certainly become significant.

Besides the problem of energy loss there is the question of the water air interface. If this interface, which is not rigid, is deformed by the action of VDW forces before contact between the water and the particle, then the work required to achieve a given penetration is increased. In order to check both the assumption that the contact between the water and the particle is not hindered by VDW forces, and the validity of neglecting energy losses, a simple model was constructed to calculate the change in the gap width and the interface deformation with time.

Consider a sphere approaching a deformable half space with which it has a repulsive surface interaction. As the sphere approaches, the wall will deform. Assume that, despite this deformation, the force law between the sphere and the wall remains the same. Assume also that as the wall deforms it takes on the same shape as the sphere, namely a spherical cap.

Let B be the centre to centre separation of the drop and the particle, H be the gap width, δ the depression in the drop

surface, and p the extent of the particle penetration into the droplet's surface (See Figure 5.5). Let the force due to the surface tension opposing the progress of the particle be \mathbf{F}_{T} , and the force due to VDW repulsion be \mathbf{F}_{S} .

The normal or radial velocity of the particle with respect to coordinates fixed at the drop centre is:

$$U_{R} = -\frac{dB}{dt} \tag{5.29}$$

Also:

$$B = a + R - p (5.30)$$

where p may take all values from -H_O, the initial gap width, to +2a for complete penetration. The particle equation of motion gives:

$$m \frac{d^2B}{dt^2} = F_s$$

where m is the mass of the particle.

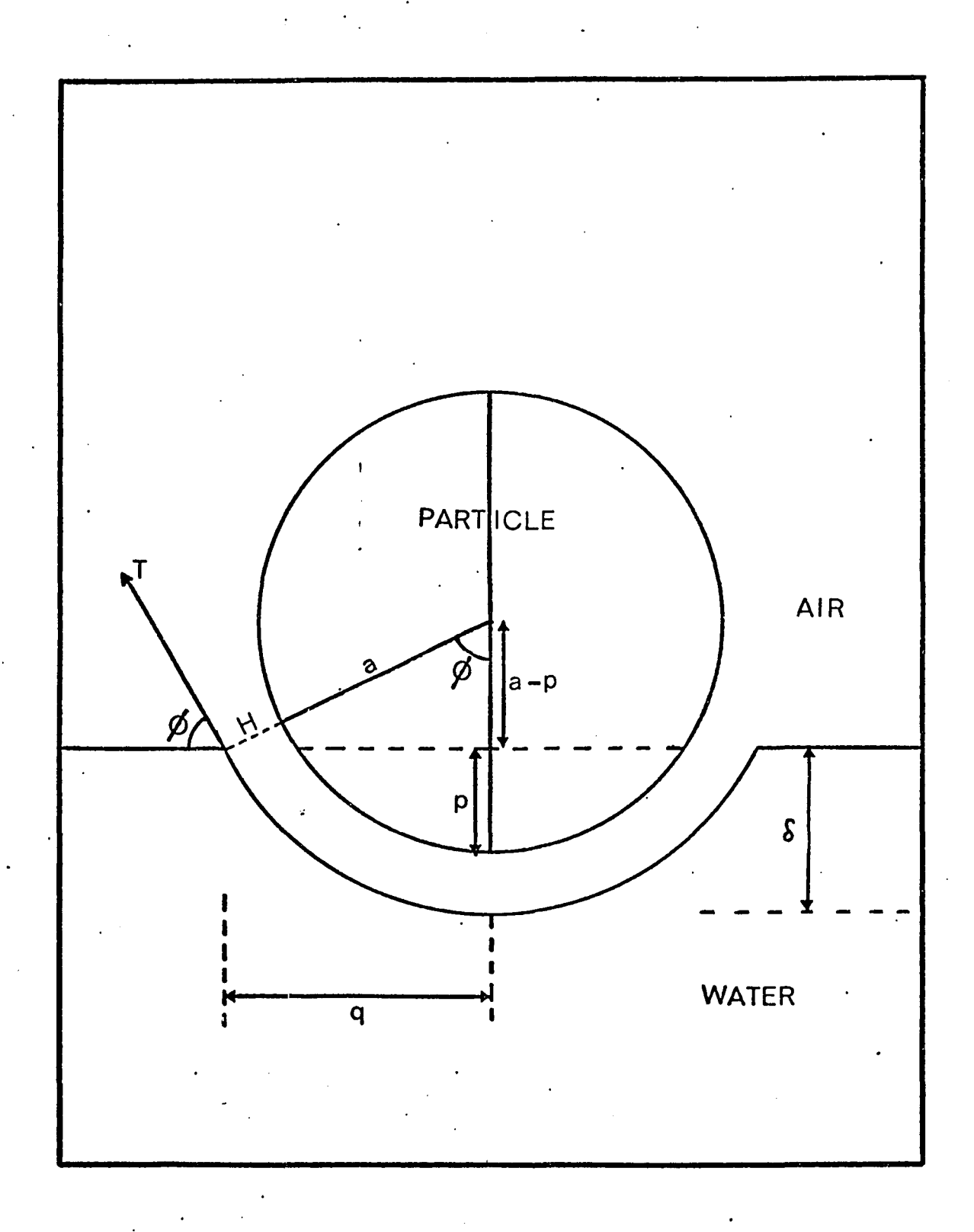
$$\therefore \frac{dU_R}{dt} = -\frac{F_S}{m}$$

$$\therefore \frac{dU_R}{dt} = -\frac{A(H)}{8H^2\pi a^2 \rho_0}$$
 (5.31)

where A(H) is a Hamaker function whose numerical value depends on gap width increasing from 0 at ∞ to A' at close separation,

Figure 5.5

APPROACH OF A PARTICLE TO
A DEFORMABLE SURFACE



and whose value is assumed calculable for any II.

The normal component of the surface tension force opposing deformation is given by:

$$F_{T} = -2\pi q\sigma \sin \phi$$

where $q = (a + II) \sin \phi$

$$F_{\rm T} = -2\pi\sigma \ (a + H) (1 - \cos^2\phi)$$

where $Cos \phi = \frac{a - p}{a + H}$

$$F_{T} = -2\pi\sigma (a + H) - \frac{(a - p)^{2}}{(a + H)^{2}}$$

$$\frac{dF_{T}}{dt} = -2\pi\sigma \left[2\frac{(p-a)}{a+H} \frac{dp}{dt} + (1-\frac{(a-p)}{(a+H)}^{2}) \frac{dH}{dt} \right]$$

Now:

$$\frac{dp}{dt} = -U_R \tag{5.29}$$

$$\therefore \frac{dF}{dt}T = -2\pi\sigma \left[-2(\frac{p-a}{a+H})U_{R} + (1-(\frac{a-p}{a+H})^{2})\frac{dH}{dt} \right]$$
 (5.32)

Equation (5.27) gives:

$$\frac{dF_s}{dt} = -\frac{1}{3} \frac{A(H)a}{H^3} \frac{dH}{dt}$$
 (5.33)

Equating (5.32) and (5.33) gives:

$$\frac{dE}{dt} = \frac{4\pi\sigma U_R (p-a)/(a+E)}{2\pi\sigma (a+E)^2 + (a-p)^2 - \frac{A(H)a}{3H^3}}$$
(5.34)

There are thus 4 equations in the 4 unknowns, B, U_R , p, H:

$$B = a + R - p$$
 (5.30)

$$\frac{dB}{dt} = -U_{R} \tag{5.29}$$

$$\frac{dU_{R}}{dt} = \frac{-A(H)}{8H^{2}\pi a^{2}\rho_{0}}$$
 (5.31)

$$\frac{dH}{dt} = \frac{4\pi\sigma U_R (p - a)/(a + H)}{2\pi\sigma (a + H)^2 + (a - p)^2 - A(H)a}$$
(5.34)

With initial conditions: at t = 0; H = H_o, U_R = U_o, B = H_o + a + R, p = -H_o, $\frac{dH}{dt}$ = -U_o, $\frac{dB}{dt}$ = -U_o, $\frac{dU_R}{dt}$ = 0.

This model is very simple and could easily be solved numerically if the Hamaker function were available. Unfortunately, the lack of any such expression makes the use of these equations very difficult. For the present purposes, the function A(H) was set at A' and the forces were arbitrarily assumed to act over a certain distance. The equations were solved numerically using the fourth order Runge-Kutta-Merson technique (40). Variations in B, U_R , H, p, and δ were computed

with respect to time for differing approach velocities and values of A'. As would be expected, the results were heavily dependent upon the starting distance at which the forces were assumed to act, and so the results are only useful in a qualitative sense. They showed that in all cases for approach velocities up to 400 cm./sec. there was some deformation of the drop surface before the gap width shrank to zero. It seems therefore likely that the surface of the droplet will be at least slightly deformed before the particle touches it by the action of van der Vaals forces.

5.3.2 electrostatic forces

The effect of electrostatic forces on the experimental results for wettable aerosols has already been discussed in Chapter 3. From Equation (3.10), the attractive force on a particle as it approaches an earthed collecting sphere of radius R in a typical aerosol of concentration 50 particles/cc. is given by:

$$F_{e} = 2.31 \times 10^{-15} \frac{R}{H^{3}} - 9.23 \times 10^{-15} \frac{RH}{(H^{2}-R^{2})^{2}}$$
(5.35)
$$- 4.84 \times 10^{-13} \frac{R^{3}}{H^{2}} - 6.93 \times 10^{-13} \frac{R^{2}}{H^{2}}$$

The energy change in moving a particle from a separation, H_1 , to a position, H_2 , nearer the collector is given by:

$$I_{e} = \int_{H_{1}}^{H_{2}} F_{e} dH$$

Thus for a 0.1 cm. diameter droplet:

$$I_{e} = \left[-\frac{8.00 \times 10^{-18}}{H^{2}} - \frac{4.62 \times 10^{-16}}{(H^{2} - 0.01)^{2}} + \frac{9.52 \times 10^{-17}}{H} \right]_{H_{1}}^{H_{2}}$$
(5.36)

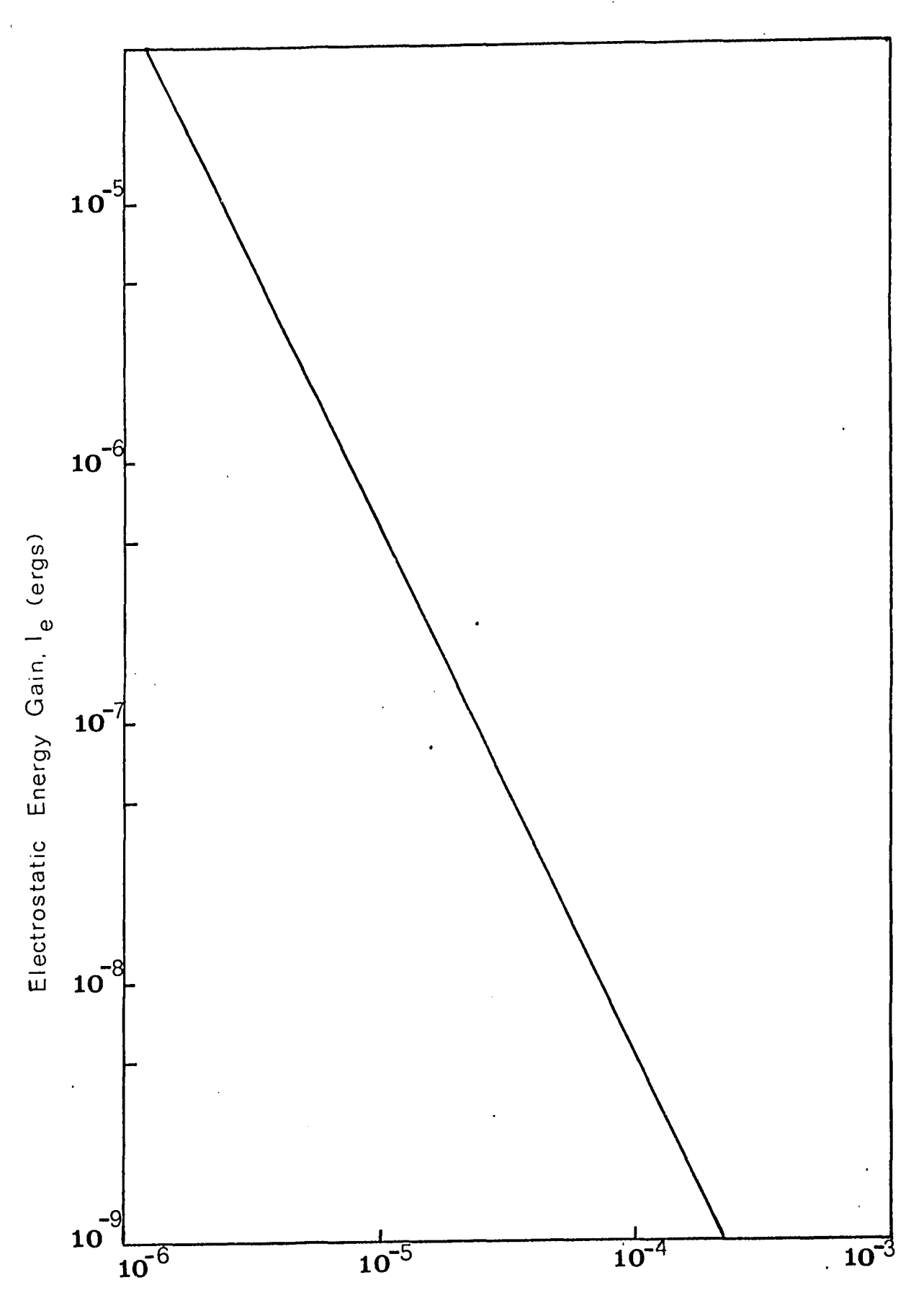
Figure 5.6 shows this function for separations H_2 between 10^{-3} and 10^{-6} cms. assuming that $H_1 = \infty$.

When the particle actually touches the droplet, it will lose its charge. Should it rebound, however, it will still be subject to the image force from the charge induced in the collector by the particles in the main stream and to the image forces resulting from charges induced in it by its neighbours. The sum of the two types of forces is represented by the third term in Equation (5.36) and the electrostatic energy lost during rebound is thus given by:

$$I_{e} = \left[\frac{9.52 \times 10^{-17}}{H}\right]_{H_{1}}^{H_{2}}$$
 (5.37)

Figure 5.6

ELECTROSTATIC GAIN AS A FUNCTION OF SEPARATION



Separation (cms)

However, this term is very small with respect to the first term in Equation (5.36) and so the electrostatic forces on rebound may be neglected.

5.3.3 viscous forces

There will be a boundary layer around the droplet at the Reynolds numbers encountered in the experiments and the fluid in the inner region of this boundary layer can be considered This fluid will have an effect on the trajectory of viscous. the particle which will lose kinetic energy to the viscous damping forces in the gap between it and the droplet. work has been done on the phenomena which occur between two approaching surfaces. As early as 1879, Lord Rayleigh was experimenting with coalescing water drops and attributed incidences of non cohesion to the viscous effects in the intervening gap. A complete review of this complicated field is beyond the scope of this work. It has been well covered by Brenner (9) and also by Bart (3) who has presented a general model for a sphere approaching any interface. The parameters of this model change according to the nature of the interface.

The approach of a rigid sphere to a deformable interface has been studied experimentally by, among others, Riolo et al (61), Hartland (30), and Hodgson and Woods (33). However, all of these experiments have been conducted in liquids and the

results obtained have only a qualitative relevance to the present situation. Two recurring features have nevertheless been observed. First, the interface will deform slightly upon the approach of the particle. Secondly, the film will not drain uniformly. A 'dimple' of the particle bearing fluid is captured between the two surfaces because the interface deforms to meet the particle in a ring coaxial with the line of collision. This dimple of air is forced into the droplet if the particle penetrates. Such an effect has been observed by Whelpdale and List (72) who followed the trajectories of air bubbles in a water drop after it has collided with another smaller droplet. There are three conclusions that can therefore be drawn from these observations. First, there will be some energy loss to viscous forces as the particle approaches the droplet surface. Secondly, there will be deformation of the droplet surface before particle liquid contact which means that a higher amount of penetration energy is required. there is the possibility of an air bubble from the draining film being trapped and forced into the drop. The formation of this bubble would require a certain amount of surface energy which would also be gained at the expense of the particle's kinetic However, these last two effects could reasonably be expected to be small and will not be considered further.

In order to estimate the relative magnitude of the viscous losses, it is necessary to be able to calculate the

forces between a sphere and the surface which it is approaching. All the literature on this subject deals, however, with quasistatic flow in a stagnant fluid so that the time dependent term in the Navier Stokes equation is negligible. This is the creeping flow regime which normally carries a constraint that the Reynolds number be much less than one for exactitude with a cut off point of Re = 1 for practical applicability of the equations. If the normal velocity of the particle relative to the collector at the outer edge of the boundary layer is considered, then the particle Reynolds number varies from 2.0 to 4.5 depending on the angle of incidence. This is not within the creeping flow regime. Furthermore, the fluid at the interface is not quiescent since it has tangential motion due to the viscous shear forces.

These factors mean that the quasistatic assumptions are not exact in the practical case. However, in order to discuss the collision process, some estimate of the energy loss to viscous damping is necessary and, since there are no published alternatives to the low Reynolds number situation, the quasistatic approach will be used as an order of magnitude approximation.

Brenner (8) and Maude (45) independently proposed exact equations for the quasistatic approach of a sphere to a solid surface and to a free surface. The free surface results that they give are:

$$\mathbf{F} = 6\pi\mu \,\mathrm{aU}_{\mathrm{R}}\lambda \tag{5.38}$$

where

$$\lambda = -\frac{4}{3} \sinh \ell \sum_{n=1}^{\infty} \frac{n(n+1)\ell}{(2n-1)(2n+3)} 1 - \frac{4\cosh^{2}(n+\frac{1}{2})\ell}{2\sinh(2n+1)\ell}$$

$$+ \frac{(2n+1)^{2}\sinh^{2}\ell}{(2n+1)\sinh^{2}\ell}$$

$$(5.39)$$

As this summation is complex, a simplification will be used. At small gap widths, it may be shown (9) that:

$$\lim_{H \to 0} \frac{H\lambda}{a} = 1$$

such that the force is given by:

$$F = \frac{-6\pi\mu a^2 U_R}{H} {.} {(5.39)}$$

This equation has been tested experimentally by MacKay and Mason (44) for nylon spheres falling through oils. They found that it gave good agreement with experiment for $H \le 0.01$ cm.

Equation (5.39) has been used to calculate the energy loss of the particle as it approaches the collector. Ignoring deceleration, the energy loss was computed from the integral of the force with respect to the gap width:

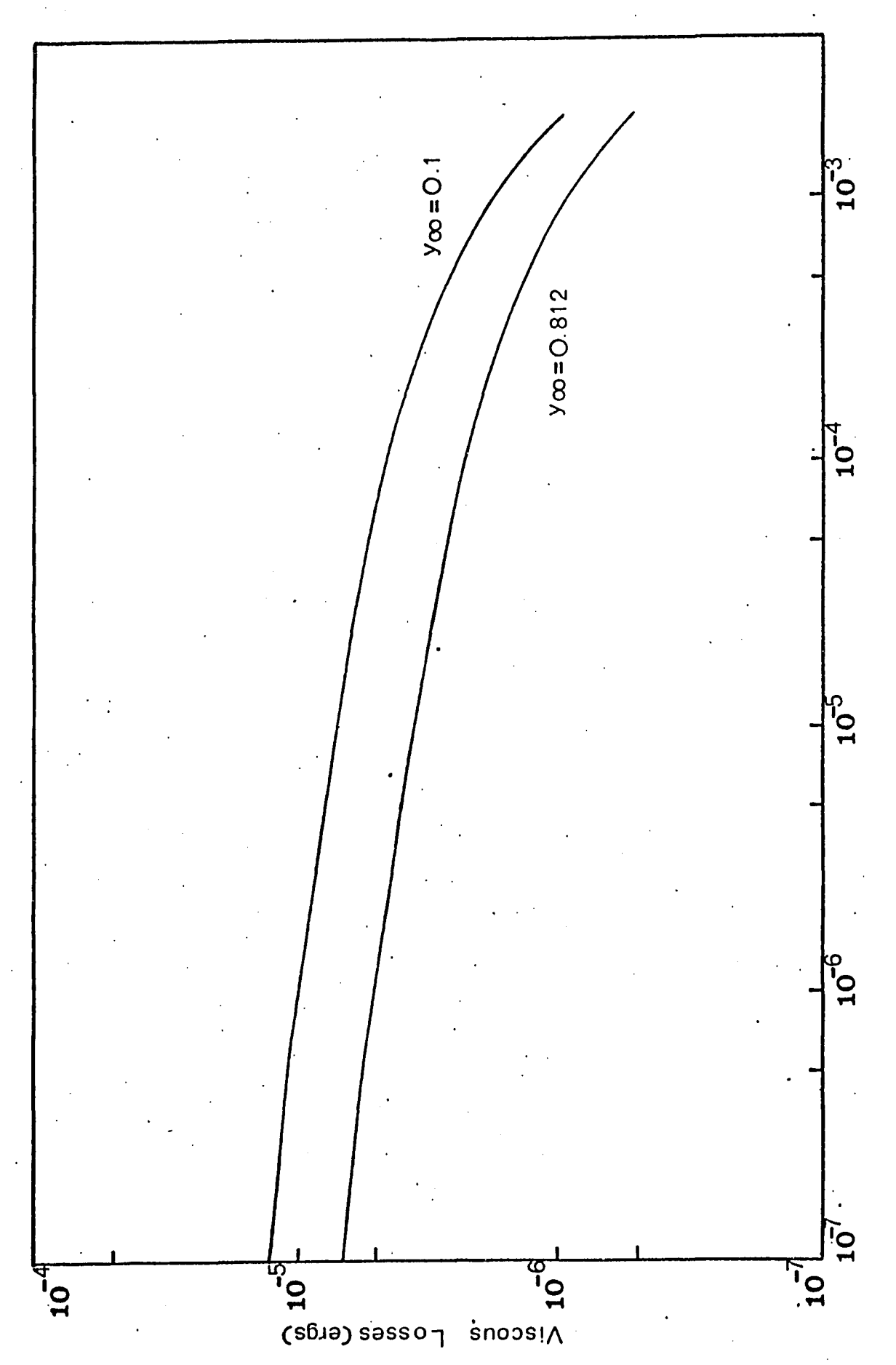
$$I_{vi} = -6\pi\mu a^2 U_R \ln \frac{H_2}{H_1}$$
 (5.40)

The values of I_{vi} calculated are relatively insensitive to the choice of H_1 . For convenience, H_1 was put equal to 0.1R which was chosen to be representative of the boundary layer thickness at the appropriate Reynolds number. It was found that doubling H_2 made only 10% difference in the values of I_{vi} . The value of 0.1R, however, provides a conservative estimate of the actual force as it is only the inner region of the boundary layer which may be considered truly viscous. The neglect of the deceleration of the particle, which makes the integration of the force equation possible analytically, also ensures that I_{vi} is overestimated. Results for the paraffin wax example are shown in Figure 5.7. The normal velocity of the particle as it impacted with the surface was calculated from its trajectory using potential flow assumptions. This was then used to calculate the energy loss from Equation (5.40).

Thus it is now possible, using the magnitudes of the various energy functions, to evaluate the two inequalities (5.5) and (5.7) and so predict whether a colliding particle will be captured by the droplet or not. This will, in effect, constitute a discussion of the experimental results and will be the central theme of the next chapter.

Figure 5.7

ENERGY LOSS TO VISCOUS FORCES
.
AS A FUNCTION OF SEPARATION



Separation, H (cms.)

Chapter 6

RESULTS AND DISCUSSION

The criterion for penetration derived in Section 5.2 is a very useful result. It is analogous to the expressions derived by Pemberton (54) and more recently by MacDonald (43). Both these authors assumed that penetration was necessary for collection, but whilst they had much to say on the subject of penetration which did not result in capture, they dwelt very little on the more likely possibility of capture without penetration.

The point of this chapter is to make good this deficiency in their discussion and to expand the theoretical outline provided in Chapter 5 to the analysis of real situations. First, the penetration criterion will be used to calculate values of 'penetration efficiency'. Secondly, these calculated values will be compared with the experimental results for hydrophobic particles. The comparison is favourable. In the light of these comparisons, it appears that there is some sort of correlation between 'penetration efficiency' and collection efficiency for the systems studied. In the final section, this correlation will therefore be discussed for the experimental conditions using both the schema proposed in Section 5.1 and the estimates of the energy losses derived in Section 5.3.

6.1 Calculation of Penetration Efficiencies

It has proved impossible to fit the long range interactive forces into the potential flow model and thereby calculate their effects on collection efficiency because of the discontinuities that they induce in the particle's equation of motion. However, the penetration criterion derived in the last chapter does not have this disadvantage. The minimum radial velocity to ensure penetration is given by:

$$U_{R}^{2} = -\frac{12\sigma \cos \theta}{d\rho_{p}}$$
 (5.19)

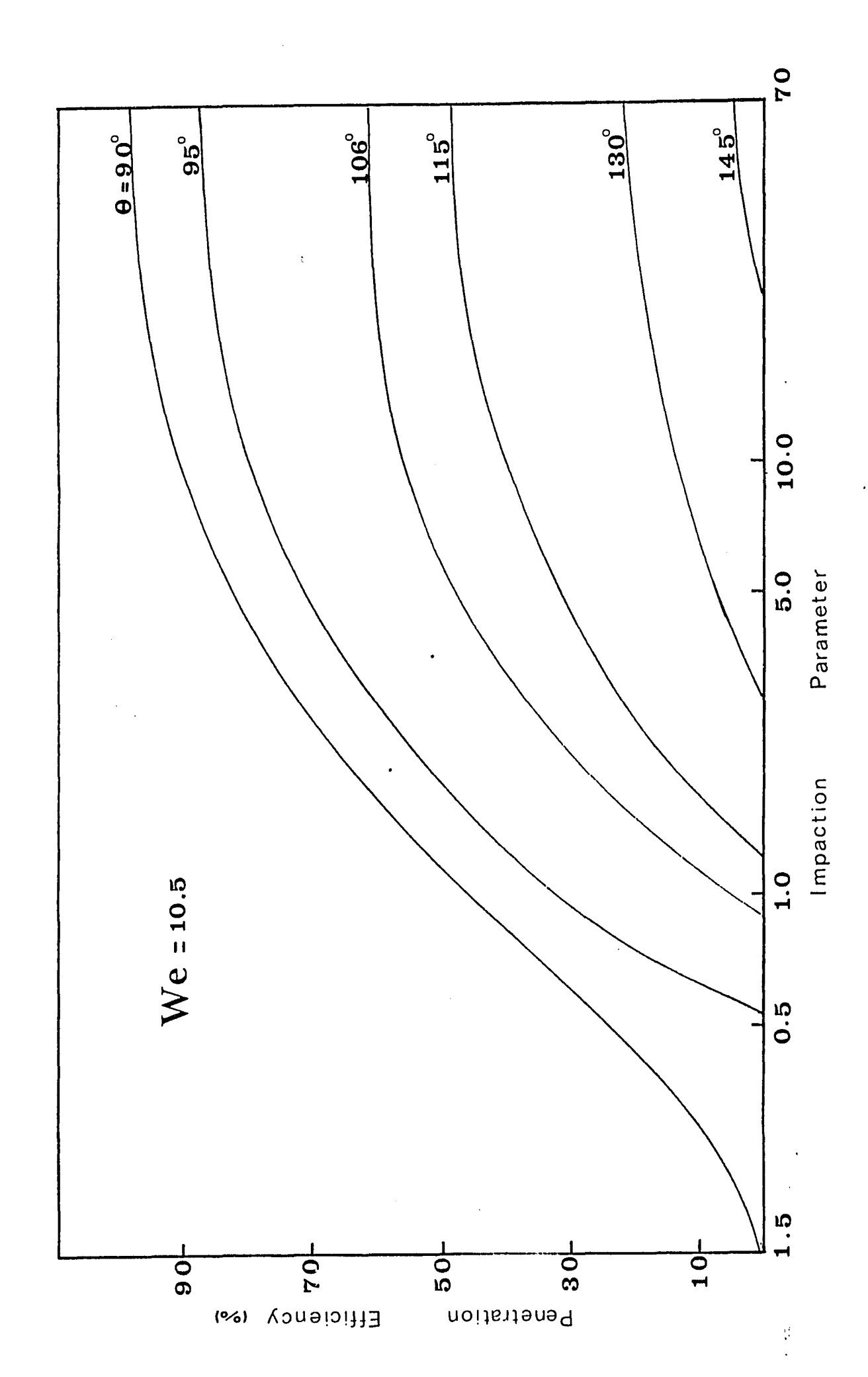
Thus the inclusion in the program of a simple boundary condition that U_R be greater than this value at the moment of impact will serve to locate the limiting trajectory for a particle which just penetrates the drop. This has been done, and the program has been used to calculate a form of 'penetration efficiency' defined, analogously to collection efficiency, as the square of the initial distance from the vertical axis of the drop of a particle whose trajectory just gives it enough normal momentum to penetrate the surface. The penetration efficiencies thereby calculated are a function of the Weber number and also of the contact angle θ . Figure 6.1 shows the variation of this penetration efficiency with impaction number for varying contact angles at a constant Weber number of 10.5. As may be seen, there is no collection at this value of We for K < 100 for

Figure 6.1

VARIATION OF PENETRATION EFFICIENCY WITH

IMPACTION PARAMETER FOR DIFFERENT CONTACT

ANGLES AT We = 10.5



contact angles above 145°. The top curve in the figure is the line for $0 \le 90^\circ$ which corresponds to the case of wettable particles. Figure 6.2 shows the variation of penetration efficiency with We at a constant contact angle of 102° which corresponds to the practical case of paraffin wax. Again the top curve represents wettable particles. The penetration efficiency was also found to be a function of a/R and of the gravitational settling velocity G. Figure 6.3 shows this variation for $0 = 102^\circ$ and We = 8.0.

An alternative way of looking at these results is suggested by Pemberton's original analysis of the situation for non-wettable particles (54). He defines a parameter that is effectively the same as the fraction of the particle's initial momentum which must be used up in penetrating the droplet surface. In the present analysis, this may be defined as:

$$M = \frac{\left(\frac{-12\sigma \cos \theta}{\rho_{p} d}\right)^{1/2}}{U_{m}}$$

M may vary between 0, for wettable particles, and 1.0, for extremely low values of We, and is effectively a dimensionless velocity. It is a very simple characterisation of any system for a practical application as it combines both the variables We and 0 into one parameter which can vary between apparently well-defined limits. MacDonald has discussed the use of this quantity in cases of partial wettability (43). It was decided

Figure 6.2

VARIATION OF PENETRATION EFFICIENCY WITH IMPACTION PARAMETER FOR DIFFERENT WEBER NUMBERS AT $0 = 102^{\circ}$

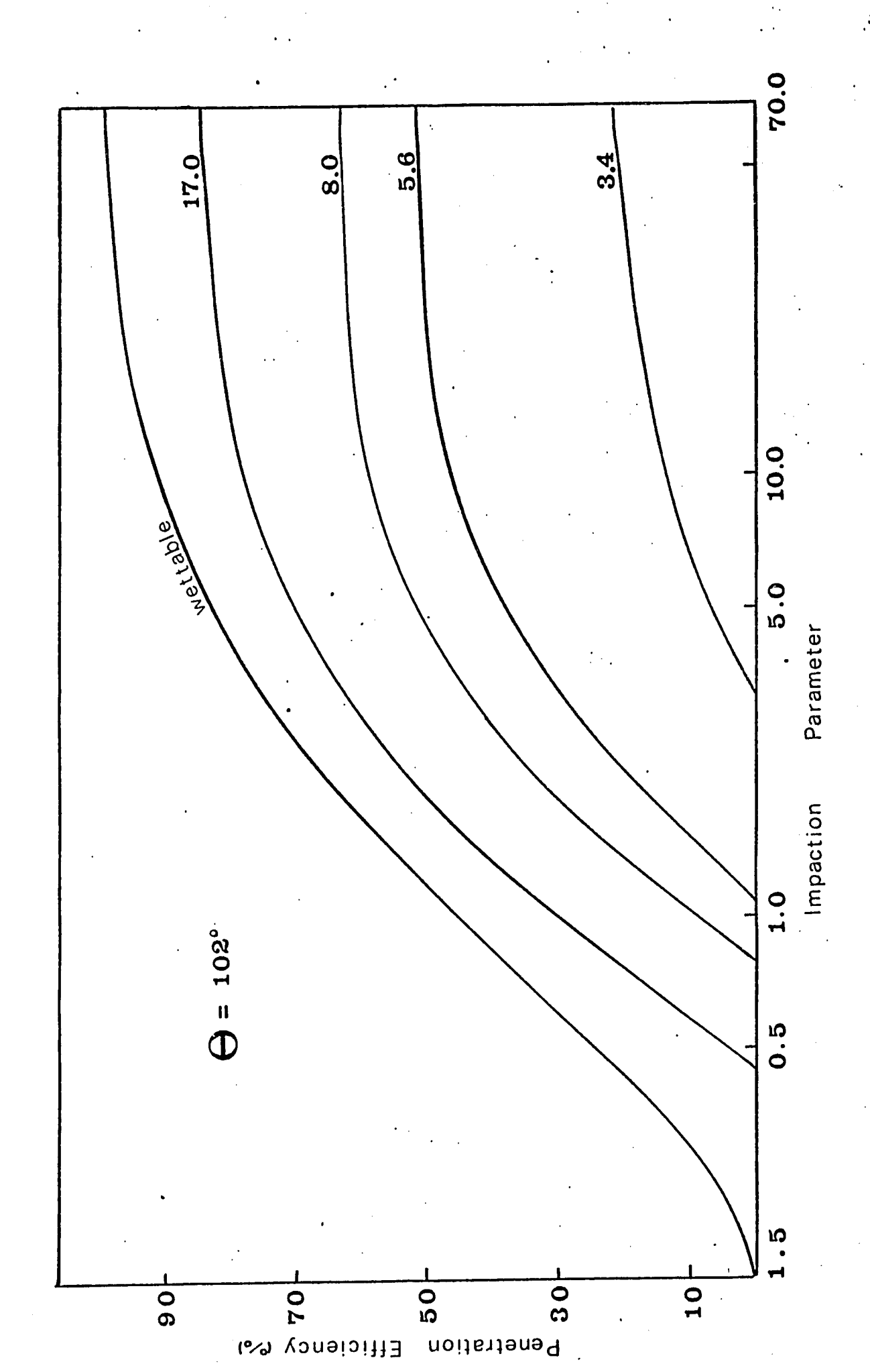
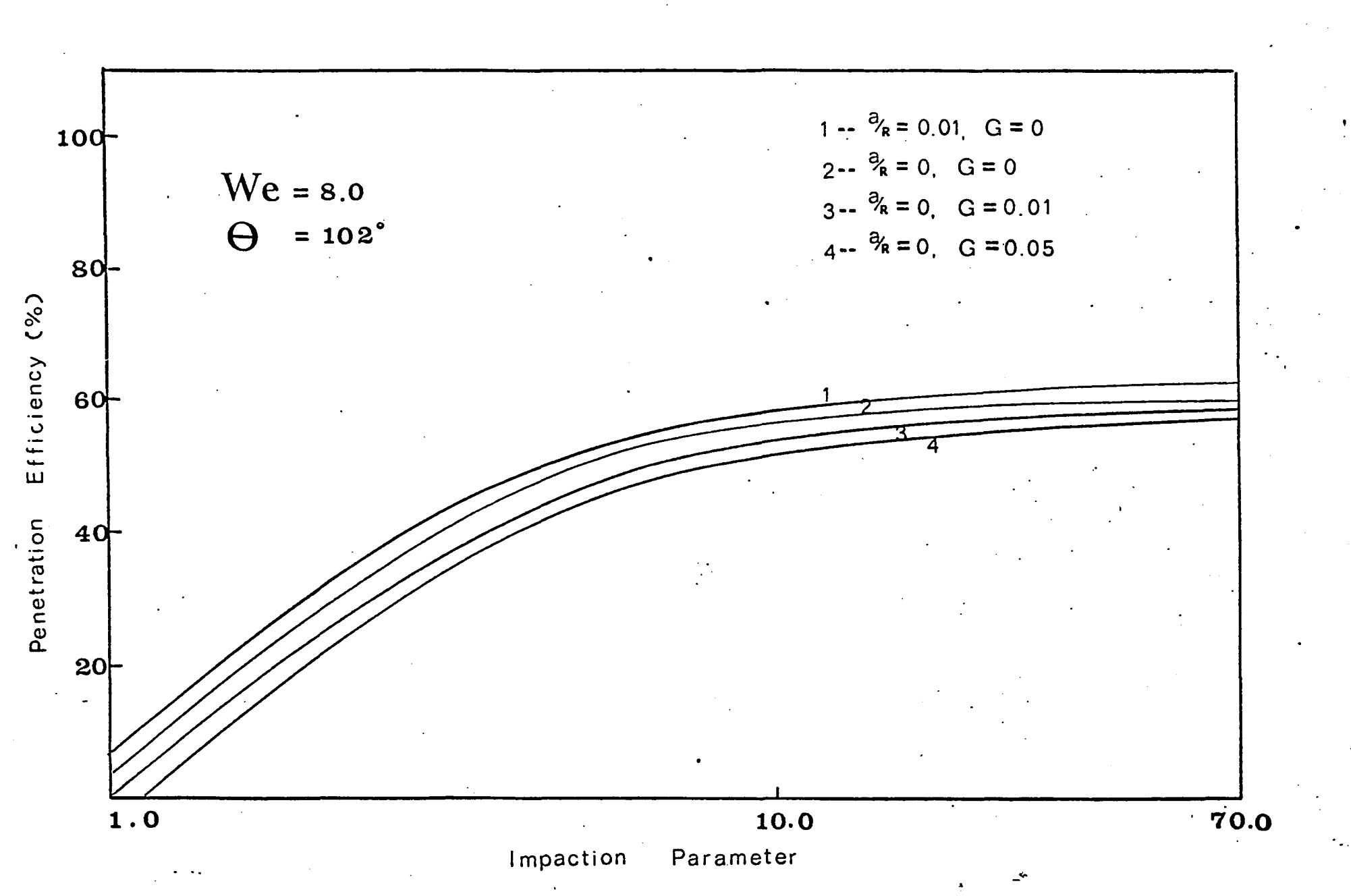


Figure 6.3

EFFECT OF RADIUS RATIO AND G
ON THE PENETRATION EFFICIENCY



to repeat Pemberton's calculations in the present work given the continued utility of this parameter as a characterisation of the penetration process. Computation of the penetration efficiencies as a function of this variable requires that $U_{\rm p}$ be greater than a specific value of M on impact. Figure 6.4 shows the results of these calculations for values of M between 0.0 and 0.9, and for values of K between 0.1 and 100. It may be seen by comparing this figure with Figure 4.1 that these results differ from those calculated by Pemberton, especially at low K for each curve. This divergence becomes important at the lower values of the penetration efficiency particularly for the minimum value of K at which penetration can occur and where there is up to a 25% variation between the two sets of results. Pemberton is very vague about the numerical procedure by which his results were obtained. The present results were calculated using a well-tried numerical technique and are in complete agreement for wettable particles (at a/R = 0and G = 0) with the curves published by other workers (20, 31). It was found that tightening the integration tolerances by a factor of 10 or, likewise, reducing the acceptable tolerance between the high and low values of y , which established the critical trajectory, made less than 0.3% difference to the computed collection. As a result, the present calculations may be considered to be more accurate.

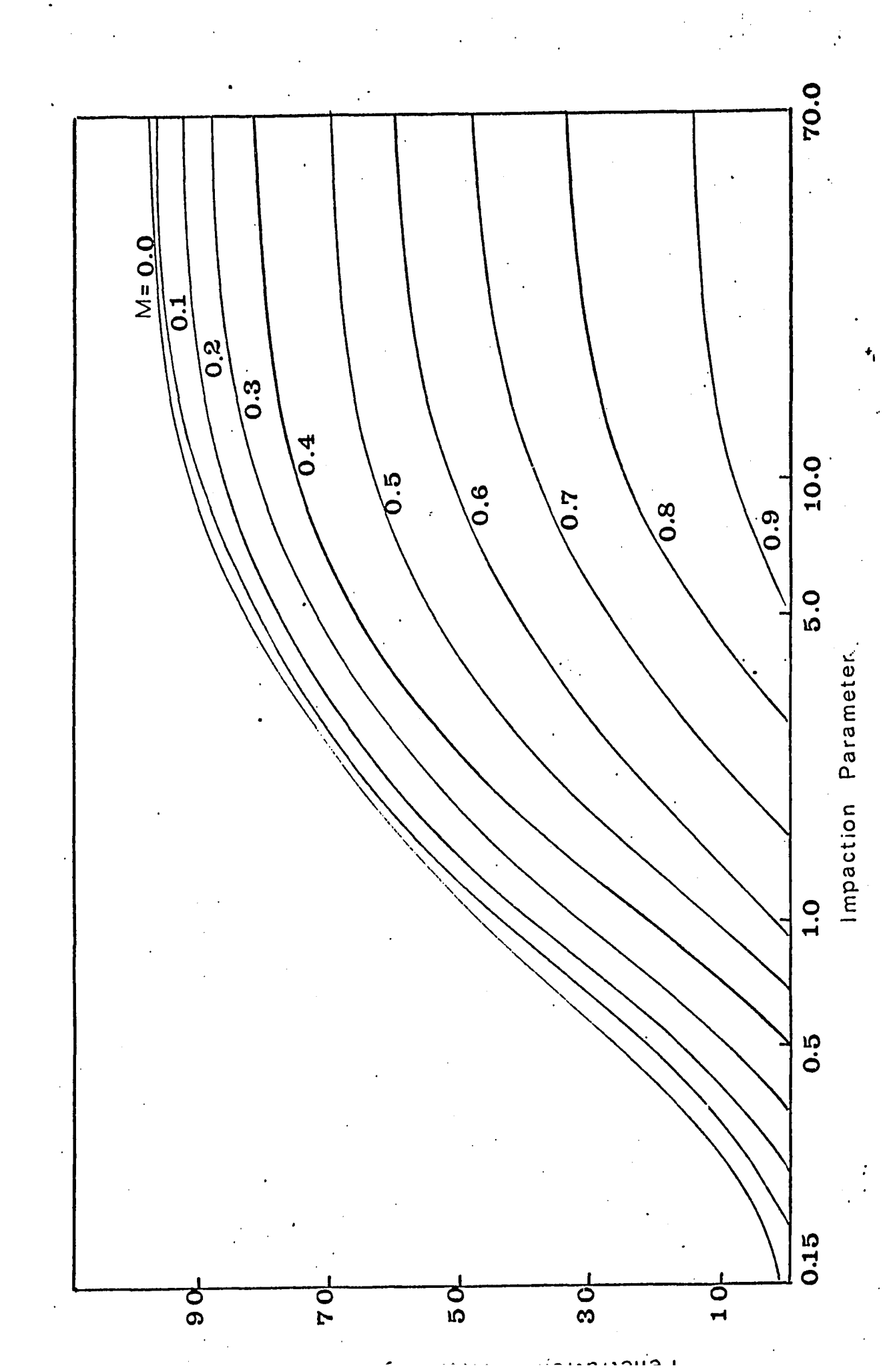
Another difference between the two sets of computations

Figure 6.4

VARIATION OF PENETRATION EFFICIENCY WITH

IMPACTION PARAMETER FOR DIFFERENT

VALUES OF M



is that the Pemberton curves go through a maximum in the region of K = 20 for $M \le 0.6$. No evidence of this maximum was found in the present work. However, Pemberton assumes that, if the particle is brought back to the surface after penetration, it is ejected into the airstream and is thus not captured by the In order to allow for this, he places the further condition upon his calculations that the particle must penetrate with enough normal velocity to travel sufficiently far into the droplet that its tangential momentum is dissipated by viscous drag within the liquid. This assumption does not correspond to reality, as will be discussed later, and the condition he develops ignores the unsteady state terms in the formulation of the viscous drag. Pemberton's assumption does not, however, account for the existence of the maxima since it was found that the inclusion of his tangential momentum condition in the present computations did not produce a maximum in any of the E versus K curves. The maxima seem, therefore, to have been produced by computational inaccuracy.

It is interesting to note from Figures (6.1 to 6.4) that there exists, for any We, θ , or M curve, a minimum value of the impaction parameter K_0 , below which no penetration occurs, and a maximum value of penetration efficiency E_m , to which the curve tends asymptotically at high values of K. When K is large and inertial effects are dominant, the particle deviates very little so that the trajectories are indistinguishable from straight

lines. For this situation, the penetration efficiency may be estimated from the fact that the collision will occur at $y = y_{\infty}$. Thus, in dimensionless terms:

$$U'_{R} = U'_{x} \cos \alpha \tag{6.1}$$

Assume:

$$U'_{x} = \frac{U_{x}}{U_{\infty}} = 1$$

$$\therefore \cos \alpha = \cos (\sin^{-1} \frac{Y_{\infty}}{R})$$

$$U'_{R} = \cos (\sin^{-1} y'_{\infty})$$

$$U'_{R}^{2} = 1 - \sin^{2} (\sin^{-1} y'_{\infty})$$

$$= 1 - y'_{\infty}^{2}$$

$$= 1 - E_{m}$$

For penetration:

$$U'_{R}^{2} = \frac{-12 \cos \theta}{We}$$
 (5.20)

$$E_{\rm m} = 1 + \frac{12 \cos \theta}{We}$$
 (6.2)

For example, at We = 3.4 and Θ = 102 , E_{m} was computed at K = 100 to be 22.12%. By Equation (6.2), it is estimated to be

26.6%. Equation (6.2) always gives an overestimate because the deceleration of the particle as it approaches the sphere is neglected. The value of $K_{\rm O}$ can be estimated in a similar way. In this case, $U_{\infty} = U_{\rm R}$ and only a particle which collides at the forward stagnation point has sufficient energy to penetrate the droplet:

$$U_{R} = U_{\infty} = \left(\frac{12\sigma \cos \theta}{d\rho_{p}}\right)^{1/2}$$
 (6.3)

This value of $\rm U_{\infty}$ may be used to calculate $\rm K_{\rm O}$. It, too, gives a conservative estimate because it does not allow for the deceleration of the particle.

6.2 <u>Comparison of Penetration Efficiencies with Experimental</u> Results

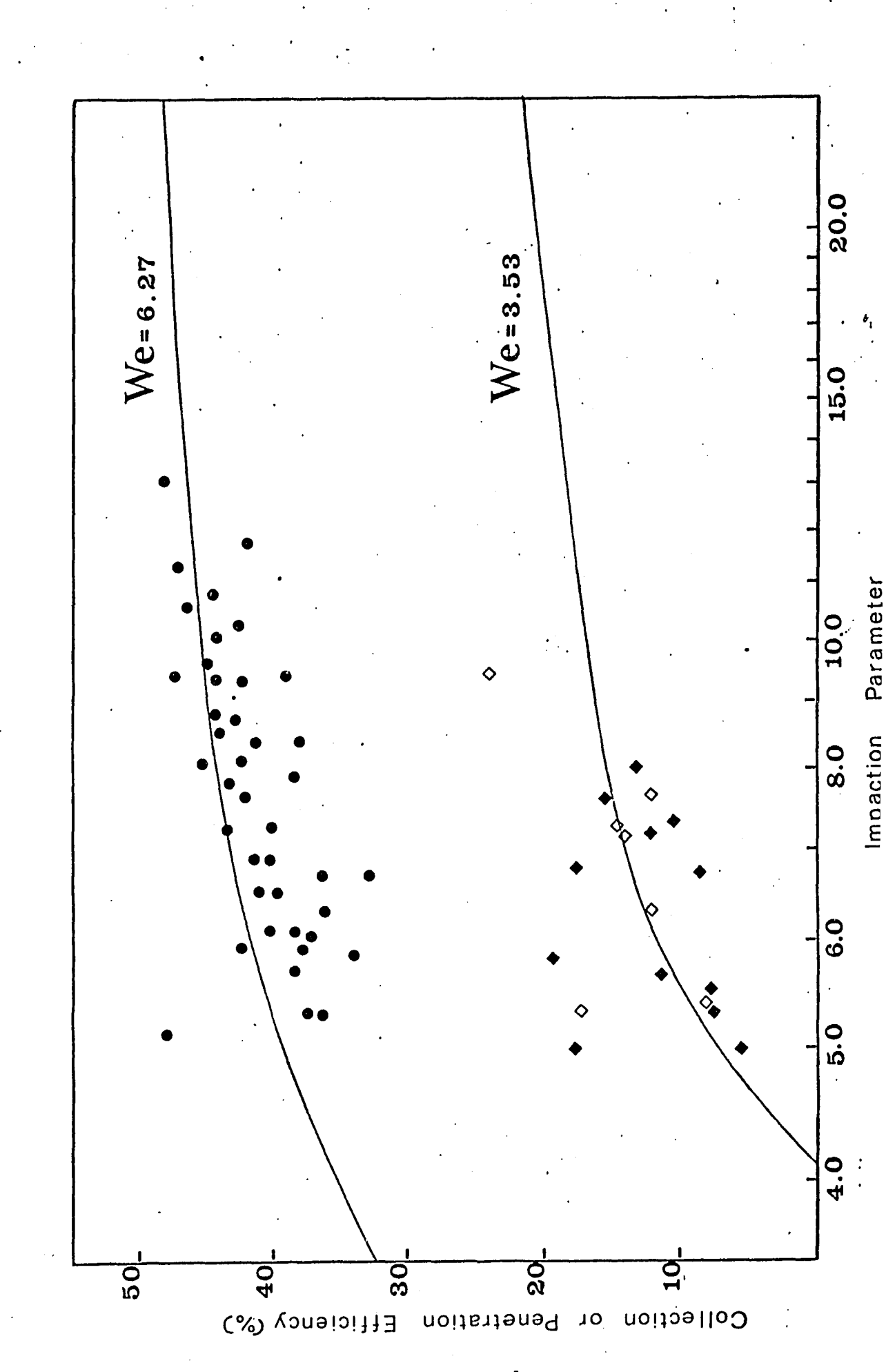
It is clearly of interest at this point to compare the theoretically computed values of penetration efficiency with the experimentally measured values of collection efficiency. Figures 6.5 to 6.11 show this comparison for the results of all the hydrophobic aerosols used. The variation of penetration efficiency with impaction parameter has been shown in the previous section to be governed by 4 quantities; 0, the contact angle; We, the Weber number of the system which is the ratio of inertial to surface tension forces during the penetration process; a/R, the radius ratio; and G, the dimensionless gravitational settling The values of a/R and G have been included in the velocity. theoretical calculations although, as in Part I, their effects are only small. Each theoretical curve has been computed using a value of G calculated from Stokes law and the average value of a/R from the plotted points.

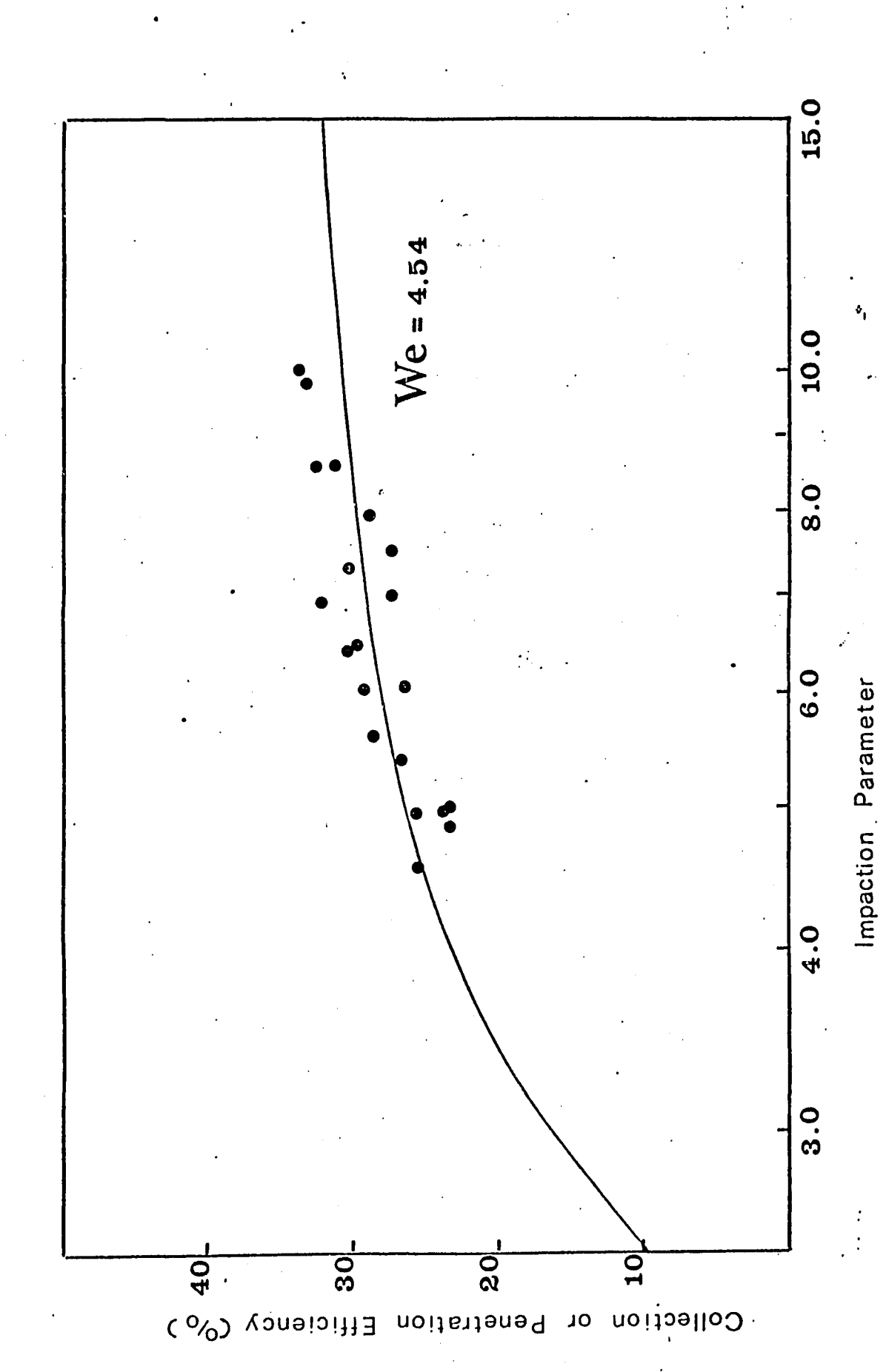
Figure 6.5 shows the experimentally measured points for paraffin wax at two different Weber numbers. The agreement in both this figure and in Figure 6.6 is very good. Variations in collection efficiency for this aerosol therefore seem to be very well correlated by the theory.

The same is true, although the agreement is not quite as good, of the results for the two liquid aerosols shown in Figures 6.7 and 6.8. The theoretical line was calculated by

EXPERIMENTAL MEASUREMENTS OF COLLECTION EFFICIENCY $AS \ A \ FUNCTION \ OF \ IMPACTION \ PARAMETER$ $PARAFFIN \ WAX \ AEROSOL, \ \theta \ = \ 102.28^{\circ}$

- We = 6.27, a/R = 0.014, G = 0.0030
- Φ We = 3.56, a/R = 0.013, G = 0.0062
- \lozenge We = 3.47, a/R = 0.015, G = 0.0063





EXPERIMENTAL MEASUREMENTS OF COLLECTION EFFICIENCY

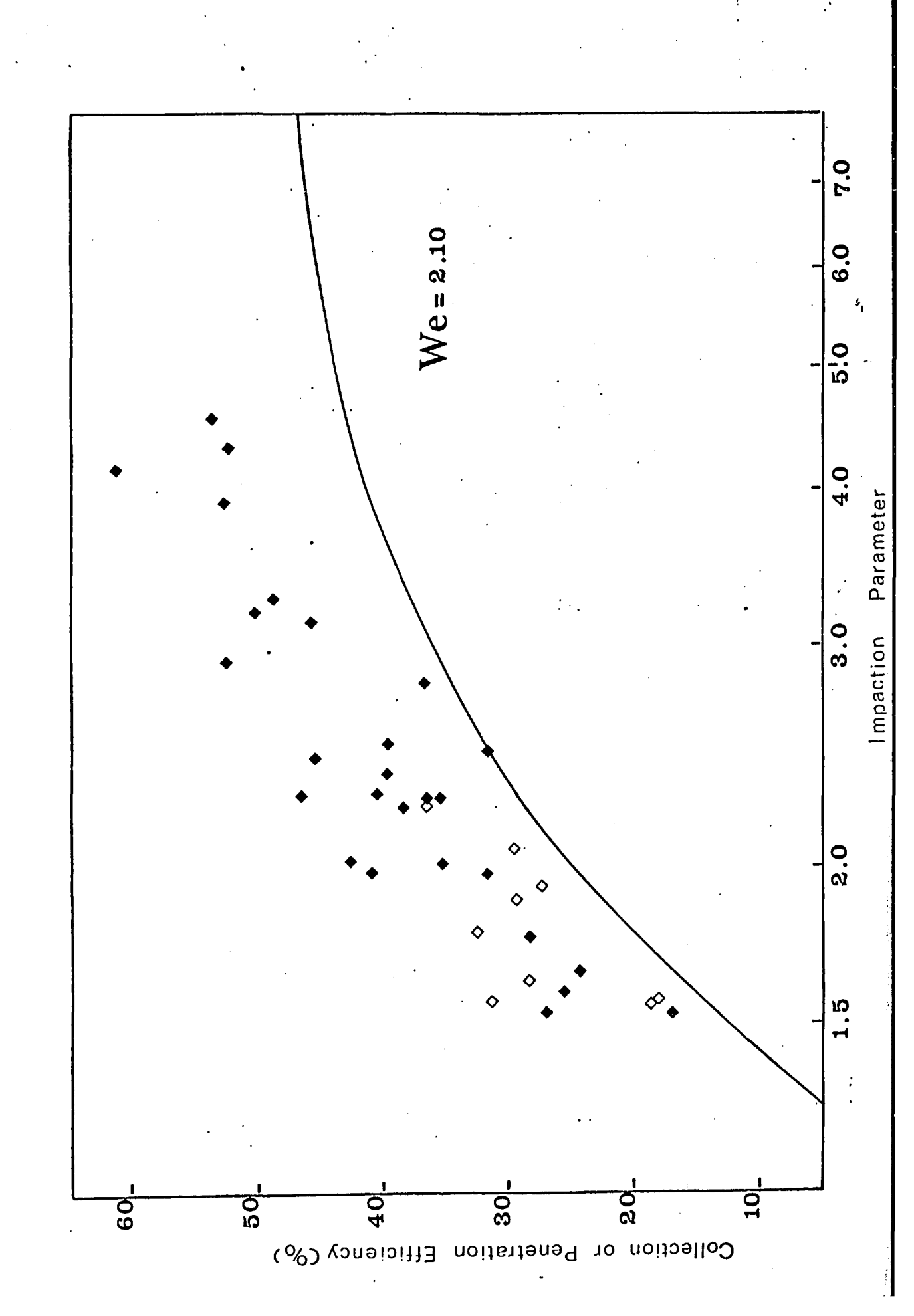
AS A FUNCTION OF IMPACTION PARAMETER

PARAFFIN OIL AEROSOL, $\gamma_{SL} = 31.54 \text{ dynes/cm.}^2$

 γ_{SV} = 35.63 dynes/cm.²

 \Diamond We = 2.14, a/R = 0.0067, G = 0.0017

 \bullet We = 2.09, a/R = 0.0099, G = 0.0017



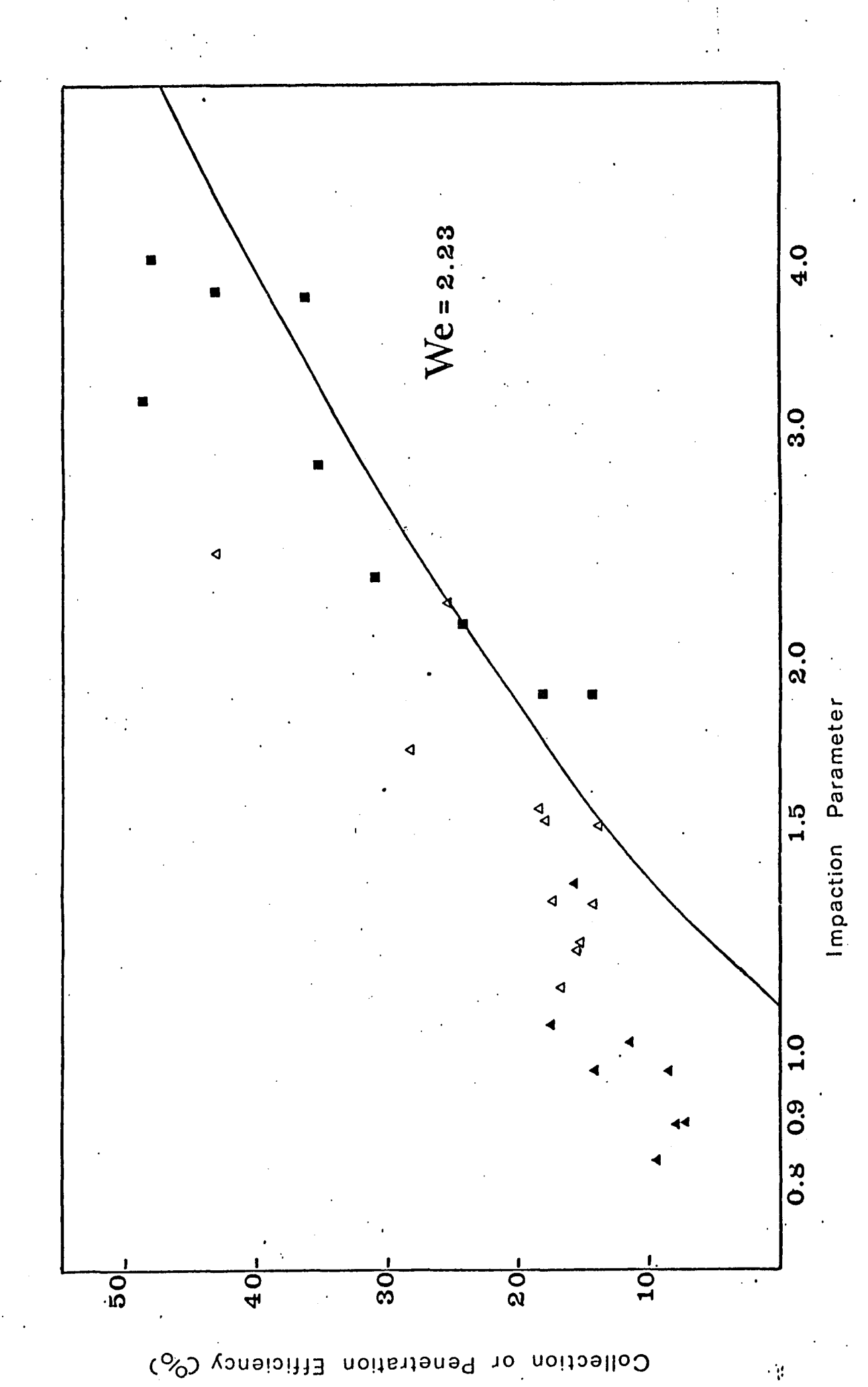
EXPERIMENTAL MEASUREMENTS OF COLLECTION EFFICIENCY AS A FUNCTION OF IMPACTION PARAMETER DIOCTYL PHTHALATE AEROSOL, $\gamma_{\rm SL}=37.84~{\rm dynes/cm.}^2$

 $\gamma_{SV} = 32.61 \text{ dynes/cm.}^2$

 \blacktriangle We = 1.98, a/R = 0.0046, G = 0.0007

 Δ We = 2.24, a/R = 0.0062, G = 0.0009

■ We = 2.43, a/R = 0.0091, G = 0.0020

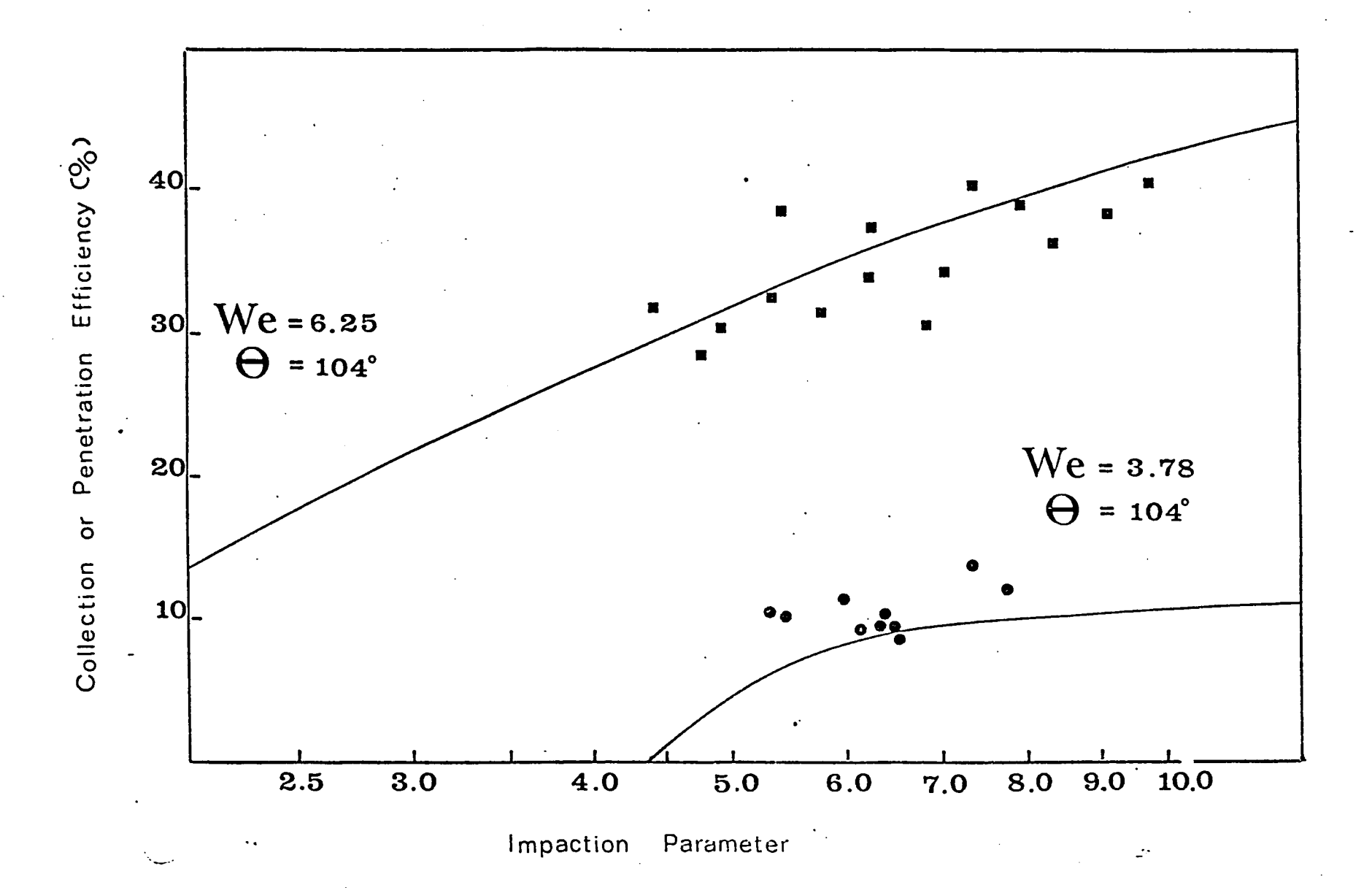


substitution of the measured values of $\gamma_{\rm SV}$ and $\gamma_{\rm SL}$ into Equation (5.18). There is a small deviation in both cases but the theoretical values of penetration efficiency are very much closer to the experimental results than would be obtained by ignoring wettability effects.

The results for the talc aerosol shown in Figures 6.9 and 6.10 do not correspond exactly to the theory. Talc is not generally regarded as strongly hydrophobic. There is also considerable variation in the published values of 0 for tale (48) ranging from 52°, for measurements using a sessile drop, to 90° using the more accurate tilting slide method. A contact angle of 90° or less should ensure that the particle behaves in a completely wettable fashion. However, collection efficiencies for talc were found to be much lower than the ideal Moreover, E was found to vary with Weber number. An attempt was made to measure the value of 0 using a sessile drop on a compressed tablet of the powder but the values obtained, in the region of 60°, were almost as low as the figure of 52° quoted by Rebinder et al (60). This low value may be attributed to the porosity at the surface of the tablet and perhaps to surface effects which may have occurred during compression. It is of no use for correlating the theory and experiments. However, it was noted that if the talc is assumed to exhibit a contact angle of 104° during the experiments then the theory correctly describes the variation of the talc results with Weber number (Figures 6.9 and 6.10).

EXPERIMENTAL MEASUREMENTS OF COLLECTION EFFICIENCY AS A FUNCTION OF IMPACTION PARAMETER TALC AEROSOL

- We = 3.78, a/R = 0.0121, G = 0.0069
- \blacksquare We = 6.25, a/R = 0.0117, G = 0.0023

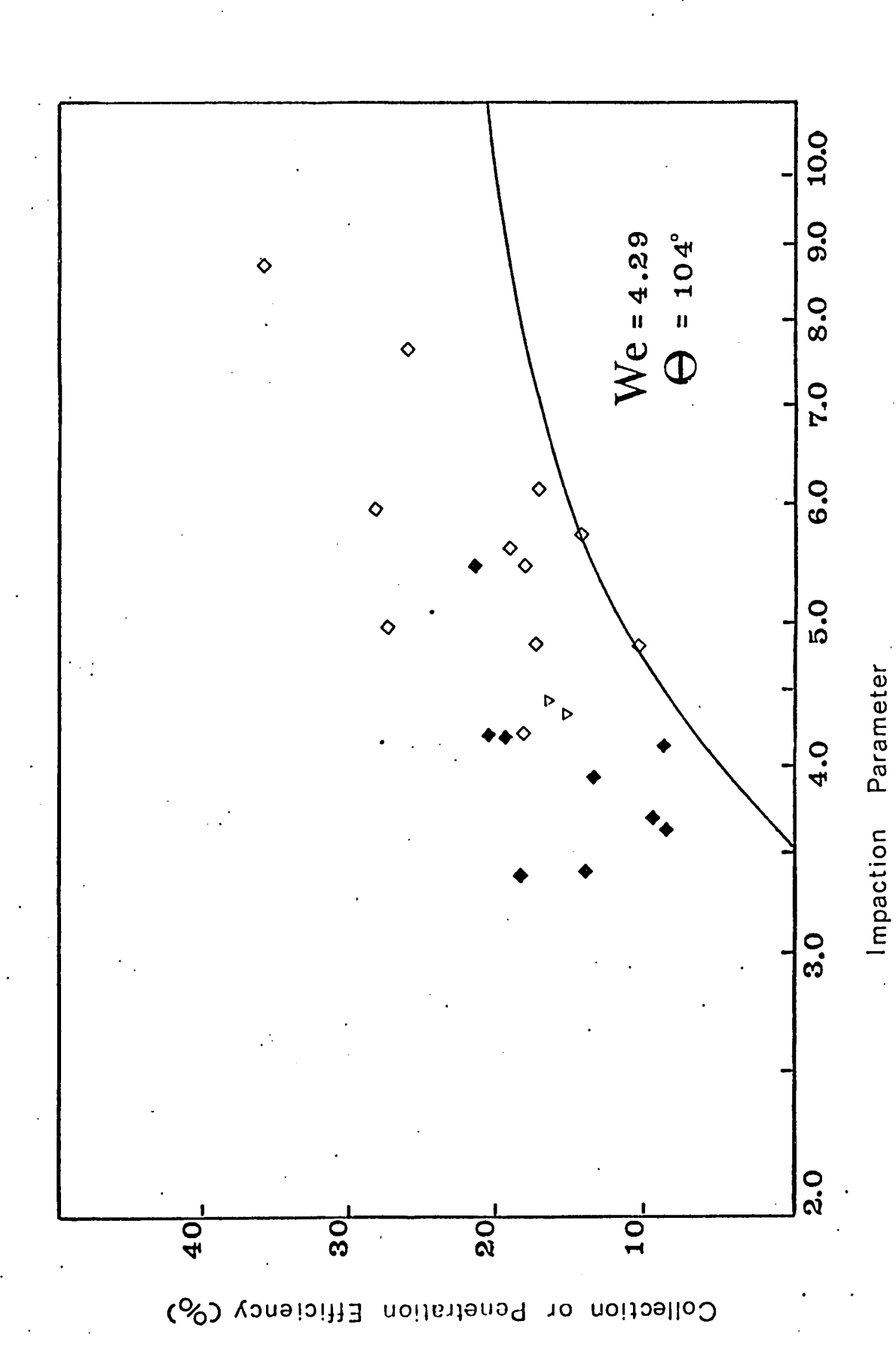


EXPERIMENTAL MEASUREMENTS OF COLLECTION EFFICIENCY AS A FUNCTION OF IMPACTION PARAMETER TALC AEROSOL

 \bullet We = 4.14, a/R = 0.0087, G = 0.0028

 ∇ We = 4.08, a/R = 0.0096, G = 0.0029

 \diamondsuit We = 4.46, a/R = 0.1214, G = 0.0027



6.3 <u>Discussion of Rebound Criteria for the Paraffin Wax</u> Example

It appears from the experimental data that there is a correlation between collection and penetration. Both Pemberton and MacDonald assume this to be the case although there is little actual basis for such an assumption. In fact, it is possible to visualize a slowly approaching aerosol particle being brought to rest on the surface of the droplet and so being captured without actually penetrating. The purpose of this section is to reduce the uncertainty in this intuitive visualisation and give it some quantitative basis for validity.

Equation (5.5) shows that, for a rebounding particle to escape capture, its approach energy must obey the inequality:

$$I_{na} \ge \frac{I_{vr} - I_{S}}{(1 - f)} + I_{vi} - I_{e} + I_{S}$$
 (5.5)

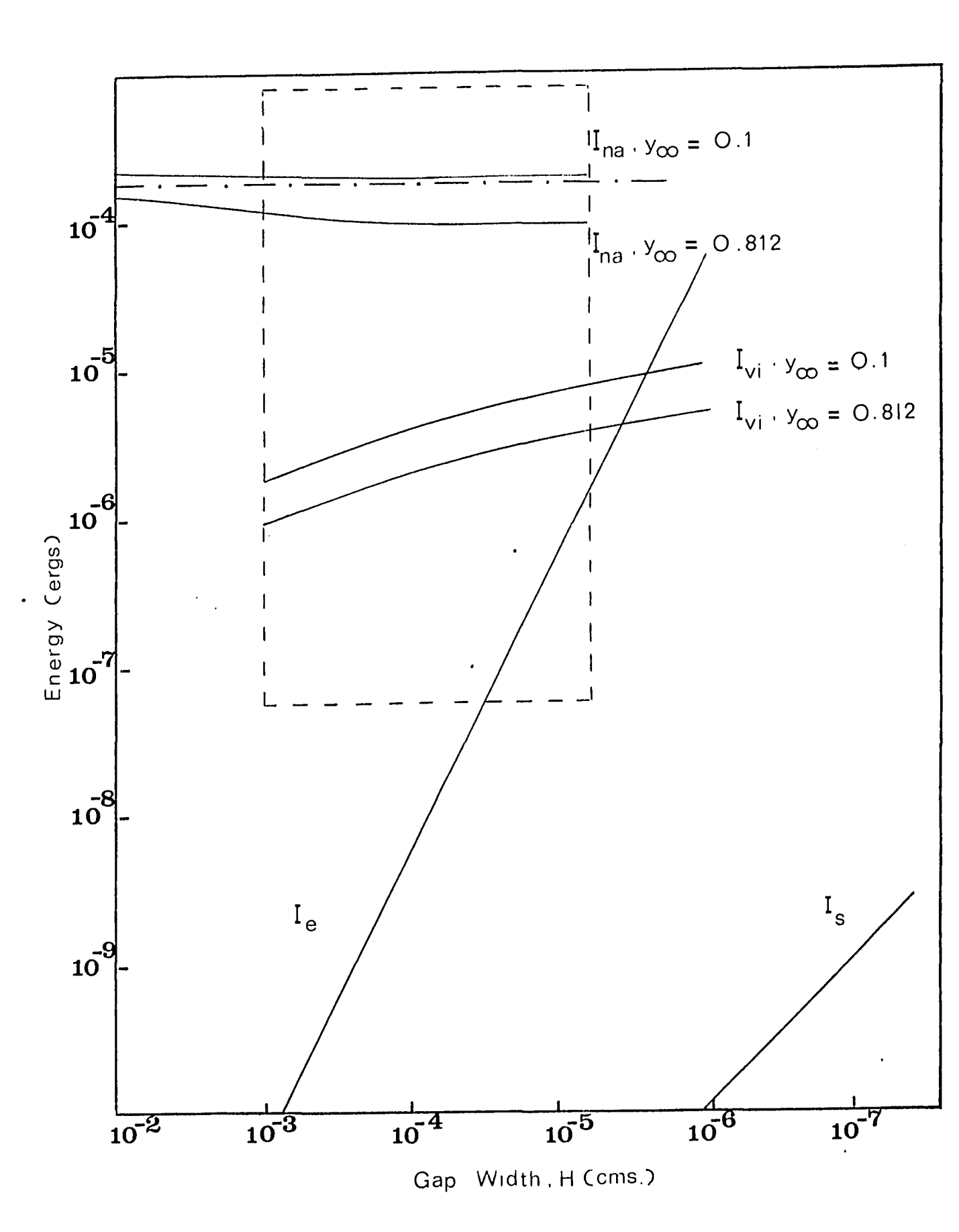
If all the particles which do not penetrate can be shown to obey this inequality under certain conditions, then the penetration efficiency and the collection efficiency must be the same. It is therefore necessary to discuss the circumstances under which the inequality is obeyed. It has been noted above that Whelpdale and List (72) have measured the quantity f for water aerosols impacting into water droplets. In this case, the impacting particle was not hydrophobic but contact between the two phases was prevented by a compressed layer of air. They measured the kinetic energy dissipation due to such factors as

surface waves and forced internal circulation within the collector, and found that it varied between 10% and 40% depending upon the angle of incidence α . This is equivalent to considering the collision to be between a sphere and an elastic surface, with a coefficient of restitution of between 0.6 and 0.9.

It is at high angles of incidence that the approach energy due to the normal velocity of the particle is lowest. Therefore, if Inequality (5.5) is not to be obeyed, it will be for large values of y_{∞} in any system. Both the total energy loss during collision (right hand side of Expression 5.5) and the approach energy are functions of the angle of incidence. It is impossible to establish general expressions for either term since I_{na} , α , and U_{R} depend on the particle trajectory which has to be computed numerically.

As was shown in Section 5.3, each of the surface interaction terms is a function of the gap width and therefore varies during the collision process. Figure 6.11 gives a comparison of the magnitudes of these terms for the paraffin wax example. It plots, on a composite graph, the energy for each of the various mechanisms versus H and, where necessary for evaluation of the viscous forces and the approach energy, it presents results from two specific trajectories with $y_{\infty} = 0.1$ and $y_{\infty} = 0.812$. The chain dotted line shows the energy necessary for penetration in this example. As may be seen, the trajectory

COMPARISON OF ENERGY FUNCTIONS WITH GAP
WIDTH FOR THE COLLISION MECHANISMS



beginning at $y_{\infty} = 0.1$ has sufficient energy to penetrate whilst the trajectory with $y_{\infty} = 0.812$ does not.

Several factors are immediately apparent from this graph. First, van der Waals forces are relatively unimportant since the energy lost to them is several orders of magnitude smaller than the approach energy. Secondly, the electrostatic forces also appear to be relatively unimportant as they rise to a significant value only at very small separations. Finally, it is apparent from Figure 6.11 that the major energy losses are due to viscous forces.

There have been many attempts to measure the film thickness at rupture between two approaching surfaces. The work has been mainly for liquid films and the results have been very However, for the purposes of this work, it may be inconsistent. arbitrarily assumed that contact between the surfaces is ensured when the gap width becomes of the same order of magnitude as the mean free path of the gas molecules. Consequently, the area in Figure 6.11 which holds the most interest is that which is enclosed within the dashed rectangle. Within these limits, it may be seen that both the electrical and van der Waals forces are unimportant and that the collision process can only be influenced by the viscous energy losses. These may be used in Equation (5.5) to predict the outcome of a collision in the present system. Both I and I may be put equal to zero and, for a successful bounce, the expression reduces to:

$$I_{na} \ge \frac{I_{vr}}{1 - f} + I_{vi}$$
 (6.4)

Under the same velocity conditions, the force on a particle receding from a surface is the same as the force on approach. However, for collisions such as those considered here, I_{vi} will not be equal to I_{vr} since both are dependent on velocity and part of the kinetic energy of the rebounding particle is lost during the contact period. As the viscous force is directly proportional to the velocity, I_{vr} is given by:

$$I_{vr} = I_{vi} \sqrt{(1-f)}$$
 (6.5)

and hence for a successful bounce:

$$I_{\text{na}} \ge I_{\text{vi}} (1 + (1 - f)^{-1/2})$$
 (6.6)

The mean free path of the air molecules has been used as the film rupture thickness. This will give an overestimate of the viscous force since the film will certainly rupture at thicknesses greater than this. The same is true of the choice of the value 0.1R as the starting distance at which viscous forces act. However, owing to the uncertainty involved in the application of Equation (5.39), it is better to keep the viscous force estimates conservative. This range of gap widths gives for I_{vi} :

$$I_{vi} = 54.16\pi\mu a^2 U_R \tag{6.7}$$

For the limiting situation of very small f such as would be the case for collisions at high angles of incidence, the total viscous energy loss is given by:

$$I_{vi} + I_{vr} = 2I_{vi}$$

and Inequality (6.6) reduces to:

$$\frac{2}{3}\pi a^3 \rho_p U_R^2 \ge 108.32\pi\mu a^2 U_R$$

or:

$$\rho_{\rm p} U_{\rm R} d \ge 324.96 \mu$$
 (6.8)

or, for the paraffin wax example:

$$U_{R} \ge 66.55$$
 (6.9)

For a particle which makes contact at the equator of the droplet, $U_{\rm R}=0$. There is, therefore, an area on the surface of any droplet onto which particles will impact with a sufficiently small velocity that they do not rebound. The upper line of Figure 6.12 shows the variation of the radial velocity on impact with the angle of incidence as computed for the potential flow assumptions for the paraffin wax example. It is clear that the velocity does not fall to a sufficiently low level to prevent rebound until angles of incidence of greater than 75°. At large angles of incidence such as these, there is very little

VARIATION OF $\mathbf{U}_{\mathbf{R}}$ WITH ANGLE OF INCIDENCE COMPUTED USING POTENTIAL FLOW AROUND THE COLLECTOR

Angle of Incidence. ∝

chance of the particle actually being captured because the very high tangential velocities in this area will sweep the particle round into the droplet's wake. The limiting velocity in Equation (6.9) is dependent on the value of f, but is not highly sensitive to it. For example, if f is equal to 90%, the limiting velocity is only doubled and capture without penetration can occur only at angles of incidence greater than 70°. It seems, therefore, that there will be no capture of particles which do not penetrate the droplet surface since they will all rebound with sufficient energy to be reentrained in the free gas stream.

Both Pemberton and MacDonald conclude that the shoot through phenomenon is not important. Thus it will not be discussed further here. However, each writer ignores the experimental observations of McCully et al (47) that hydrophobic particles form a crust on the surface of the droplet and that collected particles appear exclusively on the exterior of the water surface. These observations were confirmed in the present work where it was found that a droplet exposed either to the talc or wax aerosol stream for a period in excess of 5 minutes became covered with a visible crust of the aerosol material. This observation seems to contradict the idea that the particles must penetrate the droplet surface in order to be collected. However, it has already been demonstrated that particles which do not penetrate are not captured, at least in the case of the

illustrative example. This apparent paradox may be resolved by a closer examination of what happens to the particle inside the drop.

The circulation within droplets moving in a fluid stream is a well studied phenomenon and needs no further elucidation It is sufficient to state that, at the Reynolds numbers of these experiments, this circulation is relatively vigorous. Moreover, it appears from the experimental work of Whelpdale and List (72), that the very impaction of the aerosol particles into the droplet increases the effect. This circulation is sufficient to ensure that a particle is transported back to the surface. Once there, its own hydrophobicity causes it to be ejected from the interior of the droplet, work being done upon it by the free surface energy of the water. this process is much slower than the rebound process and so the particle is not given a sufficient impulse to allow it to escape capture. It is therefore held on the outside of the droplet where it combines with other particles similarly captured to form a crust. Given that the emergence process is exactly equivalent to that of penetration as described in Section 5.2, it can be readily proved that there is a force which holds the particle on the surface. In fact, it is likely that emergence is much nearer to a quasistatic phenomenon than penetration so that Equation (5.15) provides a more accurate description of this situation. Figure 5.4, which gives the

variations of energy with penetration, may therefore be used to indicate the relationship between emergence work and depth of immersion. It shows that there is a minimum in the energy function. The particle will come to rest in an equilibrium position at this minimum. Its depth of immersion at that point may be calculated from the fact that the derivative of the energy function must be zero and p is thus given by:

$$p = a(1 + \cos \theta)$$
 (6.10)

It is therefore concluded that, as far as the collision process for the illustrative example is concerned, only the particles which penetrate are captured and that these particles gather on the outside of the droplet. The penetration efficiency can thus be considered equivalent to the collection efficiency in this specific case. It is now pertinent to investigate in more general terms the range of experimental variables over which this conclusion is valid.

6.4 Criteria for the Neglect of the Surface Interactive Forces

In this section, order of magnitude arguments will be used to establish criteria for the neglect of each of the three surface interactive forces. If these forces can indeed be neglected then, as for the paraffin wax example, a colliding particle may be considered either to rebound or to penetrate such that no collection occurs without penetration. At moderate angles of incidence, the approach energy of the particle is of order $a^3U_{\infty}^2$. If this quantity is very much greater than the energy loss to each of the mechanisms, then they may be safely neglected.

It is easily shown that van der Waals forces are only important for very low energy collisions such as would be obtained for small particles in creeping flow around a collector. For most materials, the Hamaker constant will be of order 10^{-12} to 10^{-14} (34). Using 10^{-12} as the upper limit, and H = 10^{-5} as the rupture point of the gas film, the energy losses to VDW effects are of order a x 10^{-7} . Thus van der Waals forces may be neglected if:

$$a^2 v_{\omega}^2 >> 10^{-7}$$
 (6.11)

The smallest value of $a^2U_{\infty}^2$ used in these experiments is 0.04 and so neglect of these forces is justified.

As may be expected from the calculations for the paraffin .

wax example, the electrostatic effects are slightly more important. For an earthed collector:

$$1_{e} = O_{p}^{2} \left(1.50 \times 10^{18} \cdot \frac{D}{2H^{2}} - 7.19 \times 10^{19} \cdot \frac{D}{2(4H^{2} - 0.01)} + 4.71 \times 10^{18} \cdot \frac{D^{3}C}{H} + 1.35 \times 10^{19} \cdot \frac{D^{2}C}{H} \right)$$
(6.12)

For moderately concentrated aerosols, the first term in this equation is dominant and:

$$I_e \approx 5.66 \times 10^{27} \, O_p^2$$
 (6.13)

For particles of less than $30\,\mu$, charges of greater than 100 electrons per particle seldom occur unless the aerosol has been deliberately charged (42). Thus $\Omega_{\rm p}$ is of maximum order 1.602 x 10^{-17} coulombs and $I_{\rm e}$ is of order 1.45 x 10^{-6} ergs. The electrical effects may therefore be neglected provided that:

$$a^3 U_{\infty}^2 >> 1.45 \times 10^{-6}$$
 (6.14)

The smallest value of $a^3U_\infty^2$ in these experiments is 1.77 x 10^{-5} such that the maximum possible electrostatic energy gain is always an order of magnitude less than the approach energy of the particle for all the experimental situations.

As noted above, the viscous forces are a function of the angle of incidence and cannot therefore be dealt with by order of magnitude arguments. Instead, computations have been made of the normal velocity on impact as a function of the angle of

incidence for the case of the lowest energy of collision encountered in the experiments. This corresponds to a 9.8μ D.O.P. particle impacting onto a 0.15 cm. drop at a free stream velocity of 387.7 cm./sec. such that K = 1.5 (Run No. 107). The results are shown as the lower line in Figure 6.12. The Inequality (6.8) reduces to:

$$u_R > 61.09 \text{ cm./sec.}$$

Thus the same conclusion may be drawn as for the paraffin wax example, that viscous forces can only prevent rebound at very high angles of incidence.

From these considerations, it may be seen that the collection of the aerosol is theoretically governed by the ability of the particles to penetrate the droplet surface. The agreement of the paraffin wax aerosol measurements with the theoretical predictions substantiate this reasoning. The results for the two liquid aerosols, paraffin oil and D.O.P., also show a relatively good agreement with the theory. Both cases show a similar deviation in that the best fit line through the data points of each is about 10% above the theoretical. line over the entire range of K. This increase in the value of E could possibly be attributed to deformation of the liquid particle as it passes through the water interface. Such deformation could be expected to increase the collection of liquid aerosols by lowering the energy necessary for penetration.

The potential flow assumptions used in computing the theoretical values of collection efficiencies give a much better agreement for the paraffin wax results than for the wettable particles, the experimental points of the latter being about 6% below the theoretical line. This agreement is to be expected since the trajectories where there is greatest error involved in the assumption of potential flow close to the drop are those most nearly approaching the grazing trajectory. The condition that the particle arrive at the drop surface with a certain amount of kinetic energy eliminates such very low energy collisions.

Comparison of the present results with other data is very difficult. The only published set of experiments which are relevant are those reported by Montagna (49). However, he was working with small aerosols and his data were not taken in a comparable range. Using his experimental conditions of $9 = 103^{\circ}$ to 138° at velocities of 625 cm./sec. with a 5μ aerosol, it is easily shown, by substitution in Equation (5.19), that his particles do not have sufficient energy to penetrate. Nevertheless, even under these low energy conditions and even for $9 < 90^{\circ}$, he finds a reduction in E with increasing contact angle. It is very difficult to isolate the mechanism which caused this effect. For example, addition of surfactant to the droplet material will change the nature of the water interface with an unpredictable effect on the flow close to the drop.

Moreover, the contact angle that he finds (138) for the pure water to sulphur system is 130% at variance with the figure of 60° found by other workers This could be ascribed (25)to the method that he used for obtaining the contact angle. measured 9 from an advancing interface travelling at 5 cm./sec. Furthermore, he ignores the effect of electrostatic forces even though they could be significant. Substitution in Equation (6.14) shows that, if the particles had sufficient charge, the energy gain from electrostatic effects could be of the same order of magnitude as the kinetic energy of the particles. tentative explanation of Montagna's results stems from an analysis of Equation (5.15) which shows that any particle with $0 > 0^{\circ}$ has an equilibrium position on the surface of the drop. The force holding the particle in position and the depth of the immersion at equilibrium become smaller with increasing 0. From this finding, it could be suggested that the lowering of collection efficiency that he and other workers here observed was due to some form of reentrainment effect which would thus be more significant at higher 0.

The question of whether capture of aerosol particles is affected by surface energy phenomena for $0 \le 90^\circ$ remains to be definitely answered. There is no theoretical basis for any such effect if quasistatic assumptions are made at the interface. As soon as a particle makes contact with the water surface, it is drawn into the liquid to a certain depth which is dependent

on its contact angle. However, the velocity of impact is often quite high, especially for low α collisions, and equilibrium assumptions at the interface might not be valid. particle has penetrated beyond its equilibrium position, the line of three phase contact passing over its surface is effectively equivalent to that of an advancing interface. Under these circumstances, the dynamic contact angle will be greater than the equilibrium contact angle, and the necessary penetration work will be higher. Should the dynamic contact angle exceed 90°, then the water interface would act to expel the particle. There is insufficient knowledge of the effects of interface velocity on the contact angle to be able to say with any certainty how important an effect this could be. light of this consideration, MacDonald's finding should be modified to the effect that only acrosols exhibiting a dynamic contact angle greater than 90° have reduced capture efficiencies.

One further point arise from the discussion in this chapter. It is apparent that there are two types of collision regimes, high energy and low energy. In the high energy collision regime such as was studied in these experiments, collection efficiency has been shown to be governed by the ability of the particles to penetrate the droplet surface. The present work has been concerned exclusively with this type of collision. The low energy regime occurs predominantly for small particles diameters when the kinetic energy is so small that it may be

influenced by any of the surface interactive forces. This distinction does not seem to have been realised by other workers. It is important, however, because high energy collisions may result in quite high values of E, which has been shown to be characterised by the Weber number, the contact angle, and the aerodynamic collision efficiency. In contrast, the low energy regime is characterised by very low values of E which depend not only on the aerodynamic trajectory of the particles but also on the magnitudes of the surface interactive forces which, as noted above, cannot as yet be predicted with sufficient accuracy to define the collision process.

Conclusion

The work in this thesis has been directed towards checking the validity of one of the assumptions in the Langmuir model. It has sought to substantiate the hypothesis that not every aerosol particle which is brought aerodynamically to the surface of a collecting drop is captured. The problem has been approached from the point of view of particle wettability and tackled both by experimentation and by theoretical analysis of the collision process.

During the course of this work, an experimental technique was developed which enables collision efficiencies to be measured relatively simply and accurately. The results obtained by the method for hydrophilic aerosols show excellent agreement with the best results of other workers in the field and also with the theoretically expected values. The flexibility of the technique allows it to be used over a range of aerosol materials. Consequently, this capability was also exploited to measure the collection efficiencies of four different types of hydrophobic particles, so facilitating the fulfillment of the primary experimental objective which was to compare measurements for hydrophobic and hydrophilic aerosols taken under the same conditions. In all cases, the collection efficiency was shown to be lower for the hydrophobic particles. This conclusion has been reached before on an experimental basis for solid aerosols but

not over so wide a range of operating variables and of aerosol materials. There are no published collection efficiency data for the collection efficiencies of liquid hydrophobic particles.

The variation of collection efficiency with impaction parameter was shown to depend not only on the type of aerosol but also on the conditions under which the experiments were performed. This has been predicted theoretically in the past but not verified experimentally. It was shown to depend particularly on the aerosol velocity. This is not true for the hydrophilic particles.

The collision process between a hydrophobic particle and a water droplet has also been analysed theoretically in this thesis. A theory to calculate the work necessary for the particle to penetrate the droplet surface has been proposed. It predicts that the penetration depends on the Weber number and the cosine of the contact angle. These predictions are in line with the experimental findings. A new concept of penetration efficiency was defined and calculated on the basis of this theory assuming potential flow over the forward half of the drop. The calculated values for three aerosols agree well with the experimental results, these being described much better by the new theory than by any previously existing theory. The relationship between penetration efficiency and collection efficiency was examined and it was demonstrated that, under some conditions, the two can be equivalent. It was shown that, for high energy collisions, particles which do not penetrate

the drop surface actually rebound into the free gas stream. Particles which do penetrate are transported back to the surface of the drop where they remain. The theoretical calculations show that all particles having a contact angle of less than 90° need do no work in order to penetrate the drop and should therefore be collected as efficiently as wettable particles.

Finally it was proposed that there are two types of collision regimes for hydrophobic particles, high energy and low energy. The work in this thesis has dealt with the high energy regime in which it has been shown that the collection efficiency is determined by the ability of the particle to penetrate the drop surface. The hypothesis that hydrophobic particles are captured less efficiently than hydrophilic particles has therefore been substantiated under the conditions of this work. Thus at high values of the impaction parameter for hydrophobic particles impacting onto water droplets the Langmuir model is inadequate since not every particle transported to the drop surface is necessarily captured.

Claims to Originality

The following aspects of this work are considered to be original:

- The development of a new technique for the measurement of the collection efficiencies of suspended drops.
- The experimental finding that liquid hydrophobic particles are collected less efficiently than hydrophilic particles.
- 3. The experimental finding that, at high values of the impaction parameter, the collection efficiency of both solid and liquid aerosols varies according to the Weber number.
- 4. The development of a theory to account for the total change in interfacial energy of the system during the penetration process, and the use of this theory to calculate collection efficiencies of hydrophobic particles.

Nomenclature

Α	Wetted area of non wettable surface
A'	Hamaker constant for non retarded forces
Α"	Hamaker constant for retarded forces
A(H)	Hamaker function defined in Section 5.3.1
a	Aerosol particle radius
a f	Radius of wetted perimeter of non wettable surface
В	Centre to centre separation of collector and aerosol
	particle
b	Height of spherical cap of liquid on filter surface
С	Cunningham correction factor
C _p	Concentration of aerosol particles
С	Circumference of ring in Equation (4.2)
D	Diameter of collecting drop
D _p	Diameter of sampling probe
Ds	Diameter of spinning disc
d	Diameter of aerosol particle
d _p	Diameter of primary drops during generation
E	Collection efficiency
EA	Aerodynamic collision efficiency
E _C	Capture efficiency
Em	Maximum collection efficiency
F	Force
F '	Correction factor defined by Equation (4.2)

Force due to non-retarded VDM effects

 \mathbf{F}_{1}

```
Force due to retarded VDW effects
F_{2}
       Force due to electrostatic charge on the particle
F_{e}
       Van der Waals force
F_{s}
      Force due to surface tension
\mathbf{F}_{\mathbf{m}}
       Fractional energy dissipated during contact period
f
       Dimensionless gravitational settling velocity
G
       Acceleration due to gravity
g
       Surface to surface separation
H
H_1
       Specified values of II
H_{2}
       Original value of H
H_{\circ}
      Planck's constant (1.054 \times 10^{-27} \text{ erg. sec.})
h
h\overline{\omega}
      Lifshitz-van der Waals constant
Ι
      Energy
      Energy lost to electrical effects
I
I<sub>na</sub>
      Approach energy
      Energy due to normal motion at the moment of impact
Ini
       Energy due to normal motion of particle after rebound
Inp
       Energy due to normal motion of particle at instant of
Inr
       rebound
       Energy lost to VDW effects
I_
      Energy lost to surface energy forces
I_{\mathbf{T}}
      Energy lost to viscous forces as particle rebounds
I_{vi}
      Energy lost to viscous forces as particle rebounds
Iwr
       Impaction parameter defined by Equation (1.2)
K
```

Minimum value of K at which collection is possible

K

- K_{G} Dimensionless parameter for electrical effects defined in Equation (3.13)
- k Constant used in Equation (4.2)
- k_1 Constant used in Equation (2.1)
- L Radius of a sphere of which drop on surface forms a segment
- Cosh⁻¹(H/a) used in Equation (5.39)
- M Ratio of minimum velocity necessary for penetration to the free stream velocity
- m Mass of aerosol particle
- N Number of particles counted in 18 seconds without the drop
- N_{C} Number of particles collected by the drop in 18 seconds
- n Summation variable used in Equation (5.39)
- P Dial reading of Tensiomat used in Equation (4.2)
- p Penetration of particle into drop surface
- $\Omega_{\rm p}$ Charge on an aerosol particle
- q Radius of wetted perimeter of particle
- R Radius of the droplet
- Re Reynolds number
- R_i Radius of the laminar jet
- t Time
- U Velocity
- U Initial velocity
- U_R Radial velocity
- U_{x} Velocity in x direction

 $\mathbf{U}_{\mathbf{v}}$ Velocity in y direction

 U_{∞} Velocity of free gas stream

V D.C. output voltage from anemometer

V_a Volume of liquid drop on solid surface

V_C Volumetric flow rate through the counter

V D.C. output voltage from anemometer at zero gas velocity

 $\mathbf{V}_{\mathsf{RMS}}$ A.C. output voltage from anemometer

We Weber number $(\rho_{p} dU_{\infty}^{2}/\sigma)$

x Distance coordinate measured vertically down from the centre of the collector

y Distance coordinate measured horizontally from the centre of the collector

 y_{∞} Distance of trajectory from axis of collector at infinity

 $y_{\infty G} = y_{\infty}$ for the grazing trajectory

Greek_Letters

 α Angle of incidence

 $Y_{\text{I,V}}$ Surface free energy of water drop

 Υ_{SL} Surface energy of aerosol particle-water interface

 γ_{SV} Surface energy of aerosol particle

 δ Deformation of drop surface

Permittivity of free space (8.85 x 10^{-21} coulombs²/dynes.cm.²)

 ϵ ,"(ω) Imaginary part of the complex dielectric constant of medium j

```
ε<sub>j</sub>(iξ)
         Dielectric permittivity of medium j at imaginary
         frequency (iξ)
         Penetration angle defined in Figure 5.5
         Contact angle
         Variable defined by Equation (5.39)
         Viscosity of air
         Density of lower phase in Equation (4.2)
^{\rho}1
         Density of upper phase in Equation (4.2)
ρ<sub>2</sub>
         Air density
۴
ρ
         Particle density
n
s
         Density of feed to generator
         Surface tension of water
         Angular frequency of photon energy
ω
         Angular velocity of spinning disc
ωd
```

Subscripts

x	In x direction
У	In y direction
p	Particle
f	Fluid

Superscripts

Dimensionless variable: all quantities are rendered dimensionless with respect to drop radius and free stream velocity.

References

- 1. Adamson, A.W., <u>Physical Chemistry of Surfaces</u>, Interscience Publishers Inc., New York (1960)
- 2. Albrecht, F., Z. Phys., 32, 48(1931)
- 3. Bart, E., Chem. Eng. Sci., 23, 193(1968)
- 4. Beard, K.V., J. Atmos. Sci., 31, 1595(1974)
- 5. Beard, K.V. and Grover, S.N., J. Atmos. Sci., 31, 543(1974)
- 6. Berg, T.G.O., Gaukler, T.A. and Vaughan, U., J. Atmos. Sci., 27, 1074(1970)
- 7. Bexon, R. and Ogden, T.L., J. Aerosol Sci., 5, 509(1974)
- 8. Brenner, H., Chem. Eng. Sci., 16, 242(1961)
- 9. Brenner, II., Adv. in Chem. Eng., 6, 287(1966)
- 10. Casimir, H.B.G. and Polder, D., Phys. Rev., 73, 360(1948)
- 11. Dahneke, B., J. Colloid and Interf. Sci., 37, 342(1971)
- 12. Dahneke, B., J. Colloid and Interf. Sci., 40, 1(1972)
- 13. Dahneke, B., J. Colloid and Interf. Sci., 45, 584(1973)
- 14. Davies, C.N., ed., <u>Aerosol Science</u>, Academic Press, London (1966)
- 15. Derjaguin, B.V. and Smirnov, L.P.S., <u>Research in Surface</u>
 <u>Forces</u>, <u>Froceedings of Symposium Organized by the Inst. of Phys. Chem.</u>, U.S.S.R., Acad. of Sci., Consultants Bureau, New York (1971)
- 16. Engelman, R.J., J. Atmos. Sci., 22, 719(1965)
- 17. Environmental Research Corporation, Operation and Maintenance Manual for the Spinning Disc Aerosol Generator, St. Paul, Minnesota(1970)
- 18. Esman, N.A., Paper presented before the Div. of Air and Water Chem., Amer. Chem. Soc., Boston(1972)
- 19. Evans, L.F., Ind. Eng. Chem., 46, 2420(1954)

- 20. Flint, L.R. and Howarth, W.J., Chem. Eng. Sci., <u>26</u>, 1155(1971)
- 21. Foote, G.B., J. Atmos. Sci., 32, 390(1975)
- 22. Fox, H.W. and Zisman, W.A., J. Colloid Sci., 5, 514(1950)
- 23. Fuchs, N.A., The Mechanics of Aerosols, Pergamon Press, New York (1964)
- 24. Gillespie, T., J. Colloid and Interf. Sci., 10, 266(1955)
- 25. Goldshmid, Y. and Calvert, S., Λ.Ι. Ch. E.J., 9, 352(1963)
- 26. Good, W.R., J. Colloid and Interf. Sci., 44, 63(1973)
- 27. Hamaker, H.C., Physica, 4, 1058(1937)
- 28. Hampl, V., Kerker, M., Cooke, D.D. and Matjevic, E., J. Atmos. Sci., 28, 1211(1971)
- 29. Hampl, V. and Kerker, M., J. Colloid and Interf. Sci., 2, 305(1972)
- 30. Hartland, S., J. Colloid and Interf. Sci., <u>26</u>, 383(1968)
- 31. Herne, H., Paper presented before the Symposium on Aerodynamic Capture of Particles, Brit. Coal Board, Pergamon Press, London (1960)
- 32. Hidy, G.M. and Brock, J.R., The Dynamics of Aerocolloidal Systems, Pergamon Press, New York (1970)
- 33. Hodgson, T.D. and Woods, D.R., J. Colloid and Interf. Sci., 30, 429(1969)
- 34. Israelachvili, J.N. and Tabor, D., in <u>Progress in Surface</u> and Membrane Science, Vol. 7, Academic <u>Press</u>, New York (1973)
- 35. Jordan, D.W., Brit. J. Appl. Phys., 3(Supplement)S194(1954)
- 36. Kerker, M. and Hampl. V., J. Aerosol Sci., 31, 1368(1974)
- 37. Kraemer, H.F. and Johnstone, H.F., Ind. Eng. Chem., <u>47</u>, 2426(1955)
- 38. Krupp, H., Adv. in Colloid and Interf. Sci., $\underline{1}$, 111(1967)
- 39. Krupp, H., Schnabel, W. and Walter, G., J. Colloid and Interf. Sci., 39, 421(1972)

- 40. Lance, G.N., <u>Numerical Methods for High Speed Computers</u>, Ififfe and Sons Ltd., London(1960)
- 41. Langmuir, I., J. Meteor., 5, 175(1948)
- 41a. LeClair, B.P., Hamielec, A.E. and Pruppacher, H.R., J. Atmos. Sci., 27, 308(1970)
- 42. Liu, B.Y. and Pui, D.Y., J. Aerosol Sci., 5, 465(1974)
- 43. MacDonald, J.E., J. Geophys. Res., 68, 4993(1963)
- 44. MacKay, G.D.M. and Mason, S.G., J. Colloid Sci., 16, 632(1961)
- 45. Maude, A.D., Brit. J. Appl. Phys., 12, 293(1961)
- 46. May, K.R., J. Appl. Phys., 20, 932(1949)
- 47. McCully, C.R., Fisher, M., Langer, G., Rosinski, J., Glaess, H. and Werle, D., Ind. Eng. Chem., 48, 1512(1956)
- 48. McHardy, J., M. Sc. Thesis, Department of Mining Engineering, McGill University, Montreal(1972)
- 49. Montagna, J., Ph.D. Thesis, Department of Chemical Engineering, Wayne State University, Detroit(1974)
- 50. Montgomery, D.N., J. Atmos. Sci., 28, 291(1971)
- 51. Oakes, B., Paper presented before the Symposium on Aerodynamic Capture of Particles, Brit. Coal Board, Pergamon Press, London(1960)
- 52. O'Konski, C.T. and Doyle, G.J., Anal. Chem., 27, 694(1955)
- 53. Parsegian, V.A. and Ninham, B.W., J. Colloid and Interf. Sci., 37, 332(1971)
- 54. Pemberton, C.S., Paper presented before the Symposium on Aerodynamic Capture of Particles, Brit. Coal Board, Pergamon Press, London(1960)
- 55. Philippoff, W., Trans. A.I. Min. Metal. Eng., 193, 386(1952)
- Phillips, M.C. and Riddiford, A.C., J. Colloid and Interf. Sci., 41, 77(1972)
- 57. Picknett, R.G., Paper presented before the Symposium on Aerodynamic Capture of Particles, Brit. Coal Board, Pergamon Press, London(1960)
- 58. Ranz, W.E. and Wong, J.B., Ind. Eng. Chem., 44, 1371(1952)

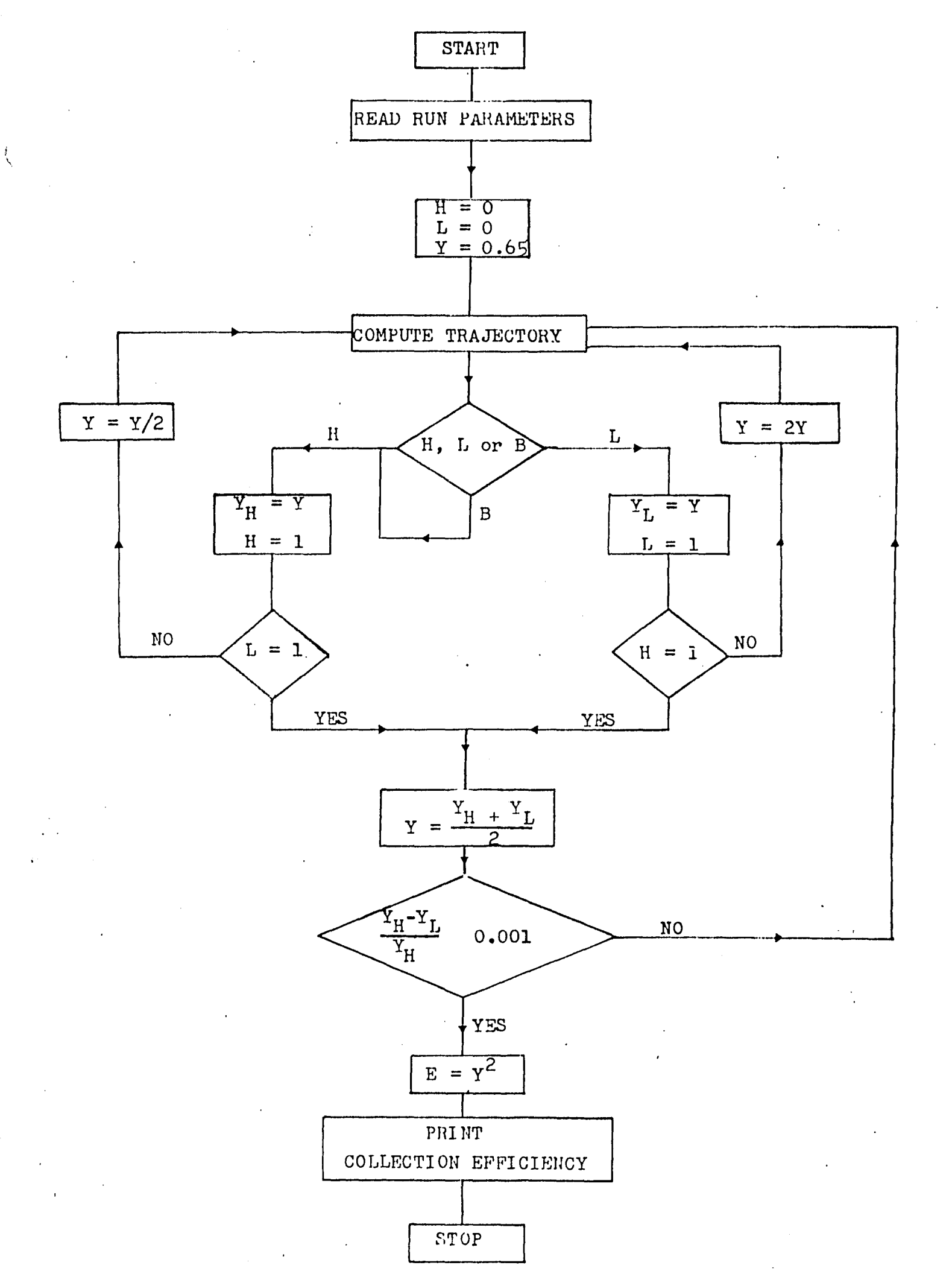
- 59. Reay, D., Ph.D. Thesis, Department of Chemical Engineering, McGill University, Montreal(1973)
- 60. Rebinder, P., Lipetz, M., Rimskaja, M. and Taubman, A., Kolloid Z., 65, 268(1933)
- 61. Riolo, E., Reed, X.B. and Hartland, S., J. Colloid and Interf. Sci., 50, 49(1975)
- 62. Rosinski, J., Stockham, J. and Pierrard, J.M., Kolloid Z. und Z. Polym., 190(1963)
- 63. Sartor, J.D., J. Geophys. Res., 65, 1953(1960)
- 64. Schenkel, J.H. and Kitchener, J.A., Trans. Farad. Soc., <u>56</u>, 161(1960)
- 65. Shimi, A.E. and Goddard, E.D., J. Colloid and Interf. Sci., 48, 242(1974)
- 66. Spielman, L.Λ. and Goren, S.L., Envir. Sci. Tech., 4, 135(1970)
- 67. Spielman, L.A. and Fitzpatrick, J.A., J. Colloid and Interf. Sci., 42, 607(1973)
- 68. Starr, J.R. and Mason, B.J., Q.J.R. Met. Soc., 92, 490(1966)
- 69. Van Quy, N., Int. J. Eng. Sci., 9, 101(1971)
- 70. Walton, W.H. and Woolcock, A., Paper presented before the Symposium on Aerodynamic Capture of Particles, Brit. Coal Board, Pergamon Press, London(1960)
- 71. Weber, E., Staub, 29, 272(1969)
- 72. Whelpdale, D.M. and List, R., J. Geophys. Res., <u>76</u>, 2836(1971)
- 73. Whipple, F.W.J., Int. Crit. Tables, 1, 71(1926)
- 74. Wu, S., J. Polym. Sci., 34, 19(1971)
- 75. Zinky, W.R., J. Air Poll. Cont. Ass., 12, 578(1962)

APPENDIX A

THEORETICAL CALCULATIONS

APPENDIX Al

LOGIC FLOW CHART OF COMPUTER PROGRAM



APPENDIX A2

LISTING OF PROGRAM USED TO CALCULATE
COLLECTION AND PENETRATION EFFICIENCIES

```
- T8T -
```

```
SPATCH WATERV CEILOGA RAYL60.991
        (1) SWATELY LONG, TIME=60, PAGES=45
             SYDEXT
             С
             С
                   NOMENCLATURE
                     K = IMPALTION PARAMETER
                     S = GRAVITATIONAL SETTLING VELOCITY
                    PPS = PAULUS RATIO
                     WE = MEBER W
                    CANS = CUNTACT ANGLE
                    X = (1)Y
                     Y(2) = Y
                     Y(3) = X VELOCITY OF PARTICLE
                     Y(4) = Y VELOCITY OF PARTICLE
                     SMIT = X
                     3 = CENTRE TO CENTRE SEPARATION
                    FRIM = THE FINAL SEPARATION TOLERANCE
                    SURFT = SURFACE TENSION OF WATER
                     JX = THE FLUID VELOCITY IN X DIRECTION
                    UY = THE FLUID VILUCITY IN THE Y DIRECTION
                    DY(5) = THE DERIVATIVES OF Y(5) WITH RESPECT TO TIME
                     CHILE = COLLECTION EFFICIENCY
                     TOLY = TULEPANCE BETWEEN HIGH AND LOW TRAJECTORIES
                    DIMENSION Y (5) DY (5)
                    TOMMON JOEP/Y/SPAD/OY/ACC/TOLKMIS)
                    COMMON K. G. RPS. RHOPEIB, BEIN, S. NUM, L. SURFT, CANS
                    COMMON EVEL, PARD, DROD, PHOP, CRIT, WE
                    PEAL K.MUAIR
                    PFAD(5.3)HIGH, HIGH. HIGH. MO.
                    IST.XCI.IA.XCI.IA.XOI.IATAMEDE
                    ICO.O.YIT
                    17 170 J=1,40
                    READES, SIK, RPS, G. WE, CANG
        10
                   F79441(5F10.0)
        11
2853891
                    ## | TE (6, 405) 4, 9, 975, #E, CANG
        12
               405 FDPMAT(*13,///.20x.*K=*.F7.3./.20x.*G=*.F7.3./.20x.*RPS=*.F10.6./.
        13
                   #20x. "HEBEK NUMBER* ". F9.5. /. 20x. "IDNTAIT ANGLE ** . F6. 2)
        14
                   1, 14=)
                    1121=0.65
        15
               128 *(11-15.0
        15
        17
                    Y141=Y(2)
                    HUMENUM+1
                    TF(NUM.ED.1) GD TD 50
        19
        20
                    25110=1Y2H-Y251/Y2H
```

```
- 182 -
```

```
TOL<M(1)=17LKM(2)=10LKM(3)=T0LKM(4)=0.0001
22
23
           EF11=0.3735
24
           X=0.3
25
           4=4
25
           A=Y(1)==?+Y(2)==?
27
           B=SCRT(A)
2 R
           1)=7=1-1=7(?)=7(2)
           F=9##5.0
23
30
           5=4-1-455
31
           11X=-1+(/(2#F)
32
           Y(3) = 1 \longleftrightarrow G
33
           Y{4}=0.3
34
           [iX=Y[]]/50
35
           PXM19=Y(1)/10000
36
          IF(*(2).L1.3.U0001)70 TO 49
37
            [FIY(1).31.3.0) 30 TO 15
39
            IF(Y(1).G1.9.25) 50 TO 415
37
            1F(Y(1).51.5.025) G7 T7 215
40
           DELX=Y(1)
41
           67 17 13
     15
42
           DEL <= Y (1) / 4
43
           60 10 13
44
     415
           DELX=Y(1)/9
45
            GO TO 13
46
     215
           DELY=Y(1)/2
47
       13 L=0
48
            CALL MERSONIC CORE X. DX. DXMIN. IFAIL, ITS. NI
49
            IF(L.FQ.10160 TO 8
50
            TELLIFORDADADAD TO 20
51
            IF(E.+0.30)93 TO 37
52
            $6(6.54.45)50 FC 41
            TETE. 50.4 /130 TO 45
53
            IF(L.50.47)50 17 47
54
55
            IF(L.FQ.5J)GO FD 51
     20
56
           WRITE (4,21)
            FORMATIONAS ISMALLER DIAMIN OR LARGER TOLKH REQUIRED FOR SUGGESSEU
.,7
     21
           DE INTEGRATION!)
59
            WRITE(5,221Y(1),Y(2),R, [FAIL
57
     22
           FORMATI///, IDX, TY CO-DRINATE #1, FR. 6, 10x, TX ID-DRDINATE #1, F9. 6,/
           X/.10x.*SEPAPATION >*.F9.6,10x.*THE VARIABLE #HIGH FAILS#*,13}
50
           63 63 100
     30
            WRITE(5.31)
4,1
     31
            FIRMATE!!!.////.ZDY.'SUCCESSFUL TRAJECTORY')
6.2
            30 70 100
1. 3
       49 49 [ 1 = (4, 93)
64
     93
            FORMATH//.10x. '7FRO COLLECTION EFFICIENCY')
1.5
            GO TO 100
t, s,
            S=P-1-2PS
4. 1
     40
7. 7
            [F(1.45].45] NO TO 845
67
            WRITE(4.41)YINT.HIGH.Y(1),Y(2),S.X
70
          . G7 T3 946
11
     845
           HRITE(5,41)YINT,HISB Y(1),Y(2),S,X
17
     846
            CONTINUE
            F78M4T1//.178.F7.4.15x.A1.14x.F9.3.12x.F9.3.14x.F7.3.15x.F7.31
13
     41
14
            Y2H=Y1"IT
            4F(NUM.LE.1) GO TO 700
15
            GO TO 201
74,
77
     233
           Y2L=0.0
73
     201
            Y(2) = (Y2L+Y2H) = 3.5
12
            GO TO 128
```

2853892

```
.
F00
```

```
51
                   5=4-1-005
        н1
                   WRITE(5,41)YINT,HIGL,Y(1),Y(2),S,X
        92
                   ASE=AIM1 ...
        93
                   IF(NJM.LE.1), 30 TO 202
        84
                   50 10 233
        25
             202
                   Y24=2=Y2L
             203 Y(2)=(Y?L+Y2H)=0.5
        86
        87
                 1 50 10 129
        HA.
              2==(C.5\(H5Y+J5Y1)=31JC3 085-
                   WRITE(4, 113) COLLE
        U
              113 FRAMATI///, TAS, "COLLISION EFFICIENCY=", F7.4)
        31
                   CONTINUE
        25
                   31.10
        93
                   END.
                   SUBROUTINE MERSONEX.DELX.DX.DX41N.TEATE.ITS.N)
        75
                   DIMENSION Y(5), YOUDES), EXES, 5), DY(5), ERR(5)
        44
                   COMMON /OEP/Y/GRAD/BY/ACC/TOLKM(5)
        97
                   COMMON K, J, RPS, RHOPE, B, EFIN, S, NUM, L, SURET, CANS
        18
                   COMMON FALL, PARD, DROD, RHOP, CRIT, HE
        39
                   REAL K
       100
                   TOLK=0.001
       101
                   115=3
       102
                   FINIS=DELX/DX+0.5
       103
                   INTS=[FIX(FIMIS)
       174
                   IFIINTS.LT.10INTS=1
       195
                   DX=DELY/IGTS
       106
                   FMULT-9X/3.
       107
                   GD TD 4
       103
                   nn 172 f=1.4
       107
                   IF(EPP(1).31.(TOLKM(1)45.0)) GO TO 20
       110
             172
                   CONTINUE
       111
                   DO 173 !=1.4
       112
                   1F(FRR(1).GT.(TOLKM(1)/32.)) GO TO 174
       111
                  CONTINUE
       114
                   GD TD 21
       115
             174
                   CONTINUE
       115
                 3 03 2 1=1+4
       117
                 2 Y(1)=YULD(1)+3.5=F<(1,1)+2.3=F<(4.1)+3.5*F<(5.1)
       118
                   ITS=ITS+1
       117
                    IF(3.LF.(1+RPS+FFIN).490.ABS(Y(1)).LE.TOLK) 50 TO 202
       120
                    P02 CT CC (CC.C.T.(1)Y.CVA.(298+1).11.P131
       121
                   60 72 703
       122
              202 L=30
       123
                   RETHRY
       174
             727
                   CONTINUE
       125
                   IF (74%7.EU.0.0)50 TO 920
       1.26
                   D=CGRT((Y(2)==2)+(Y(1)==2))
       177
                   VENS=((Y(4)*Y(21/D)*(Y(3)*Y(1)/D))**2
       129
                   C47=C446=3.141592654/190.0
       127
                   (FAJ)2CO-=RED
                   CRIT=12.0+COR/(HE=VELS)
       133
\sim
                   IF(CPIT.GT.1.0)GU TO 210
       131
g
       132
               920 L=50
\alpha
                   SELTSA
CO
       133
85.
               210 L=45
       1 14
       135
                   RETURN
2
       135
             203
                   IF(INTS.EU.1) GD TO 201
       1 3 7
                   GO TO 6
```

```
TO4 -
```

```
138
               201 L=13
       139
                   RETURN
       140
                 5 INTS=10TS-1
       141
                 4 KOLD=X
       142
                   00 5 I=1.9 -
       143
                 5 YOU ((1)=Y(1)
       144
                   145LF=U
       145
                   $3 (13.9)
       145
                20 5K=0.5#0X
       147
                   IFICK LILLKHIND GO TO 19
       14B
                   1975=19T5+1NTS
       147
                   IHALF=1
       150
                   50 10 3
       151
                  L=20
                   RET 17%
       152
                21 IFTHATF.CC.11 GO TO 3
       153
       154
                   159916=191572
       155
                   IF (CIDUBLe #2).EQ.INTS) GD TD 22
       155
                   55 10 3
       157
                22 INTS=IDUALE
       158
                   0x=2.40x
       .159
                 e Full Tank/s.
       150
                   PG 7 I=1,:
       161
                 7 Y(1)=Y0L0(1)
       162
                   X= 17L0
       163
                   CALL DERIVSIX.NI
       164
                   IF(E.E0.40)60 TO 73
       165
                   90 18 IS=1.5
       165
                   50 f0 (11,30,32,33,30), IS
                31 x=x+FMULT
       167
       168
                   50 10 30
       157
                32 X=X+0.5=FMULT
       170
                   SD TO 30
       171
                -33 X=Y7LD+UY
       172
                30 70 10 1=1.V
       173
                   Fr(IS.1): FMULT #MY(I)
       174
                   SO TO (11,12,13,14,10),15
       175
                11 Y(1)=YOLD([)+FY(1,])
       175
                   57 17 15
       177
                12 Y(1)=Y(L)(1)+3.5*(FK(1,1)+F<(2,1))
       178
                   50 10 10
       179
                13 Y(1)=Y7LJ[1]+9.375=FK(1,1)+1.125#FK(3,1)
       180
                   50 10 10
       181
                14 Y([]=YNED([]+1.5*FK([,[)-4.5*FK(3,[)+6.0*FK(4,[)
       182
                 10 SONTINUE
                   IF (15.EQ.>) GO TO 16
       183
       184
                   CALL PERIVS(X.1)
                   IFTL.E0.40160 TO 73
       185
       185
                    12 12 14
       187
                   00 17 1=1.4
             15
       188
             17
                   ERP([)=AH5(FK(1,1)-4.5*FK(3,1)+4.0*FK(4,1)-0.5*FK(5,1))
       187
                18 CONTINUE
       190
                   SO TO 1
4
       191
               73 L=40
5389
                   IF(Y(2).LI.0.00001)L=49
       192
       193
                   RETURN
       194
                   END
285
       195
                   CHAXISVIFEC BUITUCEBUZ
```

\$823895

APPENDIX A3

SAMPLE OUTPUT FOR CALCULATIONS OF COLLECTION AND PENETRATION EFFICIENCIES

	16,754	13.355	14.733	15.000	15.395	14.315	14.923	15.158	15.159	14.320	14.319
				_							
	-0.035	366 *0	2.393	0.033	5.313	-0.332	-0.331	0.028	0.327	-0.001	ccc*o-
	0.855	1.005	1.012	1.006	1.009	0.493	0.339	1.026	1,025	0.939	. 0 7 6 * 0
	ô	:	1.	1	1.	°C	°C	1	1.	•0	°
	0,519	1.728	0.427	0.255	0.191	. 255.0	0.356	0.120	0.120	0.356	0.356
50.30											
K= 1.333 5= 0.007 1PS= 0.035140 WEREN JWRER= 4.50300 CONTACT ANGLE= 0.33	٠	I	r	x	r	٦		I	I		
	0.5550	0.9753	0.8125	0.7312	\$069°C	0.6733	0.6805	0.6855	0.6830	0.6817	0.6824

thising erricitators 0.4551

,	14,354	16.91	14.523	14.445	14.445	14.354	14.354	14.445	14.354	14,354	14.354	
	\$2C*C-	\$1C*G	-0.335	520°0-	-3.355	-0.010	-0-333	-0-056	-0.002	100.001	CCC *0-	
	9,669	1.014	0.838	0.753	0.713	. 0.533	665-0	0.708	0.702	0.703	0.704	COLLISIGY EFFICIENCY= 0.4595
.37 UGO	0.737	0.157	0.551	0.643	0.641	0.733	0.730	0.547	0.729	. 621.0	9.729	COLLISION EFFI
K= 13.335 5= 0.03 4PS= 0.313990 4FRER 10.313990 CONTALT ANGLE=132.28		I	œ	æ .	æ			æ			ر	
	0.5503	0.9753	3.8125	3.7312	3.6406	0.6703	9.6805	0.6855	0.6839	0.6843	0.6849	

S823806

APPENDIX B

EXPERIMENTAL CALCULATIONS

APPENDIX B1

TABLE OF EXPERIMENTAL OPERATING CONDITIONS

Run Number	· Aerosol	Size (μ)	Velocity cm/sec.	Number of Drops	Average a/R	G	!Ye	
100	Ferrous Sulphate	10.3	162.5	14	0.00659	0.00386	0.73	
101	Ferrous Sulphate	10.8	292.3	5	0.00541	0.00215	2.36	
102	Ferrous Sulphate	12.4	382.3	6	0.00626	0.00216	4.65	
103	Talc	18.3	397.0	11	0.01214	0.00273	4.46	
104	Talc	18.3	382.6	9	0.00867	0.00283	4.14	
105	Talc	18.9	379.4	2	0.00958	0.00286	4.08	
106 .	Talc	18.3	469.9	15	0.01169	0.00231	6.25	Ti
107	D.O.P	9.8	. 387.7	8	0.00461	0.00070	1.98	i
108	D.O.P	11.4	382.3	11	0.00623	0.00096	2.24	
109	Water	7.2	390.4	22	0.00441	. 0.00034	1.51	
110	Methylene Blue	5.8	340.8	22	0.00314	0.00040	1.30	
111	Methylene Blue	5.8	337.8	12	0.00270	0.00040	1.27	
112	Talc	25.5	309.7	10	0.01211	0.00685	3.78	
114	Paraffin Oil	15.0	339.8	26	0.00989	0.00169	2.09	
115	Paraffin Oil	15.0	343.7	9	0.00673	0.00167	2.14	
116	Paraffin Wax	22.9	465.9	41	0.01389	0.00297	6.27	
117	Paraffin Wax	27.4	321.0	12	0.01334	0.00618	3.56	
118	Paraffin Wax	27.5	316.3	7	0.01479	0.00632	3.47	
. 119	Paraffin Wax	22.4	400.8	20	0.01389	. 0.00331	4.54	
120	Methylene Blue	5.0	427.6	4	0.00359	0.00024	1.76	
121	Ferrous Sulphate	11.8	163.1	23	0.00803	0.00469	08.0	
122	D.O.P.	15.7	339.6	9	0.00919	0.00209	2.43	

APPENDIX B2

LISTING OF COMPUTER PROGRAM TO REDUCE EXPERIMENTAL DATA

THIS IS THE MAIN PROGRAM FOR PROCESSING EXPERIMENTAL RESULTS. IT TAKES THE EXPERIMENTAL PRADINGS AND ANALYZES THEM TO GIVE IMPACTION NUMBER-REYNOLDS NUMBER-AND COLLECTION EFFICIENCY. IT ALSO CALCULATES THE AEROSOL VELOCITY FROM THE HOT WIRE READINGS

ON THE FIRST DATA CAND. THE MEAN PARTICLE SIZE OF EACH OF THE RANGES OF THE PARTICLE COUNTER IS READ IN. EACH IS SEPARATED BY A COMMA. IMMEDIATELY AFTER THE LAST ONE A SET OF TEMPERATURES IS READ IN. FOLLOWED BY A SET OF VISCOSITIES (OF AIR) WHICH COMPESPOND TO THOSE TEMPERATURES. NOTE: THIS IS AN UNFORMATED READ STATEMENT AND CAN ONLY BY USED ON THE WATER OF COMPILER.

THIS DATA DOESN'T NORMALLY CHANGE.
THE REFERENCE FOR THE VISCOSITIES IS 'THE HANDBOOK OF TABLES FOR APPLIED ENGINEERING SCIENCE ' PAGE 9.

ON THE NEXT DATA CARD THE FIRST 3 COLUMNS CONTAIN THE NUMBER OF CALIFFATION POINTS FOR THE PROBE. IN THE NEXT 3 COLUMNS IS THE PROBENO (MUST HE IN LETTERS NOT FIGURES). THEN TROP, ATMPR TEMPR. PSPR. AND VOPR ARE READ IN EACH WITH A FORMAT OF FIG. 0.

ON THE NEXT NOAL DATA CARDS THE DATA FOR THE WET TEST METER CALIFIRATION IS READ IN. THE HOLDGE READING IS HEAD IN FIRST FOLLOWID BY THE SAMPLE TIME IN SECONDS AND THEN THE VOLUME READING IN 10 LITRE UNITS. EACH HAS A FORMAT OF FIG.E.

THE FIRST CARD MUST HAVE DEPREVORR, TIMEQ.O, AND CFEO.O.

THE FIRST CARD MUST MAVE CORREMINER. TIMEO.G. AND CEEO.O. THIS DATA DOES NOT HAVE TO BE READ IN IF THE VENTURI CALIBRATION IS USED.

THE NEXT *NCAL* DATA CARDS ARE FOR THE VENTURE METER CALIBRATION AND ARE NOT NECESSARY IF THE WET TEST METER IS TO BE USED FOR THE CALIBRATION. ON THE NEXT NCAL DATA CARDS THE CALIBRATION DATA IS READ IN. ON FACH CARD THE BRIDGE VOLTAGE. IS FIRST.FULLOWED BY THE CORRESPONDING TRANSDUCER READING. FACH HAS A FORMAT OF FIG. 2.

THE FIRST CARD. MUST HAVE DEPREVO AND TRRESTOR.

ON THE NEXT DATA CARD THE NUMBER OF BUNS (NEXPT) IS READ IN. (12)

THE NEXT CARD CONTAINS THE PRESENT RUN NUMBER IN THE FIRST & COLS.
THIS IS FLLCZED BY A 70 COLUMN FIELD CONTAINING THE NAME OF THE SYSTEM USED. 70 CHARACTERS ARE ALLOWED AND THEY MUST ALL HE LETTERS.
NEXT DATA CARD; THE NUMBER OF THE FIRST DROP.15. THE RELATIVE HUMIDITY (AS A FRACTION AND WITH A FORMAT OF FIG.0). THE TLMPERATURE IN DEGREES F (FIG.0). THE ATMOSPHERIC PRESSURE IN MMS. MERCURY (FIG.0). THE DENSITY OF THE DISPERSED PHASE IN GYCC.(FIG.0). THE BRIDGE VOLTAGE AT ZERO VELOCITY(FIG.0). AND THE NUMBER OF DROPLETS FOR THAT RUN.

NEXT DATA CARD; THE DIAMETER OF THE PARTICLEICAN BE A NUMBER FROM 1.0 TO 14.0 CORRESPONDING TO THE SIZE RANGE ON THE PARTICLE COUNTER.OR A SPECIFIC

351212

```
SIZE OF PARTICLE CAN HE USED. IN THIS CASCUREAD IN A NUMBER 100 GREATER
           THAN THE PARTICLE SIZE IN MICRONS) .THE SAMPLE FLOW RATE IN CC./MINUTE.THE
           SAMPLE TIME IN SECONDS. THE DC READING. AND THE AC READING ARE ALL READ IN
           WITH A FORMAT OF FIG.O.
           ON THE NEXT *NEX* CARDS THE NUMBER OF PARTICLES COLLECTED. I(10).
           THE NUMBER WITHOUT THE DROP IN POSITION. 1(10). AND THE DIAMETER OF
           THE DROP ARE READ IN.
           THE NEXT DATA CARD SHOULD THEN BE ANOTHER RUN CARD.
           PRCHE CALIFRATION
           DIMENSION VELPR(40).DCPR(40).MU(6).TEMP(6).DIA(14)
           INTEGER PRCHNG.RUNNO
           CHARACTER*70 SYST
           HEAL MIC.ML
           READ.CIA.TEMP.HU
           DC 571 LL=1.3
           READ(5.1) NCAL . PROUND . TROP . ATMPR . TEMPH . PSPR . VOPR
         1 FORMAT(13.A3.5F10.0)
           WRITE(6-169)
           DUM IS A CONTROL VARIALE FOR THE VELOCITY CALIBRATION.
           IF CUM=0.0 THEN THE WET TEST METER CALIBRATION IS GOING TO BE USED.
           IF CUMPL O THEN THE VENTURE MFTER IS GOING TO BE USED.
    C
           DuM=0.0
           [F(00M+10+0+0) GO TO 750
11
12
           WRITE(6.110)PROHNO
       110 FORMAT(46x. PROPE CALIBRATION DATA (VENTURE METER) ... SAX. PROPE
13
          a NIMHEA = 1.43)
14
           WATTE (6.111)PSPR.VOPR.ATHOP. ICHPR
15
       111 FCRMAT(30x+*POWER SUPPLY VCLTAGE = *+F6+J+* VOLTS*+/+30x+*STATIC P
          SPRINE READING = ".F5.3." VOLIS"./.32%."AIMOSPHERIC PRESSURE = ".F5.
          WI. . PHZ NEDCODA.
           */*JOX**TEMPERATURE = *.F4.1.* DEGREES CENTIGRADE *)
16
           BRITE (0-112)
17
       112 FORMATIC///.14x.*HRIDGE*.7X.*TRANSDUCFR*.7X.*AIR VELOCITY*./.14X.*
          AVOLTACE!.ex. TREADING!./.14x.!(VOLTS)!.6x.!(MILLIVOLTS)!.5x.!(METRE
          #5/"EC)".//1
10
           GC TĠ 751
19
       750 WRITE(A.760)PRCHND
20
       760 FCPMAT(45x. PRCHE C/LIHRATION DATA (WET TEST METER) ... //. S8x. PROBE
          a NUMBER = 1.41.7/1
21
           WRITE(6.752) VCPR
       752 FORMATIA6X. STATIC PROHE READING # ".F6.3." VCLTS")
22
          .WRITE(6.753)
23
       753 FORMAT(////.17x.*t010GE*.T47.*AIR VFLOCITY*./.17x.*VOLTAGE*.T47.
          a * { #ETRF5/SEC } * . // }
           DO 763 I=1.NCAL
23
           IF(1.E0.24)GC TO 817
```

```
27
           GC 10 #00
28
     817
            WRITE(6.109)
29
     600
            CONTINUE
JC
           READ(5.802)DCPR(1).TIM.CF
31
       802 FURMAT( IF10.0)
32
           IF(1.50.1)63 TO 770
33
           A=(0.775#1.27)##2
34
           VELPR(1)=(CF=100001/(TIM+3.1416#A)
35
           VELPR(I)=VELPR(I)+0.01
3€
           GO TO 763
37
       906 VELPR(1)=0.0
       763 WRITE(6.7011CCPR(1).VELPR(1)
36
33
       901 FORMAT(/.15X.F7.3.T46.F7.3)
40
           GD TO 902
41
       751 NCAL=NCAL+1
42
           DO 3 I=1.NCAL
43
           IF(1.8C.14)60 TO 117
44
           IF(1.EC.34)G0 TO 117
45
           GO TO 200
     117
            WRITE(6.109)
46
47
     109
            FORMAT( 11)
     200
            CONTINUE
     C
           CALIBRATION OF PRESSURE TRANSDUCER
           READ(5.2)CCPR(I).TPPR
5C
         2 FORMAT(2F10.3)
51
           EM=1.0/3.483146
52
           POPREEM# (TRPR-TROP)
     c
    · c
           PDPH(I) IS THE PHESSURE DROP IN MM. OF WATER CORRESPONDING TO THE
           TRANSCUCER READOUT WHEN CALIBRATING THE PROBE.
           CALIBRATICS OF PROBE
53
           AT=ATMPR#13.5951
54
55
           GUNP=(1-(PCPR/AT))**A
           IF(1.EC.1)GD TO 500
56
           VELPR(1)=SCRT((2.0+287.1+(TEMPR+273.01/A)+(1-GUNP))
57
58
           60 TC 3
       500 VELPP(1)=0.0
     C
     C.
     c
           THE AIR VELOCITY IS CALCULATED HARE IN METRES PER SECOND
           BY THE FORMULA GIVEN IN THE DISA MANUAL
         3 WRITE(6.4)DCPR(1).TRPR.VELPR(1)
         4 FORMAT(/.15x.F7.3.1ux.F4.1.10x.F8.4)
62
      902 CONTINUE
           READ(5.11) NEXPT
63
        11 FORMAT(12)
           NEXPT= THE NUMBER OF RUNS.
```

```
- 1967 -
```

```
c
            NEXT THE NUMBER OF DROPLETS.
            CO 12 MN=1.NEXPT
 65
 66
            K Z = 0
 67
            GT=0.0
 68
            ART = C.O
 69
            K X = C
 70
            READ(5.58) RUNNO.SYST
 71
        58 FCRWAT(14.452)
 72
            READ(5.13)NFIRST.HUMID.TEMPR.ATM.RHOD.VU
 73
         13 FORMAT(IS.SF10.3)
            TEMBRETLMPRIAGO
      c
      c
            CORRECTION FOR HEIGHT ON PRESSURE USING THE BARDMETIC FORMULA.REFERENCE;
            "FLUID MECHANICS" BY DE NEVERS. HEIGHT DIFFERENTIAL USED WAS 64.5 FEET.
      c
      c
            ATM=ATM4EXP((-28.91*64.5)/(10.73*144*TEMPR))
 76
            TEMPRETEMPRESONO
 77
            HUMID=HUMIC+109
 78
            PEAD(5.15)CIAP.CC.AC.NEX
 79
         15 FCHMAT(3F13.C.14)
 90
            IF(DIAP-LT-105-0) GO TO 700
 eı
            DIAP=(CIAP-100.0)/(10**4)
 65
            GC TO 701
 63
        700 NHEDIAP
            DIAPECIA(NM)/(10**4)
 94
 45
       701 CONTINUE
 86
            TEN=TEMPR-400.0
 87
            TEM=(5/9)*(TEM-32)+273.15
 88
            PMCC=(288.9/(10006))0ATM/(0.62174TEM)
      C
            LINEAR INTERPOLATION USED TO FIND THE VISCOSITY
            CC 23 M=1.6
 91
            IFITEMPR.LE.TEMP(MK) 1GG TO 24
 92
         23 CONTINUE
 91
         24 A=TEMP(M)-TEMPR
 94
            PUC=PU(M)+(A/9.0)*(PU(M)-PU(M-1))
 95
            MUC=MLC#14.852/(10.0##4)
         " - CALCULATION OF THE VELOCITY.
      c
 90
            *1 = 1
 97
            M2=NCAL
 9 #
            M3+(N1+N2)/2
-30
        40C 44=N3
100
            IF (DC-CCPR(N4))401-402-403
1 C 1
        401 NZ=N3
102
            N3=(N1+N2)/2
103
            IF(N3.EG.N4)GC TO 402
104
            3C TO 430
105
        403 N1=N3
            N3=(N1+N2)/2
100
107
            IF(N3.EC.N4)GD TO 402
108
            GO TO 400
100
        402 NJ=N3+1
110
            I=N3
```

```
- 197 --
```

```
INTERPOLATION CONVERTING VOLTAGE TO VELOCITY USING A FOURTH POWER
             THE SQUARE OF THE BRIDGE VOLTAGE (DC) AND THE SQUARE ROOT OF THE
             VELOCITY ARE USED. WHEN THE INTERPOLATION IS DONE THE RESULTING VELOCITY
             IS SQUARED TO GIVE THE ESTIMATED VELOCITY.
 111
             1-1-1
 112
             D=VELFR(1)
 113
             E=OCPR(I)
 114
             [ = [ + ]
             F=VELFR(1)
 115
             G=0C₽0(1)
 117
             DC=DC*DC
             E=E*E
 118
             F=SCRT(F)
 113
             D=SCRT(D)
 120
 121
             G=G+G
             VEL=((CC-F)+(F-D)/(G-E))+D
 122
             VEL=VEL+VEL
123
 124
             AC=AC+C.CC1
             TURP=100*AC*(4=0C)/((DC+VD)*(DC-VD))
 125
 126
             VELP=VFL=100
 127
             WEERHOD# VELP# VELP#DIAP/72.8
. 128
             WRITE(6.59)5751
129
         59 FORMATI'11'+////-T30.1SYSTEM USED WAS1.AS0.////)
             WRITE(6.18)HUNNO.HUMID.TEMPR.ATM.BHOD.BHOC.HUC.DIAP.VEL.TURH.WE
130
 131
         18 FURMATERX. "RUN NUMBER". TES. "HUMIDITY". TO 7. "TEMPERATURE". TAG. "PRESS
            BURE **TSP+ *FENSITY CF*+TG4.*DENSITY OF **T70.*VISCOSITY*.TPB.*DTAM.
            adf*.tl00.*Acacsol*.filp.*foanulEnce*.fi24.*#EHER*./.f52.*bispersed
            2*.T64.*CGhTfmpDH5*.TH3.*ALPH50L*.T190.*VFLCCTTY*.T124.*NUMHEP*./.T
            a52.*PHASE*.I64.*PHASE*.IPP.*PARTICLES*./.I15.*(PER CENT)*.IP7.*(DE
            BG F1*+T40+*(MMS HG)*+T52+*(G/CC)*+T76+*(D)(SE)*+T88+*(CMS)*+T100+*
            w(MZSEC)**T112.*(PER CENT)**ZZ*T3*T5*F5*1*T27*F5*1*T4G*F6*1*T52
            a.F5.3.164.F7.5.176.FH.r.188.F7.5.1100.F5.3.T112.F5.3.T124.F5.2.//
            a//.t +.131(***)./.132(***)}
132
             #RITE(6.53)
         53 FORMAT(////:54.*DROP NUMBER*.T20.*DIAM. GF*.T35.*NUMBER*.T50.*BACK
133
            ASPRUNC **TAD: *CRLLECTION*: THO: * IMPACTION*: TOD: *REYNOLDS*: /: T20: *DRD
            aple: -. T35. *CGLLECTED *. T50. *COUNT *. T65. *FFF1C!ENCY *. T80. *NUMBER *. T9
            25. *NUMMER *./. 177. * (CMS) *. 165. * (PER CENT) *.///)
 134
             NEXHENFIRST+NFX-1
             CO 16 KENFIRST-NEXP
 1 35
             W. C. E. K. X + 1
 1 16
             READIS-171CIAD-HPARS-NCOLL
 1 17
 1 18
         17 FORMAT(F10.0.215)
 1.39
             DUMYSTANCE DIADONS THE
 LAC
             PETTVELPERHICARIAPI/(9.04MUCADIADI)=DIAP
 141
             X=FLOAT(NCCLL)/FLOAT(NPARS)
 142
             S**OAIGEAX
 143
             XXX=6.8121
             IF(HUNNC-LE-102)XXX=11.758041
 144
             EFF=X+XXXXXX
 145
             IF(KZ.EC.1)GC TO 75
 140
 147
             XXXXX/16.J
             SO TO 76
 145
         75 KK=KX/39.0
 144
 150
             CONTINUE
 151
             IF(XK.EC.1.0) GO TO 501
```

```
198 -
```

```
1F(<K.E0.2.0) GO TO 501
1F(<K.E0.3.0) GO TO 501
152
153
154
             IF(xk.FC.4.G) GO TO 501
155
             GO TO 502
154
         501 WRITE (6.109)
157
             WRITE (6.53)
158
             K Z = 1
157
         502 CONTINUE
             WRITE(6.56)X.CIAD.NCGLL.NPARS.EFF.P.RE
160
161
         56 FCGMAT(/.T5.IJ.T20.F5.J.T35.IS.T50.I5.T65.F5.1.T80.F5.2.T95.F5.1)
162
         16 CONTINUE
163
         12 CONTINUE
       571 CONTINUE
164
165
             STOP
166
             END
```

SDATA

3512134

APPENDIX B3

EXPERIMENTAL RESULTS

PRODE CALIFFATION DATA (WET TEST METER)

PROBE NUMBER = TL

STATIC PHONE READING = 4.903 VOLTS

	BRIDGE VCLTAGE	AIR VELGCITY (METRES/SEC)
	4.903	0.00
	5.421	0.416
	5.549	0.597
	5.660	0.771
	5.737	0.913
	5.845	1.153
	5.939	1.381
	6.037	1.054
	6.135	1.968
	6.231	2.298
	6.320	2.650
	6.398	2.976
•	6.442	3.203
	6.508	3-481
	6.572	3.770
	6.623	4.072
	6.698	4.356
	6.747	4.583
	6.792	4.811
	6+845	5.078
• .:	6.867	5.224

SYSTEM USED WAS FERROUS SULPHATE AFROSOL: WATER DROPLET

RUN NUMBER	PUMIDITY	TEMPERATURE	PPESSURE	DENSITY OF CISH AGED PHASE	DENSITY OF CONTINUOUS PHASE	VISCOSITY	DIAM. OF AEROSOL PARTICLES	AEROSCL VFLOCITY	TURBULENCE	WEBER NUMBER
	(PER CENT)	(DEG F)	(NHS HG)	(excc)		(POISE)	(CMS)	(M/SEC)	(PER CENT)	
100	63.0	e3.0	751.4	1 +863	0.00128	0.000189	0.00108	1.625	0.056	0.73

BACKGROUND DRUP NUMBER NUMBER COLLECTION IMPACTION REYNOLDS DIAM. CF DRCPLET EFFICIENCY NUMBER COLLECTED COUNT NUMBER (CPS) (PER CENT) 1344 22308 142.0 200 0.129 42.6 1.61 1651 22277 50.0 1.58 145.3 2 C·1 C.132 1817 159.7 202 0.145 22574 45.5 1.43 2244 20075 37.1 207.0 203 6.188 1 - 11 0.223 2973 19156 36.7 0.93 245.5 204 205 0.243 3335 19004 34.9 0.26 267.6 206 0.175 1935 20683 35.9 1.19 192.7 207 0.168 206B 22419 38.4 1.24 185.0 0-166 1763 22514 33.4 1.25 182.8 200 209 0.166 217B 21483 41.3 1.25 182.8 210 0.141 1731 20289 50.5 1.47 155.3 211 0.152 1900 20821 1.37 167.4 0-164 2278 21715 45.9 1.27 180.6 212 190.5 213 0.173 2466 21663 1.20

PROBE CALIBRATION DATA (WET TEST METER)

PROBE NUMBER = TL

STATIC PROBE READING = 8.772 VOLTS

BRIDGE VCLTAGE	AIR VELOCITY (METRES/SEC)	
8+772	0.0cc	
9.177	0.153	**
9.749	0.433	
10.663	0 • 669	
10.137	0.931	
10-019	1.252	
10.945	1 -694	
11.232	2.170	
11.549	2.738	
11-675	3.416	
12.167	4-112	
12.446	5.032	

RUN NUMBER	. HUMIDITY	TEMPERATURE	PRESSURE	DENSITY OF DISPERSED PHASE	DENSITY OF CONTINUOUS PHASE	VISCOSITY	DIAM. OF AERCSOL PARTICLES	AEROSOL VELOCITY	TURBULENCE	WEBER NUMBER
	(PER CENT)	(DEG F)	(PPS HG)	(G/CC)		(POISE)	(CMS)	(M/SEC)	(PER CENT)	
101	56.0	84.0	758.4	1.863	0.00150	0.00188	0.06108	2.923	0.017	2.36

			• • • • • • • • • • • • • • • • • • • •		•	•
DACH NUMBER	DIAM. CF DPCPLET (CMS)	NUMBER COLLECTED	BACKGROUND COUNT	COLLECTION EFFICIENCY (PER CENT)	IMPACTION NUMBER	NUMBER BEANÓTOZ
220	0-175	1675	11727	55.5	2 • 14	350.3
	C-2C3	2288	11727	55.7	1.85	406+4
222	0.201	2401	11719	59.6	1 • 26	402-4
223	0.203	1392	11670	48.7	1.85	406+4
224	0.222	2296	11649	47.0	1.69	444.4

RUN NUMBE	R HUMIDITY	TEMPERATURE	PRESSURE	DENSITY OF Dispersed Phasë	DENSITY OF CONTINUOUS PHASE	VISCOSITY	DIAM. OF AEROSOL PARTICLES	AEROSOL VELOCITY	TURBULENCE	WEBER NUMBER
	(PER CENT)	(DEG F)	(MMS HG)	(G/CC)		(POISE)	(CMS)	(M/SEC)	(PER CENT)	
102	68.0	83.0	759+0	1.863	0.00129	0.000189	0.00124	3.828	0.011	4.65

DROP NUMBER	DIAM- CF DRCPLET (CMS)	NUMBER COLLECTED	RACKGROUND CCUNT	COLLECTION EFFICIENCY (PER CENT)	IMPACTION NUMBER	REYNOLDS NUMBER
225	0.242	3777	10466 .	72.5	2.67	634.1
559	0.239	3651	10150	74.0	2.70	626.2
227	0-209	2716	10410	70.2 .	3.69	547.6
.228	0.186	2307	10179	77•G	3.47	487.4
229	0.171	1791	10430	69.0	3.78	448.1
230	0.167	1674	10040	70.3	3-87	437.6

RUN NURIII	EH HUMIDITY	TEMPERATURE	PRESSURE	DENSITY OF DISPERSED PHASE	DENSITY OF CONTINUOUS PHASE	VISCOSITY	DIAM. OF AEROSOL PARTICLES	AEROSOL VELOCITY	TURBULENCE	WEBER NUMBER
	(PER CENT)	·(DEG F)	(MMS HG)	(G/CC)		(POISE)	(CMS)	(M/SEC)	(PER CENT)	
103	69+0	80.5	761.2	1-126	0.00129	0.000189	0.00183	3.970	0.022	4.46

DROP NUMBER	DIAM. CF DRCFLET (CMS)	NUMBER COLLECTED	BACKGROUND COUNT	COLLECTION EFFICIENCY (PER CENT)	IMPACTION	REYNOLDS NUMBER
240	0.101	1210	22472	36.0	8.70	274.3
241 .	0.177	2403	25332	27.3	4.96	480-6
242	0.115	1145	27570	26 • 1	7.64	312.3
243	0.143	1172	22473	17.4	6.14	388.3
244	0.101	1883	22677	17.3	4.45	491.5
245	0.161	1556	22502	18.2	5.46	437.2
246	0.182	1176	22307	10.8	4.83	434.2
247	0.157	1526	22101	19+1	5.60	426.3
248	0.208	2571	22025	18.5	4.22	564. A
249	0.153	1133	22461	14.7	5.74	415.5
250	0-147	2006	22498	28 - 1	5.98	399.2

-

RUN NUMBEI	R HUMIDITY	TEMPERATURE	PRESSURE	DENSITY OF DISPERSED PHASE	DENSITY OF CONTINUOUS PHASE	Altenosita	DIAM. OF AEROSOL PARTICLES	AEROSOL VELOCITY	TURBULENCE	WEBER NUMBER
	(PER CENT)	(DEG F)	(MMS HG)	(G/CC)	·	(POISE)	(CMS)	(M/SEC)	(PER CENT)	
104	69.0	. 80.5	761.2	1-126	0.00129	0.000189	0.00183	3.826	0.012	4.14

DROP NUMBER	DIAM. CF DRCPLET (CMS)	NUMBER COLLECTED	BACKGROUND COUNT	COLLECTION EFFICIENCY (PER CENT)	IMPACTION Number	REYNOLDS NUMBER	
255	0.234	1586	22705 .	B • 7	3.62	612.4	
256	0.215	2115	22772	13.7	3.94	562.6	
257	0.249	3769	22811	10-2	3.40	651.6	
258	0.248	2900	22676	14.0	3.41	649.0	
257	0.202	2661	22863	19.4	4.19	528.6	
260	0.205	1258	22824	8.9	4.13	536.5	
261	C-155	1758	22887	21.8	5.46	405.6	
262	0.200	2779	22861	20.7	4.23	523.4	
263	0.229	1694	22853	9.6	3.70	599+3	

RUN NUMBER	PUHIDITY	TEMPERATURE	PRESSURE	DENSITY OF DISPERSED PHASE	DENSITY OF CONTINUOUS PHASE	VISCOSITY	DIAM. OF AERCSOL PARTICLES	AEROSOL VELOCITY	TURBULENCE	WEBER NUMBER
	(PER CENT)	(DEG F)	(PMS HG)	(G/CC)		(POISE)	(CMS)	(M/SEC)	(PER CENT)	
105	69.0	80.5	761.2	1.126	0.00129	0.000189	0.60183	3.794	0.015	4.08

אפשעטא קטאס •	DIAM. CF DRCPLET (CMS)	NUMBER COLLECTED	RACKGROUND COUNT .	COLLECTION EFFICIENCY (PER CENT)	IMPACTION Number	PEYNOLDS NUMBER
268	0.193	1724	20864	15.2	4.35	500.9
269	0.189	1804	20854	16.5	4.44	490.6

RUN NUFCEI	Y HUMIDITY	TEMPERATURE	PRESSURE	DENSITY OF DISPERSED PHASE	DENSITY OF CONTINUOUS PHASE	VISCOSITY	DIAM. OF AERUSOL PARTICLES	AEROSCL VELOCITY	TURBULENCE	WEBER NUMBER
	(PER CENT)	(DEG F)	(MMS HG)	(G/CC)	•	(POISE)	(CMS)	(M/SEC)	(PER CENT)	
106	69.0	80.5	761-2	1-126	0.00129	0.000189	0.00163	4.699	0.016	6.25

DRUP NUMBER	DIAM. CF DRCPLET (CMS)	NUMBER COLLECTED	BACKGROUND .	COLLECTION EFFICIENCY (PER CENT)	IMPACTION NUMBER	REYNOLDS NUMBER		
300	0.217	2860	14320	28.9	4.79	697.5		
301	0.124	1191	14394	36.7	6.39	398.6		1
302	G-141	1699	14359	40.5	7.38	453.2		
303	0.191	2761	14238	36.6	5.44	613.9		
3¢ 4	0.148	1598	14312	34.7	7.03	475.7		
305	0.167	1985	14201	34+1	6.23	536.8		
306	0-166	2178	14261	37.8	6.26	533.6		
30 7	0.107	976	14243	49.è	9.72	343.9		
306	C-114	1060	14287	38.9	9-12	366.4		
303	0.234	3672	14274	32.0	4.44	752.1		
315	0.194	3592	14222	32.9	5.36	623.6		
311	0.211	2829	14112	30.7	4.93	678.2		
313 .	0.180	2142	14110	31.9	5.78	578.6	•	
117	0.152	1479	14050	31.0	6-84	488.6	•	
314	6.131	1 393	14147	39-1	7.64	421.1		

ثث

SYSTEM USED WAS DIGCTYL PHTHALATE AEROSOL: WATER DROPLET

٠	RUN NUMBER	PUMIDITY	TEMPERATURE	PRESSURE	DENSITY OF DISPERSED PHASE	DENSITY OF CONTINUOUS PHASE	VISCOSITY	DIAM. OF AERGSCL Particles	AEROSOL VELOCITY	TURBULENCE	NUMBER WEBER
		(PER CENT)	(DEG F)	(MMS HG)	(G/CC)		(POISE)	(CMS)	(M/SEC)	(PER CENT)	
	107	62.0	81.5	75A.4	0.977	0.00129	0-000189	0.06698	3.877	0-017	1.98

	•					
DRCP AUMBER	OIAM. CF CRCPLET (CMS)	NUMBER COLLECTED	BACKGROUND COUNT	COLLECTION EFFICIENCY (PER CENT)	IMPACTION Number	REYNOLDS HUMBER
325	0.218	1538	15585 .	14.1	Q.98	576.8
326	0.255	1443	15788	9.6	0.84	674.7
327	0.240	1111	17009	7.7	0.89	635.0
128	0.240	1063	17402	7.2	0.69	635.0
359	C-218	992	16172	8 • 8	0.38	576.8
330	0.206	1181	16249	11.7	1.04	545.0
331	0.232	1836	17444	17.6	1.06	534.4
332	0.157	1024	17662	16.0	1.36	415.4

SYSTEM USED WAS DIOCTYL PHIHALATE AEROSOL: WATER DROPLET

RUN NUMBER	HUMIDITY	TEMPERATURE	PRESSURE	DENSITY OF DISPERSED PHASE	DENSITY OF CONTINUOUS PHASE	VISCOSITY	DIAM. OF AEROSOL PARTICLES	AEROSOL VELOCITY		WEBER .
•	(PER CENT)	(DEG F)	(PPS HG)	(G/CC)		(POISE)	(CMS)	(M/SEC)	(PER CENT)	
108	52.0	81.5	750.4	0.977	0.60129	0.000189	0.00114	3.823	0.022	2.24

DIAM. CF NUMBER BACKGROUND COLLECTION IMPACTION DROP NUMBER REYNOLDS DACPLET COLLECTED COUNT EFFICIENCY NUMBER NUMBER (CMS) (PER CENT) C.216 1123 17161 1.32 340 9.6 563.6 341 ' 0.118 1618 18226 43.4 2.42 307.9 342 0.234 2280 18064 15.7 1.22 610.6 343 0.250 2820 18452 16.7 1.14 652.3 0.232 2250 18355 344 15.5 1.23 605.4 0.167 18381 345 2144 28.5 1.71 435.8 0.190 346 1392 16703 14.0 1.50 495.8 0.215 i.33 347 2167 18097 17-6 561.0 0.184 1694 18097 18.8 1.55 480.1 348 0.168 1707 18206 18-1 1.52 490.6 J49 350 0.129 .115 178G0 25.6 2.21 336.6

SYSTEM USED WAS WATER AEROSUL: WATER DROPLET

RUN NUMBE	R HUMIDITY	TEMPERATURE	PRESSURE	DENSITY OF DISPERSED PHASE	DENSITY OF CONTINUOUS PHASE	VISCOSITY	DIAM. OF AERCSCL PARTICLES	AEROSOL VELOCITY	TURBULENCE	WEBER NUMBER
	(PER CENT)	(DEG F)	(MMS HG)	(G/CC)		(POISE)	(CMS)	(M/SEC)	(PER CENT)	
109	84.0	0.08	759.4	1.000	0.00129	0.000185	0.00072	3.904	0.020	1.51

DROP NUMBER	DIAM. CF DRCPLET (CMS)	NUMBER COLLECTED	RACKGROUND COUNT .	COLLECTION EFFICIENCY (PER CENT)	IMPACTION Number	REYNOLDS NUMBER			
356	0.209	2222	16610 .	20.9	0.58	570.7			i
357 .	0.220	3246	16316	27.0	0.55	600.7	•		į
358	C-165	1423	16497	21.6	0.74	450+6			
359 -	G-147	2319	15497	47.6	0.83	401.4	,		:
360	0.260	1566	16045	9.8	0.47	710.0			•
361	0.229	1713	17813	12.5	0.53	625.3			ļ
362	0.216	2032	18632	22.2	0.56	587+8			İ
363	0.225	2341	16553	19+0	0.54	614.4			:
364	0.195	1612	16961	17.0	0.62	532.5			!
365	0.145	2023 .	16684	39.3	9.84	395.9		•	
366	G-233	1622	17339	11.7	0.52	636.2	•		!
367	0.118	1 366	17794	37.4	1 - 0 3	322.2			•
168	0.153	1590	15656	29.6	0.80	417.8		•	<i>!</i>
369	0.233	1997	14032	17.9	0.52	636.2			
370	0.103	1156	17690	42.0	1.18	261.3			1
								•	

DROP NUMBER	DIAM. CF CRCPLET (CMS)	NUMBER COLLECTED	BACKGROUND CCUNT	COLLECTION EFFICIENCY (PER CENT)	IMPACTION Number	REYNOLDS NUMBER
371	C-143	1391	17929	25•8	0 • 85	390.5
372	0.198	2237	17206	22.6	0.61	540.7
373	0 - 104	1021	17361	37.0	1.17	284.0
374	0-116	1137	17361	33-2	1.05	316.8
375	0.233	2904	16284	22.4	0.52	636.2
376	0.243	2617	15490	19.5	0.50	663.5
377	0.090	1026	17106	50.4	1.35	245.8

PROHE CALIBRATION DATA (WET TEST METER)

PROBE NUMBER = TS

STATIC PROBE READING = 11.168 VOLTS

BRIDGE	AIR VELOCITY
VCL TAGE	(METRES/SEC)
11.168	0.000
11.810	0.335
12.223	0.603
12.653	0.992
13-149	1.565
13-345	1.827
13.764	2.508
14.056	3.079
14.335	3.713
14.411	3.852
14.474	4.612
14.908	5.142
15.422	6.615

SYSTEM USED WAS METHYLFHE PLUE AEROSOL: WATER DROPLET

RUN NUMBER	HUMICITY	TEMPERATURE	PRESSURE	DENSITY OF DISPERSED PHASE	DENSITY OF CONTINUOUS PHASE	VISCOSITY	DIAM. OF AEROSCL PARTICLES	AEROSCL VELOCITY	TURHULENCE	WEBER NUMBER
	(PER CENT)	(DEG F)	(PMS HG)	(G/CC)		(POISE)	(CMS)	(HYSEC)	(PER CENT)	
110	56.0	84.0	. 757.6	1.401	0.00129	0.000188	C.00058	3.468	0.020	1 • 30

OROP NUMBER	DIAM. CF DRCPLET (CMS)	NUMBER COLLECTED	BACKGROUND COUNT •	COLLECTION EFFICIENCY (PER CENT)	IMPACTION NUMBER	REYNOLDS NUMBER		
383	0.237	1605	17084	11.4	0.40	552.5		
384	0.220	1187	16494	10-1	0.43	512.9		
385	0.176	1474	17071	19.0	0.54	410.3		
769	0-113	1164	18371	33.8	0-64	263.4		
387	0.256	2569	18652	14+3	0.37	596.8		
386	0.215	1731	18687	13.7	0.44	501.2		
389	0-211	2210	18649	18.1	0.45	491.9		
390	0.161	1153	10010	16.8	0.59	375.3		
391	0+158	1281	19219	19.2	0.60	368.3		
392	0.249	1437	1 e 7 3 1	8.4	0.38	580.5		
393	0-172	. 274	18731	15.7	0.55	401.0		••
394	0.197	1938	18606	18.3	0.48	459.3	•	
J95 · ·	0.206	1835	17955	16.4	0.46	480.3	•	
396	0.182	1607	18310	18.C	0.52	424.3		
397	0-182	2043	18135	23.2	0.52	424+3		
							_	

DROP NUMBER .	DIAM. CF DRCPLET (CMS)	NUMBER COLLECTED	BACKGROUND COUNT	COLLECTION EFFICIENCY (PER CENT)	IMPACTION Number	PEYNOLDS NUMBER
378	0-161	1594	18135	23.1	0.59	375+3
399	0.104	1143	18039	39.9	0.91	242.5
400	0.211	1123	18152	9.5	0.45	491.9
401	0.249	1908	16323	11.4	0.38	580.5
402	0.237	2045	18658	13.3	0.40	552.5
403	0.256	1444	18284	8.2	0.37	596+8
464	0.150	1604	18781	25.9	0.63	349.7

SYSTEM USED WAS METHYLENE BLUE AEROSOL: WATER DROPLET

RUN NUMBER	HUHEOTTY	TEMPERATURE	PRESSURE	DENSITY OF DISPERSED PHASE	DENSITY OF CONTINUOUS PHASE	VISCOSITY	DIAM. OF AERCSCL PARTICLES	AEROSOL VELOCITY	TURBULENCE	WEBER NUMBER
•	(PER CENT)	(DEG F)	(PMS HG)	(GZČC)		(POISE)	(CMS)	(P/SEC)	(PER CENT)	
111	56.0	84.9	757.6	1.401	3.06129	0.000188	0.00058	3.378	0-015	1.27

DROP NUMBER	DIAM. CF DRCPLET (CMS)	NUPBER CGLLECTED	RACKGROUND COUNT	COLLECTION EFFICIENCY (PFR CENT)	IMPACTION Number	REYNOLDS NUMBER
410	0.200	1247	12889	16.5	0.47	462.2
411	0.235	1898	12742	18.4	0.40	543.0
412	G.214	P68	12360	10.4	0.44	494.5
413	0.235	1243	12483	12.3	0.40	543.0
414	0.224	1665	12258	18.4	0.42	517.6
415	0.235	1232	12370	12.3	G-40	543.0
416	0.200	1088	12367	15.0	0.47	462.2
417	0.214	1130	12513	13.4	G-44	474.5
418	0.209	1143	12769	14.G	0.45	483.0
419	0.241	1546	12962	14.3	0.39	556.9
426	0-219	1386	12517	15.7	0.43	506.1
471	6.171	1 327	12102	25.5	0.55	395•2

RUN NUMBER	YTIDIMUM S	TEMPERATURE	PRESSURE	DENSITY OF DISPERSED PHASE	DENSITY OF CONTINUOUS PHASE	VISCOSITY	DIAM. OF AERGSOL PARTICLES	AEPOSGL' VELOCITY	TURBULENCE	WEBER NUMBER
	(PER CENT)	(DEG F)	(PMS HG)	(G/CC)		(POISE)	(CMS)	(M/SEC)	(PER' CENT)	
112	72.0	96.0	757.7	1.125	0-03129	J. C00188	0.00255	3.097	0.016	3.78

OROP NUMBER	DIAM. CF DRCPLET (CMS)	NUMBER COLLECTED	BACKGROUND COUNT .	COLLECTION EFFICIENCY (PER CENT)	IMPACTION NUMBER	REYNOLDS NUMBER	
							ŗ
500	0.219	1215	19029 .	9.1	6.12	465.5	•
501 ,	0.204	1048	19324	8.9	6.57	433.6	ŕ
502	0.252	1951	1 7610	10.7	5.32	535.7	
503	0.247	. 1809	19651	10.3	5.43	525.0	
504	0.207	1132	19172	9.4	6.48	440.0	
505	0.210	1262	19763	9.9	6.39	446.4	
506	0.211	1264	19153	10-1	6.36	446+5	
507	0.226	1693	19673	11.5	5.93	480.4	
508	0.183	1269	18711	13.8	7.33	389.ò	
509	0.173	1012	18536	12.4	7.75	367.7	

RUN NUMMER	HUMIDITY	TEMPERATURE	PRESSURE	DENSITY OF DISPERSED PHASE	DENSITY OF CONTINUOUS PHASE	VISCOSITY	DIAM. OF AERCSOL PARTICLES	AEROSCL VELOCITY	TURBULENCE	WEBFR NUMBER
	(PER CENT)	(DEG F)	(WMS HG)	(CVCC)		(POISE)	(CM5)	(M/SEC)	(PER CENT)	
114	71.0	85.0	754.0	0.880	0.00158	0.000188	C.00150	3.398	0.020	2.09

	OROP NUMBER	DIAM. CF DRCPLET (CMS)	NUMBER COLLECTED	BACKGROUND COUNT •	COLLECTION EFFICIENCY (PER CENT)	IMPACTION NUMBER	REYNOLDS NUMBER	
_ •	550	0.092	1162	16273	57.4	4.32	213.2	
	551 ,	0.197	3758	15430	42.B	2.02	456.4	
	552	0.174	3167	15432	46.2	2 • 28	403-1	!
-1	553	C-141	1680	15652	36 - 8	2.82	326.7	
- 4	554	0.162	2657	15149	45.5	2 • 45	375.3	
	555	G-174	2387	15123	35.5	2.28	403-1	!
	556	0.201	3639	15020	40.9	1.98	465.7	
	557	0.121	1731	16561	48.8	3.28	280.3	İ
;	558	C+C95	1347	16621	61.2	4.18	220.1	
Ì	559	0.250	3864	16717	25.2	1.59	579-2	Ì
	560	0.135	2304	16472	52.3	2.94	312.8	į
53	561	0.174	2661	16475	36.3	2.28	463-1	ļ
21	562	0.198	3337	16311	35.5	2.01	458.7	
51	563	0.158	2483	17012	39.8	2.51	366-1	
3	364	0-177	2983	16937	38+3	2.24	410-1	.

RUN NUMBE	R HUMIDITY	TEMPERATURE	PRESSURE	DENSITY OF DISPERSED PHASE	DENSITY OF CONTINUOUS PHASE	VISCOSITY	DIAM. OF AEROSOL PARTICLES	AEROSOL VELOCITY	TURBULENCE	WEBER NUMBER
	(PER CENT)	(DEG F)	(NNS HG)	(G/CC)		(POISE)	(CMS)	(M/SEC)	(PER CENT)	
115	71.0	85.0	754.0	0.880	0.60128	0.000188	0.00150	3.437	0.050	2.14

DROP NUMBER	DIAM. CF DRCPLET (CMS)	NUMBER COLLECTED	BACKGROUND COUNT .	COLLECTION EFFICIENCY (PER CENT)	IMPACTION NUMBER	REYNOLDS NUMBER
,						
580	0.227	3783	15340	32.6	1.77	531.9
saı .	0-174	2353	14350	29.7	2.07	454.6
รคอ	0.179	2177	12972	35.7	2.25	419.4
583	0.260	2 38 5	12732	18.9	1.55	609.3
584	0.258	2189	12162	18.4	1 • 56	604.6
รสร	0.207	2179	12742	27.2	1 - 94	485.1
586	0.213	2 3 7 0	1 2080	29.5	1.89	499.1
587	0.246	3061	12056	28.6	1.63	576.4
568	0.257	3629	12042	31.1	1.56	602.2

SYSTEM USED WAS PARAFFIN WAX AEROSOL: WATER OROPLET

10310

1970

0-186

614

	RUN NUMBER	HUMIDITY (PER CENT) 68.0	TEMPERATURE (DEG F)	PRESSURE (WMS HG) 763+2	DENSITY OF DISPERSED PHASE (G/CC)	DENSITY OF CONTINUOUS PHASE 0.00130	VISCOSITY (POISE) 0.000189	DIAM. OF AEROSOL PARTICLES (CMS)	AEROSOL VELOCITY (P/SEC)	TURBULENCE (PER CENT) 0.011	WEBER NUMBER	
:						, .		•	•			•
•	********		********	********	*******	**********	• • • • • • • • • • • • •	*******	********		********	1
•	********		********		********	********	******	******		*********	******	•
												- ;
!	DROP NUMB	BER DIAM. DACPLE (CMS)		BER LECTED	HACKGROUND COUNT	COLLECTION EFFICIENCY (PER CENT)	NUMBER	CN REY	NOLDS BÉR			i
												:
	600	0.221	31	47	10248 .	42.8	5.96	706	• 0			
	ec ı	0.215	282	21	10162	40.1	6.12	686	. 8			į
:	602	0.195	18	35	10286	33.0	6.75	622	• 9			•
•	6¢3	0.208	24	42	10579	36.3	6.33	664	• 5			į
:	604	0.216	27	4 3	10695	37.4	6.09	690	• 0			,
	605	0.221	29	16	10713	38.0	5.96	706	• 0			ļ
	606	0.161	170	68	10241	45.4	8.17	514	• 3			
	607	0+154	. 15	88	10352	44-1	8.55	492	• 0			;
	608	0.150	. 14	89	19473	43.0	8.77	479	•2			
-	609	0-165	1 0	4.4	10584	38.9	7.78	527	- 1		٠	ļ
	610	0.156	15	26	19278	41.6	8.44	498	• 3			:
	611	0.156	. 13	92	10216	38.1	8.44	498	•3			•
	612	0.161	16	75	10299	42.7 .	6.17	514	. 3			į
	613	0.171	16	87	10452	42.1	7.70	546	• 3		•	

40.2

575.0

7.31

	DROP NUMBER	DIAM. CF DÀCPLET (CMS)	NUMBER COLLECTED	E A CK GROUND	COLLECTION EFFICIENCY (PER CENT)	IMPACTION NUMBER	REYNOLDS NUMBER
	615	0.181	2170	10391	43.4	7.27	578•2
	616	C•231	3537	11623	38.8	5.70	737.9
i	617	0.190	2507	11372	41.6	6.93	. 607.0
_ :	618	C+190	2409	11306	40.2	6.93	607.0
3	619	0.201	2763	11346			
	620	0.195			41.1	6.55	642.1
-] . -i	•		2548	12525	36.4	6.75	622.9
3	621	0.215	3276	12434	38.8	6.12	686.8
	. 622	0.247	4215	12558	37.5	5.33	789.0
4	657	0-115	1199	13103	47.1	11.44	367.4
1	624	0.124	1404	13397	46.4	10.61	396±1
1	625	0.256	6376	13727	48.3	5.14	917.8
: 1	626	C.224	3424	1 3641	34 - 1	5.ea	715.6
	627	0.122	1 30 1	1 3271	44.9	10.79	389.7
1	628	0-111	1026	1 3492	42.0	11.86	354.6
	629	0.248	4488	13671	36.4	5.31	792.2
إنت	63C	0:127	1349	13306	42.8	10.36	405.7
İ	631	0.140	1530	1 3604	39.1	9.40	447.2
	632	02131	1489	13318	44.4	10.65	418.5
	633	0-136	1650 .	13424	45.3	9.68	434.5
	634	0.167	2353	13303	43.2	7.88	533.5
1	635	0.139	1812	13393	47.7	9.47	444.0
S	636	C-140	1692	13275	44.3	9.40	447.2
	637	C-141	1662	13330	42.7	9.33	450-4

DROP NUMBER	DIAM. CF DRCPLET (CMS)	NUMHER COLLECTED	HACKGROUND COUNT	COLLECTION EFFICIENCY (PER CENT)	IMPACTION Number	REYNOLDS NUMBER
638	0.100	931	13179	48.i	13-16	319.5
639	C-202	3173	13234	40.0	6.52	645.3
640	0.149	1939	13269	44.8	e•e3	476.0

- 223 -

SYSTEM USED WAS PARAFFIN WAX AEROSOL: WATER DROPLET

RUN NUMBER	HUPIDITY	TEMPERATURE	PRESSURE	DENSITY OF DISPERSED PHASE	DENSITY OF CONTINUOUS PHASE	VISCOSITY	DIAM. OF AEROSOL PARTICLES	AEROSCL VELOCITY		WEBER NUMBER
	(PER CENT)	(DEG F)	(NMS HG)	(G/CC)		(PO ! SE)	(CMS)	(M/SEC)	(PER CENT)	
117	64.0	82.0	763.9	0.918	0.00130	0.000189	0.00274	3.210	0.013	3.56

DROP NUMBER	DIAM. CF DRCPLET (CMS)	NUMBER COLLECTED	BACKGROUND COUNT .	COLLECTION EFFICIENCY (PER CENT)	IMPACTION NUMBER	REYNOLOS NUMBER
650	0.236	1735	27221	7.e.	5.51	521.1
651	G-171	1796	26875	15.6	7.61	377.6
652	0 • 2 30	2361	26983	11.3	5.66	507.9
053	0.172	2567	27027	17.0	6.78	424.0
654	C.174	1298	26992	8.7	6.71	428.4
655	0.244	1744	26889	7.4	5-23	538.8
656	0.177	1261	26842	10.2	7.35	390.9
657	0 - 273	3795	26703	19.5	5.83	492.4
658	0.260	1509	27103	5.6	5.00	574.1
659	0.162	1 37 4	26931	13.2	8.03	357.7
660	0.260	^733	27053	17.6	5.00	574 - 1
661	G-101 '	1583	26897	12.2	7.19	399.7

RUN NUMBER	* HUMIDITY	TEMPERATURE	PRESSURE	DENSITY OF DISPERSED PHASE	OFNSITY OF CONTINUOUS PHASE	VISCOSITY	DIAM. DF AERGSGL PARTICLES	AEROSCL VELCCITY	TURBULENCE	WEBER NUMBER
	(PER CENT)	(DEG F)	(MMS HG)	(G/CC)		(POISE)	(CMS)	(M/SEC)	(PER CENT)	
118	56.0	62.0	755.4	0.918	0.00130	0.000189	0.00275	3.163	0.010	3.47

Dugb profiles	DIAM. CF DRCPLET (CMS)	COLLECTED COLLECTED	RACKGROUND COUNT	COLLECTION EFFICIENCY (PER CENT)	IMPACTION Number	NUMBER
680	0.240	1923	27645	8•2	5-38	523+2
681	0.180	1867	27748	14-1	7.18	392.4
965	0.177	1834	27032	14.8	7.30	385.9
683	C-168	1 37 3	27329	12.1	7.69	366.3
484	0.204	2009	27297	12.C	6.33	444.8
685	0.242	2842	27090	12.2	5.34	527.6
686	0.137	1849	27871	24+1	9.43	298.7

SYSTEM USED WAS PARAFFIN WAX AERUSUL: WATER DROPLET

RUN NUPHE	H HUMIDITY	TEMPERATURE	PRESSURE	DENSITY OF DISPERSED PHASE	DENSITY OF CONTINUOUS PHASE	VISCOSITY	DIAM. OF AEROSOL PARTICLES	AEROSOL VELOCITY	TURBULENCE	WEBER NUMHER
	(PER CENT)	(DEG F)	(PMS HG) ·	(G/CC)		(POISÉ)	(CMS)	(M/SEC)	(PER CENT)	
119	74.G	81.2	758.6	C.718	6.00129	0.000189	0.00224	4.C08	0.011	4.54

DROP NUMBER	DIAM. CF DRCPLET (CMS)	NUMPER COLLECTED	BACKGROUND CCUNT	COLLECTION EFFICIENCY (PER CENT)	IMPACTION Number	REYNGLDS NUMBER
70C	0.237	3384	16012	25.6	4.58	648.2
701	0.222	2691	15997	23.3	4.89	607.2
702	0.217	2623	15921	23.8	5.00	593.5
703	0.201	2518	15036	26.9	5.40	548.9
704	0-193	2439	15852	28.8	5.62	527.9
705	0.218	2853	15793	25.9	4.98	596.2
706	0.126	1155	15771	31.4	8-61	344.6
707	C-11C .	926	15703	33.2	9.86	300.9
708	0.154	1515	15722	27.7	7.C4	421.2
709	C-126	1193	15677	32.7	8.61	344+6
710	0-148	1519	15655	30.2	7.33	404.B
711	0.108	906	15621	33.9	10.04	295.4
712	0.168	1970	15607	30.5	6.46	459.5
713	0.215	2464	15636	23.2	5.04	588.0
714	C-156	. 1783	15521	32.2	6.95	426.7

DAGP NUMBER	DIAM. CF DRCPLET (CMS)	NUPAER COLLECTED	BACKGROUND COUNT	COLLECTION EFFICIENCY (PER CENT)	IMPACTION Numher	REYNOLDS NUMBER
715	0-136	1224	15530	29.0	7.98	372.0
716	C-179	21,31	15507	29.2	6.66	489.6
71 7	0.178	1919	15580	26.5	6.09	486.8
718	0.144	1299	15496	27.5	7.53	393.8
719	0.167	1876	15347	29.9	6.49	456.7

SYSTEM USED WAS METHYLENG MUUE AEROSOL: WATER DROPLET

RUN NUFUEI	Y TIOIMUH S	TEMPERATURE	PRESSURE	DENSITY OF DISPERSED PHASE	DENSITY OF CONTINUOUS PHASE	VISCOSITY	DIAM. OF AEROSOL PARTICLES	AFROSCL VELOCITY	TURBULENCE	WEBER NUMBER
	(PER CENT)	(DEG F)	(MMS HG)	(G/CC)		(POISE)	(C#5)	(P/SEC)	(PER CENT)	
120	69.0	81.0	761.0	1.401	0.30129	0.000189	0.00050	4.276	0.015	1.76

DRCP NUMBER DIAM. CF NUPHER BACKGROUND COLLECTION REYNOLDS IMPACTION DRCPLET COLLECTED COUNT . EFFICIENCY NUMBER NUMBER (CMS) (PER CENT) 7.º C 0.136 957 15397 22.9 0.65 398.0

952 386.3 721 -0-132 14703 25.0 0.67 722 0.132 1107 15259 28.4 9.67 386.3 1205 723 C-160 15373 20.9 0.55 468.2

SYSTEM USED WAS FERROUS SULPHATE MERCSOL: WATER DROPLET

RUN NUPE	ER HUMIDITY	TEMPERATURE	PRESSURE	DENSITY OF DISPERSED PHASE	DENSITY OF CONTINUOUS PHASE	VISCOSITY	DIAM. OF AEROSOL PARTICLES	AEROSCL VELOCITY	TURBULENCE	WEBER NUMBER
	(PER CENT)	(DEG F)	(PMS HG)	(G/CC)		(POISE)	(CMS)	(M/SEC)	(PER CENT)	
121	63.0	83.0	762.2	1 • 86 3	0.00130	0.000185	0.00118	1.631	0.016	0.80

DROP NUMBER	DIAM. CF DRCPLET (CMS)	NUMBER COLLECTED	BACKGROUND CCUNT .	COLLECTION EFFICIENCY (PER CENT)	IMPACTION NUMHER	REYNOLDS NUMBER	<u>!</u>
							:
730	0.260	3638	10362	35 - 4	82.0	297.7	į
731	0-206	2628	10533	40 - 1	1.24	235.9	į
732	0.234	3555	10577	41.8	1.09	267.9	!
733	0-160	2050	10519	51.9	1.59	183•2	!
734	3.144	1654	10432	52.1	1.77	164.9	:
735	0.191	2608	10328	47.2	1.33	218.7	į
736	0.176	1837	10109 .	40.0	1.45	201.5	•
737	0-109	908	10006	52.0	2•33	124.8	
738	0.167	2661	10921	59.5	1.52	191.2	
739	0.190	2269	10034	42.7	1.34	217.5	. !
740	0.177	2226	10096	47.9	1.44	202.6	
741	0.249	3436	10013	37.7	1.02	285•1	
742	0.242	2626	10115	30 • 2	1.05	277.1	;
743	0.130	1421	10115	56.6	1.96	148.8	• :
744	0+134	1445	10136	54+1	1-90	153.4	ı

!	DROP NUMBER	DIAM. CF DRCPLET (CMS)	NÙMHER COLLECTED	BACKGROUND COUNT	COLLECTION EFFICIENCY (PER CENT)	IMPACTION NUMBER	REYNOLDS NUMBER
	745	0.114	1119	10024	54.5	2.23	130.5
	746	G-145	1041	10009	53.1	1-76	166.0
	747	0.077	786	10226	69.2	2.93	99•6
1	748 -	0.132	1445	19181	55.5	1 • 93	151-1
	749	0.120	1324	10198	61.4	2 • 12	137.4
	75G	0.105	1006	10114	61.5	2.42	120.2
	751	0.103	944	10612	60.5	2.47	117.9
	. 752	0-114	1125	10165	58.0	2.23	130.5

RUN NUMBER	FUMIDITY	TEMPERATURE	PRESSURE	DENSITY OF DISPERSED PHASE	DENSITY OF CONTINUOUS PHASE	VISCOSITY	DIAM. OF AEROSOL PARTICLES	AEROSCL VELOCITY	TURBULENCE	WEBER NUMBER
	(PER CENT)	(DEG F)	(MMS HG)	(CVCC)		(POISE)	(CMS)	(M/SEC)	(PER CENT)	
122	63.0	ac.o	702.2	0.977	0.00130	0.000185	G-CG157	3.396	0.012	2.43

2	CCMPILE TIME=	1.21 SEC.EXEC	UTION TIPE=	4.97 SEC. WA	TFIV - VERSION	LEVEL 3 PARCH	1971	DATE=	75/1
	DIAGNOSTICS	NUMBER OF ERRORS		0. NUMBER OF WARNINGS=		O. NUMBER OF EXTENSIONS=		0	
	CORE USAGE	OBJECT CCDE=	8080 HYTES.	ARRAY AREA=	424 HYTES.TOTAL	AREA AVAILABLES	118784	BYTES	
	, 7e3	0.260	2656	tař :	18+1	1.89	620.0		
	782	0.174	2312	14701	35.3	2.83	414.9		
	781	C.128	1533	14727	43.3	3.64	305.2		
	786	0.122	1574	14853	48+5	4.03	270.9		
1	779	0.211	3023	14876	31-1	2.33	503-1		
1	778	0.155	2519	14577	49.C	3.17	369.6		
1	777	0.130	1 336	14073	36.7	3.79	310-0		
į	776	0.260	2157	14788	14.7	1.69	620.0		
	775	0•230	2872	14954	24.7	2.14	548.4		
	OROP NUMBER	DIAM. CF DRCPLET (CMS)	NUMUER COLLECTED	BACKGROUND COUNT	COLLECTION EFFICIENCY (PER CENT)	I MPACTION NUMBER	REYNCLO: NUMHER	s	
;									